DISTRICT MORPHOLOGY IMPACT ON ENVIRONMENTAL CONTROL, ENERGY PERFORMANCE,INDOOR AND OUTDOOR COMFORT

A Thesis

by

Ayşe Özlem DAL

Submitted to the

Graduate School of Sciences and Engineering
In Partial Fulfillment of the Requirements for
the Degree of

Master of Science

in the
Department of Architecture

Özyeğin University
May 2023

DISTRICT MORPHOLOGY IMPACT ON ENVIRONMENTAL CONTROL, ENERGY PERFORMANCE, INDOOR AND OUTDOOR COMFORT

Approved by:

Assist. Prof. Turaj Arda Aşrafi,
Advisor,
Department of Architecture
Özyeğin University

Assist. Prof. Neşe Ganiç Sağlam,
Department of Architecture
Özyeğin University

Assist. Prof. Gözde Gali Taşçı,
Department of Interior Architecture
Beykent University

Date Approved:

To all the children who lost their lives in the earthquake on February 6 in Turkey…

ABSTRACT

Technological developments have provided significant architectural changes in the developing world in the last century, as in all other sectors. Nowadays, it cannot be denied that all the changes cause challenges like increasing carbon emissions, climate change, scarcity of resources, depletion of fossil fuels, population growth, and urbanization. Therefore, providing an efficient living environment, economy, and society are essential current targets for countries. The European Commission, which provides regulations to decrease the negative impacts of the building sector, is shifting the attention from the building level to the urban level. Since urbanization and the growth rate of the population is increasing rapidly, all countries like Turkey, need to take the responsibility of decreasing the adverse impacts of building stock.

This study aims to evaluate the impact of district morphology on environmental control, energy performance, and comfort levels in different climatical regions of Turkey. The prominent uniqueness of the thesis is the integration of three key parameters. These are examining environmental control parameters for the urban morphologies' sun and wind potential, analyzing indoor and outdoor thermal conditions, also indicating energy performance calculations. Therefore, it is aimed to do inclusive research by considering the environment, energy, and human being together.

In the methodology, a case study urban block is selected to analyze in Ankara, Turkey. It has 76,183 m² and includes approximately 2,400 dwellers. The case study urban block investigated two different climatical conditions. Ankara has a temperate-dry climate, and İzmir is selected as the representative city of a hot-humid climate. The

research methodology consists of three main steps: arranging parametric modeling, conducting performance simulations, and making a comparative assessment. The parametric modeling includes data collection of the site, determining urban scenario variables, and organizing alternative urban block models. Regarding the urban scenario parameters, 28 alternative urban models are arranged. The performance analysis and comparative assessment process are conducted in Grasshopper/Rhinoceros software using a variety of plug-ins like Ladybug 1.4.0, Honeybee 1.4.0, Butterfly 0.0.05, and ClimateStudio1.1.9.

The results show that all the beneficial alternatives have a 135° orientation regarding solar radiation analysis, energy performance simulations, computational fluid dynamic analysis outdoor and indoor comfort simulations. The best optimum urban scenario for Ankara belongs to the alternatives of *Irregular X-Axis*. The model produces the highest electricity thanks to solar streets and provides the lowest final district T.P.E. The final district T.P.E. of Ankara's best district model is 33% lower than the current value. The best optimum urban model for İzmir belongs to the *Detached* category. The model provides the lowest final district T.P.E, nearly half of the existing situation's final district T.P.E.

Eventually, comprehensive research is needed to ensure the best optimum district morphology regarding the urban context and climate. Conducting all important parameters as much as possible highlights the best solution regarding environment, energy, comfort, and renewables.

ÖZETÇE

Son yüzyılda yaşanan teknolojik gelişmeler dünyada önemli gelişmeleri beraberinde getirirken da bazı olumsuzluklara da sebep olmaktadır. Bunların başında iklim değişikliği, kaynakların kıtlığı, fosil yakıtların tüketimindeki artış, nüfus ve kentleşmenin artışı gelmektedir. Mimarlık ve inşaat sektörünün sera gazı emisyonlarının ve enerji tüketiminin önemli bir kısmından sorumlu olduğu bilinmektedir. Yapı stoğunun sebep olduğu olumsuzlukların etkisini azaltmak için hem bina hem de kent ölçeğinde çalışmalar yapılmasına dikkat çekilmektedir. Son yıllarda, kentleşme ve nüfus oranlarındaki artış göz önüne alındığında tüm ülkeler de olduğu gibi Türkiye'de de kent ölçeğinde araştırmalar yaparak yapı stoğunun olumsuz etkilerini azaltmak için çalışmalar sürdürülmesi gerekmektedir.

Bu çalışma, yerleşke morfolojisinin fiziksel çevre kontrolünü, enerji performansını ve konfor seviyesini nasıl etkilediğinin araştırılması amaçlanmıştır. Bu durumda Türkiye'nin farklı iklim bölgeleri de göz önünde bulundurulmuştur. Çalışmanın özgünlüğünü belirleyen üç durum vardır. Birincisi, çevre kontrolü, enerji performans çalışması ve termal konfor beraber ele alınmıştır. Çevre kontrolü incelemelerinde güneşin ve rüzgârın parseldeki hareketi incelenmiştir. Ayrıca, termal konfor hem dış çevrede hem de iç ortamda analiz edilmiştir. İkinci durum, kent senaryoları oluşturulurken hem homojen hem de heterojen parsel dokusu oluşturmaya gayret edilmiştir. Üçüncü olarak, yenilenebilir enerji kaynaklarından güneş enerjisinin farklı yerleşke morfolojisindeki potansiyelleri analiz edilmiştir. Bu yüzden, yapılan araştırmada çevre, enerji ve insan kapsayıcı bir bakış açısıyla incelenmiştir.

Tezin yöntemi aşamasında öncelikle Ankara'da 76,183 m²'lik bir yerleşke seçilmiştir ve yerleşkede yaklaşık 2,400 kişi ikamet etmektedir. Ankara ılımlı-kuru iklime sahiptir. Çalışmada iklimin etkisini incelemek için ayrıca sıcak-nemli iklim bölgesinde yer alan İzmir ili seçilmiştir. Araştırmanın yöntemi üç temel aşamadan oluşmaktadır: modellemenin yapılması ve alternatiflerin düzenlenmesi, performans simülasyonlarının yapılması ve karşılaştırmalı değerlendirme için analizlerinin yapılmasıdır. Modelleme aşamasında parselde yeni alternatiflerin oluşturulması için değişkenler belirlenmiştir. Bu bağlamda 28 adet alternatif yerleşke modeli oluşturulmuştur. Yapılan analizler *Grasshopper/Rhinoceros* programı kullanılarak tamamlanmıştır. Algoritmik simülasyon modellerinin oluşturulması için *Ladybug 1.4.0, Honeybee 1.4.0, Butterfly 0.0.05, ve ClimateStudio 1.1.9* gibi eklentiler kullanılmıştır. Güneş radyasyonu, enerji performans analizi, akışkan dinamiği simülasyonu, dış ve iç konfor analizleri tamamlanmıştır.

Araştırmanın temel sonuçları şu şekildedir. Ankara ve İzmir için başarısını koruyan alternatiflerdeki binalar 135° yönelime sahiptir. Ankara için en başarılı sonuç veren alternatif *"IrregularX-Axis"* grubuna aittir. Bu alternatifte yerleşkenin final primer enerjisinde Ankara için %33 oranda bir düşüş sağlamaktadır. İzmir iklimi için en başarılı model "*Detached*" kategorisine aittir. Bu alternatifte yerleşkenin final primer enerjisinde %52 oranında bir düşüş sağlanmaktadır.

Kapsamlı bir araştırma yürütmenin önemli olduğu vurgulanan bu çalışmanın çıktıları değerlendirildiğinde; çalışma alanı genişletilebilir, değişken sayısı arttırılarak daha fazla alternatif değerlendirilebilir, peyzaj ile ilgili değişkenler de eklenerek araştırmanın kapsamı genişletilebilir. Ayrıca, *"solar street"* fikrinin öneminin anlaşıldığı için bu fikir daha fazla geliştirilerek kent ölçeğine nasıl daha verimli şekilde entegre edilebileceği ile alakalı çalışmalar ortaya çıkartılabilir.

ACKNOWLEDGMENTS

I must express deep gratitude to my entire family, especially my mother and father. They encouraged and motivated me with their endless love throughout my life. Their compassion and peace are the unique features that make me who I am. This thesis could not have been completed without the invaluable support of Assist. Prof. Turaj Arda Aşrafi, the thesis advisor. Through my graduate education, he taught me not to be afraid to try new ideas, to continue researching, and always move forward without giving up. Therefore, I would like to thank him for every contribution to my academic career and life. I offer my sincere appreciation for sharing his profound experiences and valuable time with me. Lastly, I am appreciative of the jury members, Assist. Prof. Neşe GANİÇ SAĞLAM, and Assist. Prof. Gözde GALİ TAŞÇI, thanks for their precious contribution.

May 2023 Ayşe Özlem DAL

(Architect, Research Assistant)

TABLE OF CONTENTS

LIST OF TABLES

LIST OF FIGURES

CHAPTER I

INTRODUCTION

In the world, buildings are one of the biggest consumers of energy like 40% of total energy consumption and 36% of carbon dioxide emission [1,2,3]. Energy Performance Building Directive 2018, the which is the latest version, has the goal of decreasing greenhouse gas emissions by at least 40% by 2030 when it is compared to 1990 [4]. It is figured that to reduce the negative impacts of the building sector European Commission is shifting the attention from the building level to the urban level by pointing to “district-level energy efficiency”, “post-carbon cities”, “net/nearly zero energy districts” [2,5]. Therefore, it is essential to use sustainably mitigate energy consumption and use the potentials of the urban context. It is also beneficial to meet by renewable energy that is self-produced within the neighborhood to avoid climate change and carbon emission [2,6]. All these targets are to cope with today’s challenges for planning and designing a sustainable environment, economy, and society against increasing carbon emissions, climate change, scarcity of resources, depletion of fossil fuel, population growth, and urbanization [7].

One of the current problems is urbanization and the population’s growth rate, which means the increasing number of people in urban areas [8]. The urban population rate in the world is assumed to increase by 2.7 billion by 2050, especially in developing countries [9,10]. Turkey, one of the developing countries, shares the same essential problems since the growing rate of urbanization is 2% per year. Thus, every year 100.000 new building is added to the existing building stock, which has about 9.1 million buildings and 23 million dwellings in Turkey. Related to the energy demand, of building sector has responsibility for 1/3 of the country's total energy consumption, and gas and electricity use is responsible for 2/3 of the sector's total energy demand [11]. Currently, Turkey is in the adaptation process for European Union and needs to take the responsibility of decreasing the negative impacts of building stock by making an effective evaluation of urban design, which has a critical effect on building energy performance and comfort level [9].

When the significant relation of the building sector on energy consumption and carbon dioxide emission and other related issues like climate change is considered, the design of buildings and the organization of those which refers to urban form [12]. Urban morphology is defined as the formation of settlements over time as the central placement theory [13]. It is vital to focus on producing high-quality living environments for indoor, outdoor, and building energy performance to overcome cities' current problems. However, recent studies generally focus on the improvements at the level of individual buildings [12]. The research problem of the thesis is based on evaluating the relationship of urban block form with energy performance and comfort levels both indoors and outdoors with the basis of environmental control parameters for different climates in Turkey.

1.1 Purpose of Thesis

Chapter I displays this thesis's research problem; the purpose is to investigate the relationship between district form, environmental control, building energy performance, and comfort level through simulation. The case study urban area is in Ankara, Turkey. It has a temperate-dry climate. To evaluate the impact of the climate, İzmir is also considered in the study as a hot-humid climatic region.

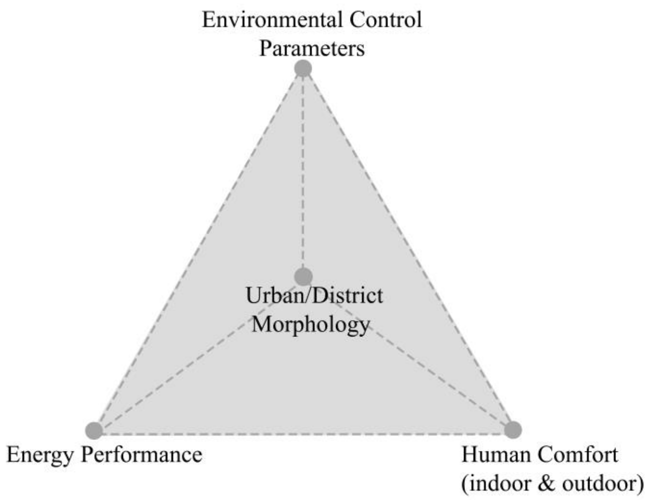

Figure 1: Main keywords of the thesis

There is much significant research about the relationship of urban or district form with environmental control parameters, energy performance, indoor and outdoor comfort, which is mentioned in Chapter II in detail. The difference between this thesis from previous research is evaluating the relationship between three: urban block morphology, energy performance, and indoor and outdoor comfort. This defines the unique part of the thesis. Figure 1 indicates the main keywords examined in the thesis to understand their relationship. In general, this study has the following aims:

- To investigate the impact of district morphology on environmental control parameters
- To examine the relationship between district form and energy performance
- To evaluate the impact of urban block morphology on indoor and outdoor comfort
- To examine the relationship between three topics: district morphology, energy performance and, indoor and outdoor comfort

- To define a proper strategy to ensure the most optimum district morphology for temperate-dry climate zone and hot-humid climate zone and upgrade them by integrating renewable energy solutions

1.2 Hypothesis

Every city inevitably has its characteristic challenges, like climate conditions. At the same time, there can be similar issues in urban areas like climate change, urbanization, increasing the total energy consumption and carbon dioxide level of buildings, and urban heat island impact, especially in city centers. By considering these consequences, it is critical to design urban areas that are proper for their standards for pedestrian, building, and urban levels. Therefore, the thesis hypothesizes that district morphology considerably impacts environmental control parameters, energy performance, and comfort level. It also affects the potential of renewable energy system integration. The urban areas designed according to the vision can direct a way to cope with the century's challenges and improve architectural solutions.

CHAPTER II

LITERATURE REVIEW

The literature review of the study focuses on the research and investigations in the field of district morphology relations with environmental control, energy performance, indoor and outdoor comfort. The publications in “ScienceDirect”, “Scopus” and “Web of Science” were examined by combing the keywords of “urban morphology”, “district morphology”, “passive systems”, “energy performance”, “indoor comfort”., and “outdoor comfort”. Furthermore, the “YÖK Tez Tarama” and “TÜBİTAK Veri Tabanı” databases have been investigated.

2.1 State of Art Related to The Impacts of Urban Morphology on Environmental Control Parameters

The quote “learning from the past” is a frequent paradigm in both architecture and urbanism by referring to “passive urbanism” which is stated as generating the urban form with the base of the climatic characteristic of the region as an adaptation strategy since it advocates the evaluation of the performance of urban layout in respect to the solar accessibility, wind pattern, thermal and mass balance based on the morphological examination [14].

Oke (1988) was called one of the first researchers to use the urban canyon concept [15]. Oke [16] tried to offer alternatives for outdoor climates to provide optimum conditions, such as maximization of shelter, dispersion of pollutants, urban warmth, and solar access. Oke *(1988)* states that there are infinite combinations considering the climate, urban geometry, and design solutions; therefore, there is no universally optimum geometry as one single solution [16,17]. The most important decision is choosing the best optimal solution for the context. *Meşe* [18] made the seven categorizations about proper integration of passive strategies as a critical point for urban design by considering urban form and density [19], location selection and orientation, building form, solar volume and direction, the direction of the prevailing wind, street design considering building height and street width, landscape design regarding location, size, and type of tree.

2.1.1 Wind Pattern

Urban typology has an impact on the wind effect, which is one of the renewable energy potentials since building layout, space between buildings, and height of them have a significant impact on wind direction, which affects the integration of natural ventilation into the building [19,20].

Hassan et al. [8] researched to evaluate the relationship between urban morphology and wind potential to promote indoor and outdoor air quality on the urban residential block in Port Said City, Egypt. The study uses the computational fluid dynamic analysis by using Ansys Fluent software on four different urban alternatives, including the maximum number of forty buildings. The urban morphologies are arranged according to the yearly prevailing wind pattern with three scenarios as parallel, perpendicular, and oblique. The urban scenarios of the study are shown in Figure 2. The result of the research is that the proposed alternatives reduced the dispersion of air pollutants by approximately 20–85% compared with the existing case by utilizing proper natural ventilation [8].

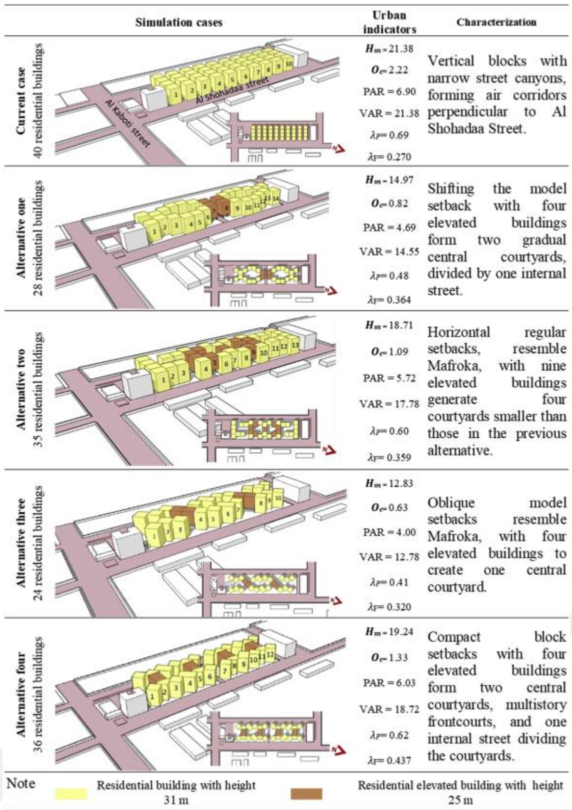

Figure 2: Urban scenarios of the article [8] *(Hassan et al., 2020, p.7)*

Ramalho Fontenelle et al. [21] examine the two urban morphologies regarding a representation of the urban transformations of Rio de Janeiro between 1976 and 2013. The research analyses the impact of morphological change in the case study urban area on the airflow pattern by using the RANS k-ϵ turbulence model. The results show an enlargement in wind velocity at the pedestrian level and a rise in the pressure difference between the building facades. New high-rise buildings increase the stagnation area, especially for the leeward region since the boundary layer height and the turbulence level increase [21].

Hang et al. [22] aim to examine two main city models as round -square form and rectangular form, to understand wind behavior. The wind pattern is evaluated by the CFD simulation tool. Nine urban scenarios are organized regarding the number of streets, street length ratio, aspect ratio H/W, and wind direction. There are three main wind directions at an angle of 15°, 30°, and 45°. The simulations demonstrate that if the city model is round with two crossing streets, the non-parallel wind direction provides a more robust wind pattern for the whole urban morphology. On the contrary, if the round model with a narrow street, the parallel wind direction cannot blow for the entire street [22].

2.1.2 Solar Radiation

Another environmental control parameter is the integration of solar energy with the impact of urban form. Sarrelde et al. [23] conducted research in London, which has mild winters and temperate summers, to understand the solar energy potential through urban form. The five urban forms are analyzed based on solar energy integration to increase renewable energy potential on a neighborhood scale. Python programming language is linked with Geographical Information Systems by using the ArcGIS ArcMap 10.0 software. The software uses the Area Solar Radiation tool to analyze the solar potential on the roof. Also, the Solar Access Analysis tool of the Autodesk Ecotect Analysis 2011 software is used to analyze solar irritation on facades.

There are five main categories and 18 descriptors for arranging the urban alternatives. The building typologies include detached houses, semi-detached houses, terraced houses, and apartment blocks. The vertical and horizontal distribution category has the descriptors of building height and distance between buildings. The land-use group indicates the share of the area covered by domestic buildings, the share of the area covered by roads, and the share of the area surrounded by gardens. According to building geometry, there are descriptors of average building volume, average building perimeter, and average building orientation. The last group is building density. There are five categories: plot ratio, site coverage, total floor area, the total area covered by buildings, and the total neighborhood area.

The study's main result is that thanks to the optimization of combinations on eight urban form variables, the solar potential of roofs could be increased by 9%. At the same time, the rate could be an increase on façades up to 45% in London [23]. There are some international research initiatives such as *‘‘COST Action TU1205”* and *“the IEA SHC Task 51 00Solar Energy in Urban Planning”* to evaluate the integration of solar energy into building design and planning in the world [24].

Shi et al. [24] investigated 18 urban typologies in Singapore to analyze the interactions between solar energy use and urban morphology using a parametric methodology. For the study, typical vernacular urban typologies are formulated by Urban Block Generator, in Rhinoceros, Grasshopper. The formulation generates a proper urban form by combining block dimensions, building patterns, floor area ratios, and site coverage. While analyzing vernacular building typologies to arrange the formulation in the parametric tool, different software like OpenStreetMap and ArcGIS is used. DAYSIM examines the generated urban forms for solar radiation simulation. The solar energy penetration assessment and the photovoltaic panels' capital costs for these block typologies are analyzed using City Energy Analyst software. The research results show that the impact of floor area ratio is dominant, followed by site coverage and building pattern on the on-site solar energy use [24].

Esch et al. [25] discuss the effect of urban design parameters and building design parameters on solar access and the passive solar heating strategies in residential buildings in the Netherlands in a moderate climate. Urban design parameters include street width orientation, while building design parameters consist of roof shape and building envelope design. The reference situation has a 15m street width; the other three alternatives are 10m, 20m, and 25m. Two street direction alternatives are arranged as north-south and east-west, which refers to the existing direction. There are three types of roof shade flat, gable, and single-pitched. The gable-type roof shade is the current situation. Also, there are two types of envelope design alternatives conventional and solar. Trigonometric equations are used for calculating solar access to the urban canopy with the base of the sun’s position in the sky and the geometry of the canyon.

Solar access to the urban canyon is studied for three typical days of the year; the 21st of December for the shortest day for winter, the 21st of March for spring and autumn, and the 21st of June as the longest day of the year to represent the summer season. TRNSYS simulation tool calculates the passive solar heating potential about heat demand and solar heat gain in different urban forms to provide proper solar irradiation in colder seasons and shade in warmer seasons. Street width significantly influences the total global radiation of urban canyons, as the wider ones have higher global radiation. In summer, the narrow streets enable limiting excessive heating for high densities. In winter, increasing the street width is preferable to enlarge the heat demand, especially in the east-west direction [25]. Also, for cold climates, changing the street to 5 m provides a solar radiation gain of 19% in winter and 25% in summer [9,15,25].

Zhu et al. [26] explore the relation between urban morphology and solar potential of a high-density area in Shanghai that has a subtropic climate. The constant variables are site, surrounding, and building form. The variables to manage the urban forms which is shown in Figure 3, are seven main orientations, three layout alignments, six-building heights, building density alternatives. Seven main orientations are 135°, 150°, 165°, 180°, 195°, 210°, 225°. Three layout alternatives are linear (both row and column alignment); east-west (just row alignment) and south-north (just column alignment). 12, 18, 33, 54, 78, and 99 m are the building height alternatives. The building density: 3, 4, 5, 6, 7, and 8 are the number of rows while 4, 5, and 6 are the number of columns. According to the combination of variables, 1260 urban scenarios were analyzed to define solar irradiation potentials.

The solar irradiation for the scenarios was simulated by Ladybug what is the tool of Grasshopper. Excel and SPSS are used for data processing and analysis. The meteorological data for the simulation of solar irradiation is linked with derived the Energy Plus weather database. The results of the new urban alternatives display a strong correlation with solar energy performance when it is compared with the existing situation. The best results are obtained by reducing the building height and increasing the number of buildings, adjusting the building to a suitable orientation [26].

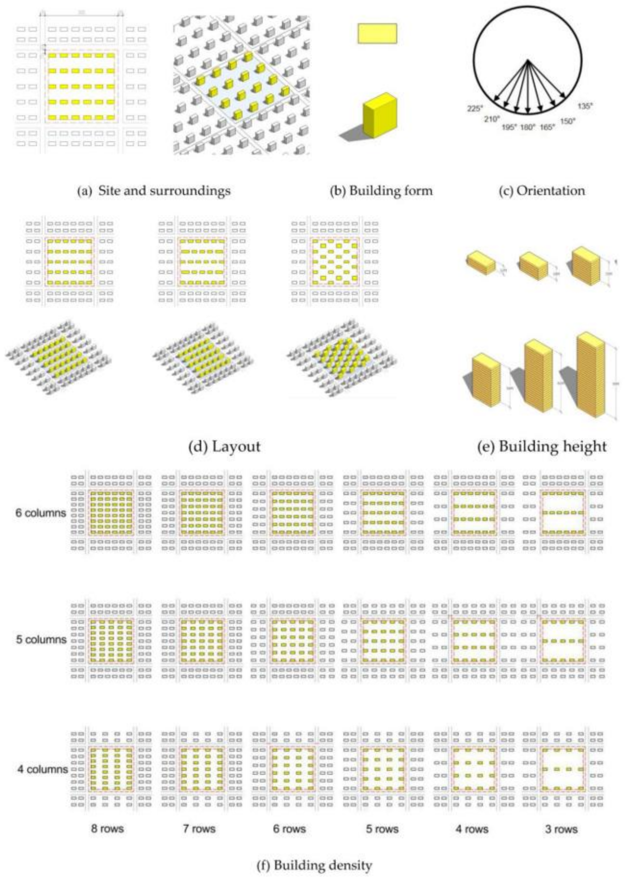

Figure 3: Urban scenarios of the research [26] *(Zhu et al., 2020, p.6)*

Khalid [27] specifies the proper urban morphology for sub-tropical regions with the four-case study area in Pakistan. The study analyses the climate-responsive passive design parameters to define the characteristic regional behavior such as ventilation strategies, thermal design of envelope, and architectural details of the vernacular buildings. The research has main results for the different climatic characteristic areas. The highland site has cold winter and warm summer. The primary materials are timber, stone, and brick. Using skylights, light ways, terraces, and courtyards are defined as the passive design strategies. Low land climate has hot summers and cool winters.

The basic material is brick. According to passive design strategies, there are thick walls, roof shadings, and porches. In this case, the facades have small windows with a specific traditional pattern. The coastal climate has a moderate temperature. The general construction material is mud and cement sand blocks. The ceilings are high to ensure cross ventilation, and there are wind catchers. The arid climate part has rock and stone as the primary construction material. There are ventilators, thatched roofs, traditional ponds, and wells as a passive design strategy. In four cases, the primary insulation material is glass wool [27].

Dallal and Visser [28] evaluate the climate-responsive design strategies in a hot-dry climate in Egypt by using a parametric tool. The evaluated urban forms are organized according to different passive strategies to improve outdoor comfort, also reduce energy consumption in the early design stage [28].

Table 1 shows the articles related to the impact of urban morphology on environmental control parameters. As a result, urban morphology has a strong correlation with environmental control parameters, which is based upon vernacular architecture as the adaptation of the climatic characteristic of the site. With the base of the climate, buildings in the urban block can impact differently, especially on wind behavior and solar integration. Hence, changes in the urban density, orientation, street width, geometry of the buildings, dimension of the buildings, and landscape design mainly affect the integration of passive systems, especially for the wind and solar radiation as the features of ventilation and daylight.

Table 1: Articles regarding to urban morphology and environmental control

No	*Authors*	*Year*	*Keywords*	*Main Features*	*Method*	*Tools*
[8]	Hassan et al.	2020	Outdoor air quality, Passive strategy, Urban morphology, PM10 dispersion, CFD simulation,	Environmental Control Urban Morphology	1-Selection of the case study parcel 2- Defining the prevailing wind direction 3-Validation of the simulation 4- Determination of 4 urban forms 5- Conducting CFD simulation	Ansys Fluent software (CFD analysis)
[21]	Fontenelle et al.	2015	2015	Environmental Control Urban Morphology	1- Defining the 2 urban morphology 2-Analyisng wind pattern of morphologies 3-Comparing the results	RANS k-ϵ turbulence model
[22]	Hang et al.	2009	City form Numerical simulation Urban morphology Wind conditions	Environmental Control Urban Morphology	1- Defining the 9 test cases 2- Conducting CFD simulation 3-Analysis of the results	CFD simulation
[23]	Sarrelde et al.	2015	London Neighborhood Renewable energy Solar potential Urban morphology	Environmental Control Urban Morphology	1- Generation of 5 urban forms based on 18 parameters 2- Analyzing solar potential 3- Discussion of the analyses	Python, ArcGIS, ArcMap, Area Solar Radiation tool, Autodesk Ecotect Analysis

No	*Authors*	*Year*	*Keywords*	*Main Features*	*Method*	*Tools*
[24]	Shi et al.	2021	Solar energy penetration, Capital costs, Urban form, Block typology, Energy-driven urban design	Environmental Control Urban Morphology	1- Collecting data from 6 dense areas 2- Creating architectural formulations 3-Creating 18 urban forms 4- Analyzing solar energy, and calculating capital cost of PV panels	Grasshopper-Urban Generator, ArcGIS, OpenStreetMap, DAYSIM, City Energy
[25]	Esch et al.	2012	Solar access, Solar exposure, Passive solar design, Street layout, Building geometry	Environmental Control Urban Morphology	1- Determination of street width, street direction, and building envelope scenarios about the Dutch urban forms 2- Calculation of solar access on 21st December 21st March, and 21 June 3- Calculation of heating demand and solar heat gain	TRNSYS
[26]	Zhu et al.	2020	High-density residential area, Ladybug Morphological parameters, Multiple linear	Environmental Control Urban Morphology	1- Choosing typical urban block in Shanghai 2-Calculation solar irradiation for 72 directions 3- Definition of 6 main criterias 4-Calculation of solar potential for the 1260 scenarios	Rhinoceros, Grasshopper (Ladybug) EnergyPlus
[27]	Asma Khalid	2020	Architectural morphology, Built environment, Housing, Passive design, Urban Vernacular	Environmental Control Urban Morphology	1- Specify the 4 climatic zones zones in Pakistan 2-Collecting the data of vernacular houses like plans, passive design issues and thermal comfort solutions and construction materials	Site observation

2.2 State of Art Related to The Impacts of Urban Morphology on Energy Performance

The fastness of the growing urban areas and making wrong decisions in urban planning regarding energy efficiency cause environmental problems and economic and social drawbacks by decreasing green areas, increasing dense settlements, and unfavorable thermal comfort conditions [15,19,29]. Therefore, urban scale parameters cannot be considered separately from building energy performance [30].

Globally, with the impact of the growing rate of urbanization, cities are responsible for almost 75% of primary energy use and nearly 65% of greenhouse emissions [10,15,24]. For over 30 years, final energy consumption related to the urban areas increased by at least 20% [31]. Hence, urban sustainability focuses on building cities that minimize the use of land and energy consumption due to the possibility of dense future cities. However, the energy performance of dense urban areas still needs to be questioned [32]. Recently, the term "energy-conscious morphological layout" was mentioned as prioritizing assessing the energy consumption of the urban form to provide a massive saving at the urban level [14].

2.2.1 Temperate Climates

Energy use in urban areas has turned a vital interest worldwide by correlating with greenhouse gas emissions [33]. In the case study of Agua Branca in Sao Paulo, Brazil, Marins [33] analyses the impact of energy efficiency potential and emissions on an urban scale. In France, buildings are responsible for consuming half of the final energy, which is calculated as more pollutant than transportation and industry [31].

De Lemos Martins et al. [31] aim to identify urban design factors regarding buildings' energy demand and the solar energy potential in Toulouse, France, which has a temperate climate. There are three case studies to represent the typical French urban archetypes. Belfort represents the compact city block with continuous buildings in a closed urban city block. Castors refer to pavilion city as a semi-continuous urban form. Hers is a slab city with continuous pavilions as an open city block. They evaluate the existing urban typologies regarding four main criteria as an urban block, building, envelope, and energy budge.

Figure 4 explains the urban archetype parameters. Urban block evaluation indicates floor area ratio, plot ratio, shape factor, courtyard/patio aspect ratio, street width, and building height. Building evaluation concerns roof surface, orientation, height, width, length, and solar protection device. Envelope measures are wall and glazing U value, glazing ratio, and façade orientation. The energy budge consists of heating, cooling demand, and solar potential on the roof. CitySim software is used to simulate the heating and cooling demand of buildings and their solar energy potential at the urban district scale. The software allows the simulation of buildings according to thermal needs, daylighting, and solar energy.

The result of the study shows that traditional urban compact blocks in Belfort positively impact the heating demand of buildings for approximately 50%. However, the building and envelope factors have more influence by over 60% for pavilions and slabs urban blocks like Castors and Hers, respectively [31].

Urban Archetypes *Toulouse Urban Area* *43.617 43° 37'N | 1.450 1° 27'E*		Continuous buildings into closed city block **« Compact city »** (Belfort)	Semi-continuous pavilions **« Pavilion city »** (Castors)	Continous pavilions into open city block **« Slab city »** (Hers)
Typo-morphological factors by scale of analysis				
URBAN BLOCK	Floor Area Ratio	3,2	0,35	0,6
	Plot Ratio	0,75	0,17	0,2
	Shape Factor	0,3	0,53	6
	Courtyard/Patio aspect ratio	3,5	-	-
	Aspect ratio	2,1	0,6	1,0
	Street Width (m)	8	10	10
	SDV Height (m)	4,05	2	2
BUILDING	Roof surface (m^2)	528	135	345
	Orientation	Nord-est - Sud-ouest	Nord-est - Sud-ouest	Est-Ouest
	Height (m)	18	6	9
	Building Width	8	16	45
	Building Length	12	8	8
	Solar protection device	non	non	non
ENVELOPPE	Albedo	0,3	0,2	0,4
	Ground Albedo	0,2	0,25	0,25
	Wall U-value	1,3	0,9	0,9
	Glazing ratio	0,4	0,1	0,2
	Glazing G-value	0,4	0,6	0,6
	Glazing U-value	1,8	1,1	1,1
	Façade orientation	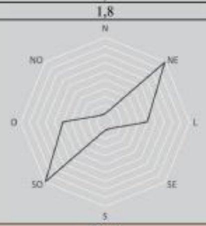		
ENERGY BUDGE	Heating demand (kWh/m^3.an)	**38,8**	**32**	**25,8**
	Cooling demand (kWh/m^3.an)	**14,1**	**2,5**	**10,1**
	Solar potential on roof (kWh/m^2.an)	**1100**	**900**	**1211**

Figure 4: Urban archetype features of the study [31] *(*De Lemos Martins et al., *2019, p.365)*

The research was conducted in temperate-dry climates by Kalaycıoğlu and Yılmaz [6]. They proposed to analyze achieving nearly zero energy levels by considering cost-optimal levels in the district scale by implementing the energy efficiency measures for the case study area in Eskişehir, Turkey. Therefore, the case district area with 42 buildings is evaluated according to climate properties, building type and number of the buildings, building locations, their distances, their shading patterns, district system configuration.

Energy-related measures include the three alternatives of the insulation layer thickness both for roof and wall, three glass types according to U-Values, three options for lighting system improvement, two kinds of infiltration rate, three types of heating, and two types of cooling, and two alternatives of renewable energy integration. Renewable energy alternatives include integrating solar panels, photovoltaic panels, and both. By combining single measures, 59 scenarios were analyzed using Design Builder and Energy Plus. Also, district-level energy calculations are performed by the EnergyPro simulation program. The global cost is calculated according to EN 15459:2007 Standard, and the cost-optimal level is decided according to Energy Performance Building Directive (2010). The result of the study is that to achieve nearly zero energy levels both in buildings and districts, usage of renewable energy is inevitable. Thermal solar and PV panels are used in this case. On the contrary, there can be a limitation for renewable energy integration at the building level due to the high investment costs [6].

İstanbul has a temperate-humid climate in Turkey. Uçlar and Buldurur [29] state that there is a lack of examination on an existing settlement to examine the relationship between urban form and building energy performance. They focus on analyzing different urban textures in İstanbul by considering heating energy consumption [29].

Mangan et al. [9] study the impact of different urban configurations on building energy and cost efficiency in İstanbul for residential buildings. For the examination of 120 urban form alternatives are generated based on urban and building design parameters. The effect of 120 urban alternatives on building performance was calculated on final energy consumption and energy-related CO2 emissions. Final energy consumption includes heating, cooling, lighting, total energy consumption, also life cycle costs. Design Builder and Energy Plus software conduct the energy analyses. A special formulation is used to calculate annual carbon dioxide emissions. To complete the cost analysis, the life cycle cost for 30 years is calculated by the net present value formulation.

To obtain the climatic data of İstanbul Meteonorm 7.0 is used to include outside air temperature, outside air humidity, solar radiation, and wind. The data from the Turkish Statistical Institute indicates a schedule of building usage, occupant density, occupant activity level, and occupant clotting type. The Housing Development Association (TOKI) was reviewed to generate the typical Turkish residential building model to determine plan types, floor area, building heights, and context urban geometries. TS 825 standard is used to identify the proper layering system of the construction for the opaque and transparent components in İstanbul. With the basis of these, alternatives of plan types, number of floors, h/w ratio, urban typologies, and orientations were combined. The urban scenario parameters are shown in Figure 5. Rectangular and square are the plan types of alternatives. There are four-floor varieties 3,5,10, and 15. For building height and street width ratio (h/w), there are three alternatives 0.5, 1.0, and 2.0. Pavilion and slab are the urban typology alternatives. There are four orientation alternatives 0°, 45°, 90°, and 135°.

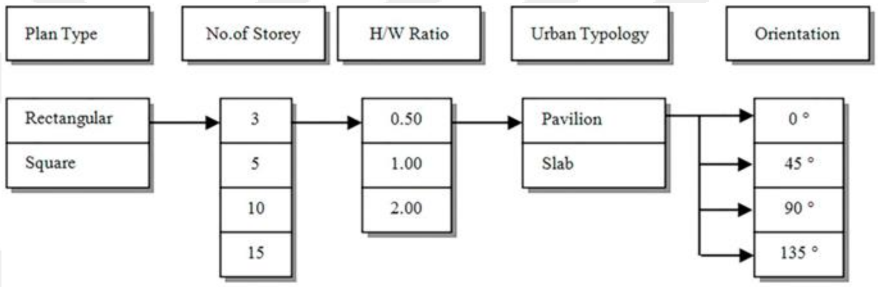

Figure 5: Urban form variables of [9] *(Mangan et al., 2021, p.6)*

The main results of the research are that building height and h/w ratio play a more significant role than orientation in the energy and cost performance regarding three urban forms. According to plan type and urban typology, the total energy consumption of rectangular urban alternatives results from more than square pavilions by 8% and 15%, respectively. The CO2 emission results decreased by 13% for rectangular pavilions and 17% for square pavilions. Regarding the impact of urban typology on building energy and cost calculations, both pavilions achieved a 9% decrease in total energy consumption and a 7% decrease in CO2 emissions [9].

To optimize urban morphology relating to energy systems in Athens, Greece; Perera et al. [34] conducted a study based on fifteen influencing parameters for twenty distinct neighborhoods. The urban morphology systems are displayed in Figure 6.

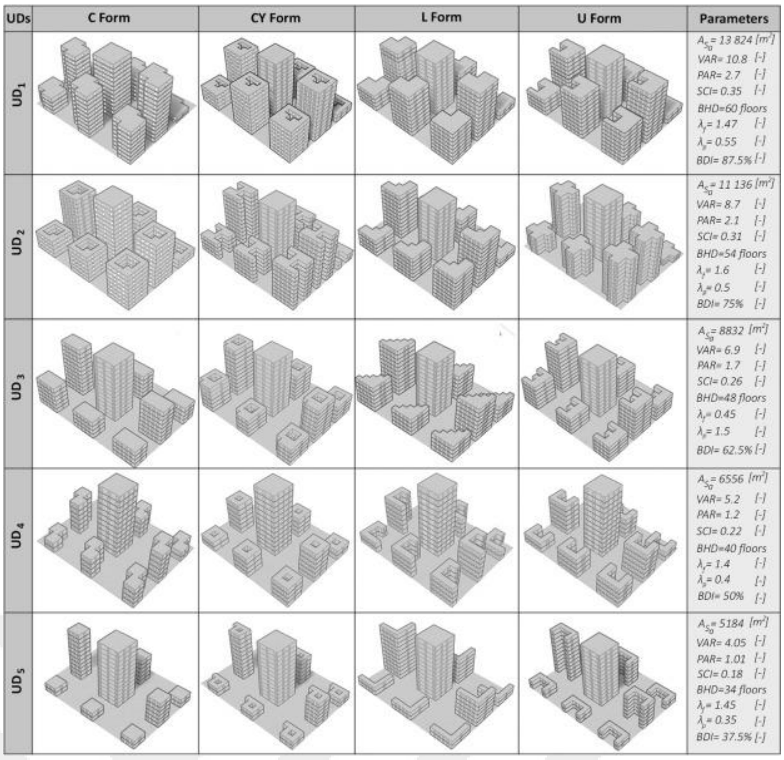

Figure 6: District morphologies of the study [34] *(Perera et al., 2021, p.7)*

The urban alternatives are generated by Building Modular Cell. The fifteen urban parameters include two main categories as urban density and urban form. Urban density-related parameters are volume-to-air ratio, plot-to-area ratio, site coverage index, building density index, urban plan area density, frontal area density, relative compactness, building materials, and occupant density. The urban form-driven parameters are building layout, height distribution, neighborhood size, building function, urban street pattern, and urban canopy pattern. The climate data includes extreme warm and cold weather databases, mainly focusing on three time periods to represent future climate variations to assess climate resilience. The three type periods are 2010 to 2039, 2040 to 2069, and 2070 to 2099. The Global Climate model is used to simulate future climate. The microclimate around buildings is simulated by Rossby Centre RCM for a maximum of 30 years [34].

The result of the study shows a strong correlation between urban form and building energy performance since proper urban morphology based on climatic data can decrease building energy consumption and cooling loads by at least 10% [8,34]. An appropriate urban form can increase ventilation by more than 15% [8,34].

The study by Salvati et al. [35] is applied to 10 case studies in Rome, Italy, and Antofagasta, Chile to calculate the air temperature, wind speed, solar access, and surface temperature modifications for an urban context by using the tool TRNSYS. Also, the calculations of urban air temperature and urban surface temperature are conducted by Urban Weather Generator. The urban alternatives are evaluated according to the urban parameters of roughness length urbanized terrain, site coverage ratio, a facade to site ratio, average building height, and the ratio of building length to street width. Mediterranean climates need both heating and cooling like Rome. Hence, the local urban heat island intensity and the shadow impact of surrounding buildings share the highest energy impact. Also, for the low-density urban textures, the urban radiant environment and decrease in the wind speed cause a direct increase in cooling demand. In Antofagasta, cooling energy is necessary. Therefore, urban shadows have an enormous impact on the cooling demand of buildings especially the urban blocks with high buildings. The common result of both cases is that site coverage ratio and building height have a prior impact on building energy performance [35].

2.2.2 Hot-Dry Climates

Dubai, a desert climate, needs to enhance outdoor thermal performance to minimize cooling energy consumption [36]. Shareef [36] analyzes to find an optimized urban block typology to reduce the cooling load in Dubai. The existing urban block is chosen as a case study area which includes 24 buildings with five stories. This means the case study area has a regular urban form with the same heights. The variables are chosen to evaluate the relationship between urban morphology and the cooling load, such as building height diversity and orientation. Two main group urban configurations are organized as height diversity along the short axis and height diversity along the long axis. It is represented in Figure 7.

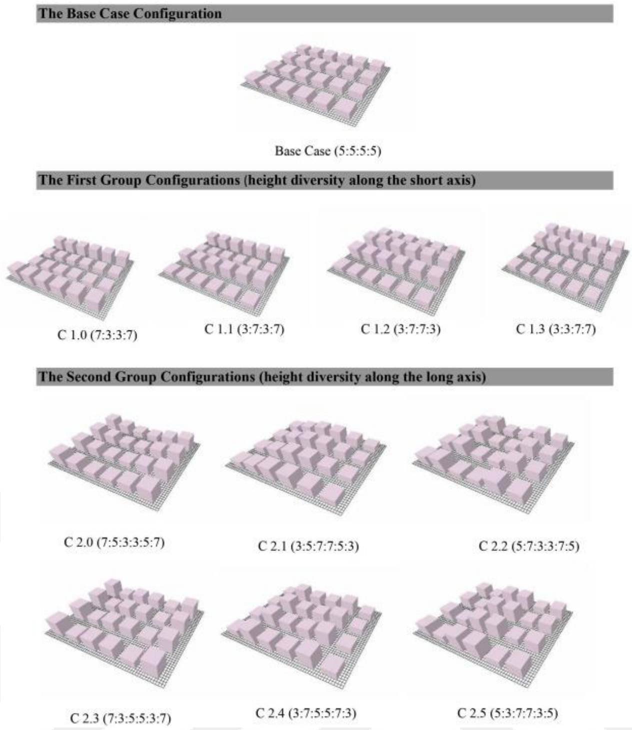

Figure 7: Urban scenarios of [36] *(*Shareef, *2021, p.6)*

The first configuration had 4 alternatives while the second group has six alternatives. ENVI-Met 4.4.3 simulation software is used to simulate the outdoor microclimate parameters like air temperature, wind speed, and relative humidity and to calculate the indoor energy consumption of the urban block. IES-VE simulation software is used to calculate specifically the cooling energy consumption.

The results show that orientation is the most influential variable for the reduction in cooling load thanks to controlling building solar gain and solar radiation. Concerning the orientation, north-south-oriented urban forms provide a 13% reduction for the direct solar gain. This means the cooling load reduction by 6.4% between these two orientations. Specifically, C 2.1 (3:5:7:7:5:3) configuration is the best configuration by having the lowest solar gain and highest shading provided in all orientations. Furthermore, reducing outdoor air temperature and solar gain by designing the urban block with different building heights results in a cooling load reduction of 4.6% compared to the base case. Therefore, the C 1.2 (3:7:7:3) configuration recorded the best performance in the north-south orientation compared to the base case in the northeast-southwest orientation. The study proves the implementation of irregular urban configuration on building energy performance in hot climates regarding proper orientation [36].

2.2.3 Cold Climates

The research about urban morphology's relation with building energy performance and cost-efficiency was conducted in a severely cold region city, Harbin since Leng et al. [37] stated that there is little research on urban morphology-related heating energy consumption for cold climates. Hence, the study aims to examine 73 office buildings with seven urban morphological factors on heating energy consumption. The factors are building site cover, floor area ratio, building height, road height-width ratio, total wall surface area, external influence rate, and lower green space ratio. By combining the parameters, 54 urban forms are analyzed using OpenStudio, the interface of EnergyPlus.

The results show that regarding the reduction of heating energy consumption, road network density has no relation with urban morphology, while the other six parameters have a strong relationship. Increasing the building site coverage, floor area ratio and building height total wall surface area positively impacts heating energy performance. However, increasing the green space ratio leads to a lower heating energy performance. The floor area ratio is the most critical factor for saving heating energy up to 10.820 kWh/m2/y for cold climates [37].

2.2.4 Humid-Subtropical Climates

The urbanization rate is also rapidly increasing in China and the energy consumption, respectively [38]. Wang and Li [30] aim to evaluate the impact of urban form on energy consumption by using Data Envelope Analysis for five central districts in Shanghai. These five districts examine building area, energy use, floor area ratio, and tax ratio of the modern service sector [30]. Wang et al. [38] conducted research based on achieving energy-efficient urban design. The optimization goals are having maximum solar energy utilization, solar lighting on the first floor, and minimum building energy demand. The 42 urban blocks with 539 residential buildings in Jianhu, China. The morphological variables of the study are orientation, floor area ratio, building density, the average number of floors, scattered degree, height to width from four directions, open space ratio, shape coefficient, and perimeter-to-area ratio. The methodology of the study is shown in Figure 8.

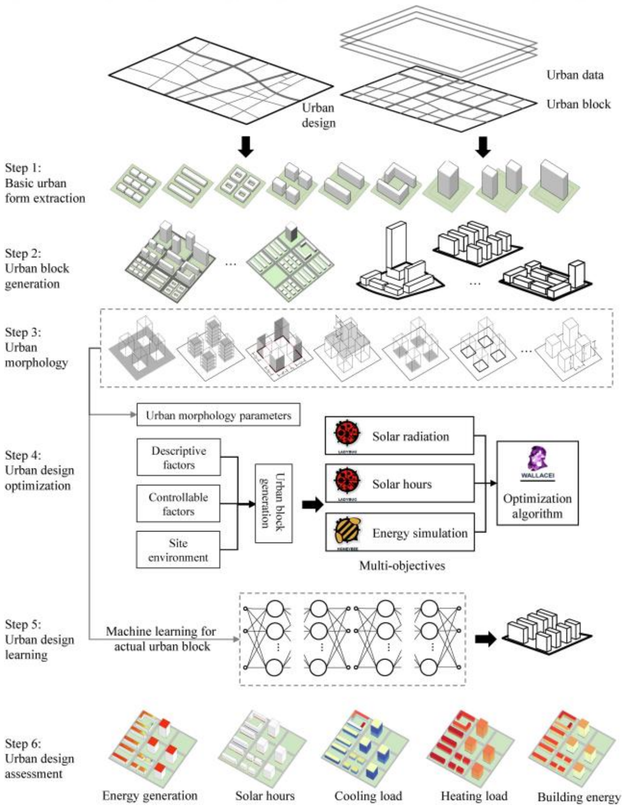

Figure 8: Methodology diagram of the article [38] *(Wang et al., 2021, p.2019)*

In the methodology, generated urban morphologies are optimized for having maximum energy generation of PV, maximum solar hours for first floors of buildings, and minimum building energy demand by using Rhinoceros, Grasshopper. The process conducted using the Wallacei, a plug-in tool in Ladybug. The next step, the application of a machine-learning algorithm includes an urban energy modeling for providing energy-efficient urban design by calculating energy demand and renewable energy potential. The model integrates the long-short term memory network algorithm to expose energy-saving opportunities for an existing urban block. The result of the study is that long short-term memory can achieve the best accuracy of 1.21% for energy generation of photovoltaic and 1.37% for total building energy use [38].

Cody et al. [39] study the shading impact of three different urban morphologies for four different climatic regions on the heating and cooling effect of buildings by using the IES Virtual Environment tool for energy analysis and dynamic thermal performance simulations of buildings. The four representative countries are Helsinki, Finland; Dublin, Ireland; Vienna, Austria; and Athens, Greece. The three urban alternatives include irregular building distribution, block form, and courtyard form in one block. The choice of typology matters shows the least results in Vienna, but the chosen typologies show 40 percent higher results in Helsinki [39].

Table 2 shows the articles about urban morphology and energy performance. Consequently, related to the growth rate of urbanization, the impact of the building sector greatly influences energy use in the world. Urban texture in different climates affects both potential and drawbacks. The main parameters that impact energy use can be summarized as building plan types, the height of the building, building height and street width ratio, the orientation of buildings, also opaque and transparent components.

Table 2: Urban morphology and energy performance

No	*Authors*	*Year*	*Keywords*	*Main Features*	*Method*	*Tools*
[6]	Kalaycıpğlu and Yılmaz	2017	EPBD Costoptimal methodology, District energy systems Nearly zero-energy	Energy Performance Urban Morphology	1-Evaluation of 42 buildings 2-Definition of the energy performance measures 3-Calculation of energy performance and global costs	Design Builder EnergyPlus EnergyPro
[9]	Mangan et al.	2021	Urban form, Residential building performance, Energy, Cost efficiency, etc.	Energy Performance Urban Morphology	1-Definition of 120 urban alternatives 2- Calculation of energy and cost 3-Usage of LCC tool for cost analysis 4-Evaluation of results	Design Builder EnergyPlus Meteonorm 7.0
[30]	Wang and Li	2017	Energy efficiency Urban form Shanghai city	Energy Performance Urban Morphology	1-Definition of 120 urban alternatives 2- Calculation of energy and cost 3-Usage of LCC tool for cost analysis 4-Evaluation of results	Design Builder EnergyPlus Meteonorm 7.0
[31]	De Lemos et al.	2019	Building energy multi-scale modeling Sensitivity analysis Urban form Temperate climate	Energy Performance Urban Morphology	1- Choosing 3 French urban archetypes 2- Assessing the urban types regarding the heating and cooling demand of buildings and their solar energy potential 4- Discussion of the results	CitySim
[34]	Perera et al.	2021	Energy systems Interconnected infrastructure Sustainable cities Urban form	Energy Performance Urban Morphology	1-Generating 20 urban morphologies 2-Generation of future weather datasets 3- Conducting energy simulations 4-Assessing renewable energy potential 5-Collecting techno-economic data	Global Climate Model, Rossby Center RCM Building Modular Cell

No	*Authors*	*Year*	*Keywords*	*Main Features*	*Method*	*Tools*
[35]	Salvati et al.	2020	Building performance simulation, Urban energy Urban heat island, Urban morphology	Energy Performance Urban Morphology	1- Definition of 10 urban forms 2-Evaluation of site coverage, facade to site ratio etc. 3-Simplifying the urban model on solar and wind pattern 4-Calculation of urban air temperature and urban surface temperature	TRNSYS Urban Weather Generator
[36]	Sundus Shareef	2021	Urban morphology Microclimate, Energy consumption,Cooling load, IES-VE Dubai/ UAE	Energy Performance Urban Morphology	1-Designing an urban block with 24 buildings 2- Defining the variables 3- Analyzing outdoor and indoor thermal performance 4-Calculation of cooling load	Envi-met, IES-VE
[37]	Leng et al.	2020	Energy, Office, Cold region Thermal performance,	Energy Performance Urban Morphology	1- Data collection on existing buildings 2- Definition 7 variables 3- Conducting energy simulations 4- Discussion of the results	Open Studio EnegyPlus
[38]	Wang et al.	2017	Low-energy, Solar energy utilization, Urban building energy model, Urban morphology etc.	Energy Performance Urban Morphology	1-Generation of urban forms 2-Optimizing the solar radiation, solar hour, and energy by Wallagei algorithm 3-Application of a machine learning algorithm with the predictive technique of the long short-term memory	Rhinoceros, Grasshopper (Ladybug, Honeybee, Wallagai)
[39]	Cody et al.	2018	Operational energy Urban fabric etc.	Energy Performance Urban Morphology	1- Choosing 3 typologies 2- Calculation of shading impacts and heating and cooling demand	IES Virtual Environment

2.3 State of Art Related to The Relationship Between Environmental Control and Energy Performance

Implementing environmental control parameters decreases energy consumption and enhances a sustainable economy since integrating proper daylight and natural ventilation reduces the need for mechanical heating and cooling by decreasing active systems' load, like air conditioning [19,40]. According to research in Libya, which has a hot climate, energy consumption in buildings is responsible for approximately 31% of total energy consumption since contemporary buildings mainly adopt air conditioning systems to provide a comfortable area [41]. Understanding the buildings' dynamics based on the current climatic condition of the place and designing the urban geometry according to the passive systems to overcome the negative impacts of climates can be guided to decrease excessive energy consumption. Hence, cities of tomorrow must provide and optimize the existing infrastructure to minimize the waste of energy while maximizing the benefits of natural resources [42].

2.3.1 Daylight Availability

Trepci et al. [19] evaluate 54 alternatives on the effects of urban context height, distance, and orientation on cooling load in a hot climate by using Rhinoceros software with the Honeybee plug-in of Grasshopper for shading effect and daylighting simulation and EnergyPlus software for analyzing the energy performance. The alternatives include two building types: residential and commercial. Three types of sizes are low-rise, mid-rise, and high-rise. Three alternatives of context height are low, medium, and high. Low context height is half of the existing height. Medium context height is the same height as the current situation. High context height refers to the double measurement of the existing situation. The context distance alternatives are small, medium, and large. Small context distance is the minimum allowed setback distance as 4.57 m for residential buildings and 6.1 m for commercial buildings. The buildings higher than 10.97 m have an extra distance as the addition of half the measurement of the building's height. Also, there are two types of orientation. 0 refers to the current rotation in the north-south direction; 90 gives the rotation to the east-west direction.

The research results show that the combined effects of urban context with different heights, distances, and orientations can significantly reduce cooling demand by up to 26% for total cooling loads and 24% for peak cooling loads, thanks to the dense and compact organization. The urban form related to passive design strategies can reduce the energy intensity of building systems [19].

Jayaweera et al. [43] evaluate the shading impact of the urban context in terms of daylight and annual energy savings, especially for yearly cooling energy, annual daytime lighting energy, and spatial daylight autonomy. Seventy-five urban typologies were generated in a tropical climate for high-residential buildings using parametric modeling. For the study, Rhinoceros software with Grasshopper was used for the Diva4 and Archsim plug-ins. They estimate the simulation models' daylight availability and energy use, respectively. Therefore, RADIANCE and Daysim work within DIVA4 for daylighting analysis, while Archsim is based on EnergyPlus. The main results are that the optimum solar access is defined for a high-rise residential building, achieving 75 spatial daylight autonomy by annual energy savings of 28%-36% in the east-west and 8%-12% in the north-south directions. All case studies have yearly energy savings of 26%-31% and 9%-15%, respectively, in the east-west and the north-south directions [43].

Loeffler et al. [12] aim to identify the vital parameters of urban planning with energy demand and energy generation of buildings regarding passive design measures in

Vienna, Austria, which has a temperate humid climate. The purpose case study area is to evaluate the impact on heating and cooling energy demand, overheating potential, daylight availability, and solar potential. The five influencing factors are the orientation of buildings, window area, thermal insulation of building envelope, solar heat gain coefficient of the transparent building parts, and the site coverage variations as compactness. The orientation of the building has three variations as 0°,45°, and 90°. Window area has two variations, with 20% and 40% for north, west, south, and east facades. The thermal insulation factor has three alternatives for walls, windows, roofs, and ground floors. Moreover, the transparent building parts' solar heat gain coefficient has three variations: 0.6, 0.48, and 0.30. The site coverage percentage has three alternatives 40, 30, and 8.

After the combinations of the variations, 243 scenarios were examined using Rhinoceros, Grasshopper parametric tool. The overheating potential, daylight availability, and solar potential are evaluated by using Ladybug, Honeybee, and Radiance. EnergyPlus calculate heating and cooling energy demand. The study results as the high compactness of the buildings to have lower the heating energy demand is decreased by improving the thermal insulation of the building envelope. Moderate compactness can reduce the energy demand for cooling and lighting and increase the solar potential of buildings [12].

Morello et al. [44] evaluate the impact of urban geometry on the total energy balance thanks to the proper use of natural daylight for the case study settlement in Milan, Italy. The energy performance of existing urban layouts is calculated according to European Standards. Several schematic urban layouts are examined related to urban solar admittance. Solar admittance is assessed to the percentage of shadowed areas on the urban facade related to the solar potential [44].

Camporeale and Mercader-Moyano [45] analyze the reduction of primary energy consumption for high-rise housing typologies by optimizing their shapes by considering passive strategies. The research focuses on urban forms from the four cities in a temperate climate. These cities are Resistencia and Buenos Aires in Argentina and Seville and Madrid in Spain. In every case, an urban block is chosen. Octopus generic algorithm is used by Rhinoceros 6, Grasshopper, and EnergyPlus for the energy performance simulation. The window-to-wall ratio inputs, plot limits, orientation, climate, and envelope thermophysical data are indicated as constant; floor area, width, length, and height data are the variables. Nearly 15 alternatives are evaluated using minimum annual primary energy, maximum passive volume ratio, and roof-best-oriented surfaces. The result shows that the complex urban design evaluation in the early stages can balance energy savings and reduction of greenhouse gas emissions [45].

Strømann-Andersen and Sattrup [17] aim to highlight the effects of urban geometry on building energy consumption in Copenhagen. The main variables are density and orientation to investigate the impact of solar radiation distribution and daylight on the total energy consumption for building heating, cooling, and artificial lighting [12,17,31]. In the research, urban types have three levels. Types of the urban canyon are street, square, courtyard, and garden. There are two building types housing and office. According to the building types, there are two types of daily and weekly occupancy use patterns. The variables are decided by evaluating Copenhagen's typical urban typologies, street width, building height-street width ratio, and plot ratio.

The radiation calculations are conducted by Autodesk Ecotect Analysis 2010. The RADIANCE-based simulation environment, DAYSIM, is used to simulate indoor illuminance. IES-Virtual Environment 6.0.2 is used to calculate the energy calculations. ApacheSim/RADIANCE tool is a fully integrated thermal and daylight simulation that provides a detailed electrical energy consumption output for lighting, mechanical ventilation, heating load, cooling load, and indoor operative temperature [17]. The research results prove that the geometry of urban canyons, especially the building height-street with ratio (aspect ratio), inevitably impacts total energy consumption by up to 30% for offices and 19% for residential buildings [12,15,17,31].

2.3.2 Natural Ventilation

Jurelionis and Bouris [46] stated that a strong relationship exists between external air movement and the morphological parameters of buildings and surroundings, like building height and street cavity ratios. The computational fluid dynamics method is used with two wind directions for three chosen city models to calculate the surface pressure distributions on building surfaces. The three real urban morphologies are determined from Zürich, Switzerland; Kaunas, Lithuania; and Athens, Greece. They are displayed in Figure 9. Pressure differences and air change rates relate to the heating load required to overcome the heat losses due to air infiltration. In examining three urban textures, the simulations result in a difference of 41% percent in air change rates and heat losses caused by air infiltration. The sideward wind direction for the urban layout caused higher air change rates and heat losses [46].

Cardinale et al. [47] point out the impact of natural ventilation on cooling capacity in the Mediterranean region by focusing on traditional materials and techniques. The three main orientations are decided as southwest, south, and southeast to provide better solar radiation and wind integration. The calculations are conducted by AIOLOS software. The result of the study shows a critical correlation between natural ventilation potential for the proper direction of the form to reduce cooling load, especially in summer. Furthermore, using a material with appropriate thermal insulation, high thermal inertia for diminishing the daily temperature differences, and a combination of a solar control unit is the most valuable parameters for the research as a passive cooling technique [47].

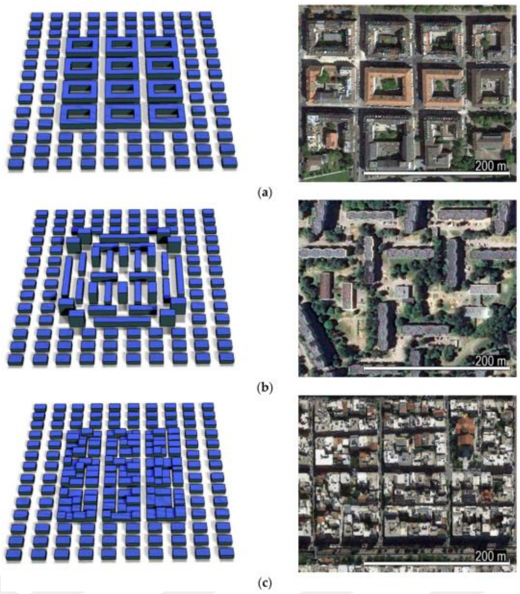

Figure 9: Case studies of the article [46] *(Jurelionis and Bouris, 2016, p.3)*

Javanroodi et al. [48] investigate the impact of urban morphology on cooling load reduction by enhancing natural ventilation for the high-rise buildings in Tehran, Iran. The site has a semi-arid climate. Three urban parameters are decided as urban density types, building forms, urban patterns. There are five urban density alternatives as proposed density by codes of Tehran Municipality (60%), maximum density (85.6%), minimum density (35.8%), mean density (70.24%), middle density (50%). Building forms are “L” forms, “U” forms, cube forms, and courtyard forms. There are four configurations of the urban pattern. P01 means no street between buildings. P02 has a 4 m width street (H/W: 12). P03 has a 6 m width street (H/W: 8). P04 means 8 m width street (H/W: 6). By combining the parameters 1600 urban morphologies are arranged by using the Building Modular Cells tool.

The wind flow is simulated by Autodesk Inventor for Autodesk CFD analysis. The calculation of cooling load is conducted by Rhinoceros, Grasshopper. The Archsim plug-in is used coupled with EnergyPlus. 16 urban configurations are represented as having the lowest cooling load and highest natural ventilation potential. The result of the research is that the proper urban morphology can decrease the cooling load by 10% and increase the potential of natural ventilation by 15%, compared to the current condition [48].

2.3.3 Daylight Availability and Proper Natural Ventilation

Gros et al. [49] examine a new district in La Rochelle, France, called Atlantech by comparing two building densities on the impact of solar irradiance, wind airflows, building indoor temperatures, and energy demand. The two scenarios are based on floor area ratios of 1.0 and 1.5. The aim is to achieve a zero-carbon district. For the analysis, EnviBatE and SOLENE-Microclimate simulation is used. For the airflow model, the Computational Fluid Dynamic model is used with the code of SATURNE. The tools evaluate the building energy consumption at a district scale, including solar irradiance and sky luminance. The result of the research is that if the wind velocity decreases up to 80% for the 1.5-floor area ratio, the effect of solar radiation on nearby buildings reduces by 7% [49]. Moreover, *Baker and Steemers (2000)* proved that renovation in Carlo Ratti's settlement form causes a change in energy consumption by over 10% [15,50].

The research proved a correlation between building energy performance and passive energy systems, especially for wind and solar behavior, with the impact of urban morphology. Wind patterns can affect the natural ventilation potential of buildings to optimize cooling load. At the same time, the solar behavior in the urban form can be related to the daylight potential of building for improving heating load on the urban scale. Each urban texture parameter plays a crucial role in energy use and environmental control based on the characteristic of climate. Table 3 shows the articles and some critical information.

Table 3: Relationship between environmental control integration and energy performance

No	*Authors*	*Year*	*Keywords*	*Main Features*	*Method*	*Tools*
[12]	Loeffler	2021	Energy efficiency, Energy-efficient urban planning, Passive design measures, Sustainable spatial planning, etc.	Environmental Control, Energy Performance Urban Morphology	1- Determination of variables about orientation, window area, envelope materials, the orientation of the buildings, and urban compactness. 2- Choosing a case study area 3- Examining the alternatives with 243 scenarios	EnergyPlus, Grasshopper (Radiance)
[17]	Stroman n and Sattrup	2011	Urban density, Energy use, Daylight, Solar radiation, Integrated design	Environmental Control, Energy Performance Urban Morphology	1- Analyzing the existing urban pattern 2- Calculation of urban canyon radiative environment and daylight 3-Calculation of energy consumption	ECOTECT, Radiance DaySim, IES-VE, ApacheSim
[19]	Trepci et al.	2021	Passive design, Urban context, Energy efficiency, Cooling, Hot	Environmental Control, Energy Performance Urban Morphology	1- Selection 54 urban alternatives 2- Designing experimental models 3- Analyzing of shading, daylight 4- Analysis of energy performance	Grasshopper (Honeybee) EnergyPlus
[43]	Jayawee ra et al.	2021	Solar access, Urban tropics, Parametric modeling, Daylight, Cooling energy	Environmental Control, Energy Performance Urban Morphology	1- Determination of high-rise urban block 2- Optimization of solar access 3- Analyzing daylight	EnergyPlus, Grasshopper (ArchSim, Diva4, Radience)
[44]	Morello et al.	2009	Daylighting, Digital elevation models, Sustainable urban design, etc.	Environmental Control, Energy Performance Urban Morphology	1-Choosing a case urban block in Italy 2- Identify alternatives 3- Evaluation of the solar potential 4-Calculation of energy consumption according to European Standards	Formulation based on European Standards

No	*Authors*	*Year*	*Keywords*	*Main Features*	*Method*	*Tools*
[45]	Campore ale and Moyano	2019	Building shape optimization, Energy consumption, etc.	Environmental Control, Energy Performance Urban Morphology	1-Definition of alternatives and variables (Floor area, width, length, and height) 2- Modelling the case studies 3- Generation of the different urban alternatives	EnergyPlus , Grasshopper (Octopus)
[46]	Jurelioni s and Bouris	2016	Air infiltration, Computational fluid dynamics (CFD) predictions, Energy performance of buildings, etc.	Environmental Control, Energy Performance Urban Morphology	1- Choosing the urban morphologies from Zürich, Switzerland; Kaunas, Lithuania; and Athens, Greece 2- Simulating air speed and building surface pressure distribution 3-Calculation of energy performance	Computational fluid dynamics (CFD)
[47]	Cardinel li et al.	2003	Energy saving Natural ventilation Thermal comfort	Environmental Control, Energy Performance Urban Morphology	1- Collecting data on case study area 2- Evaluating the main sun and wind direction	AIOLOS
[48]	Javanro odi	2018	Cooling load High-rise buildings Hot-arid climate Urban energy Urban morphology Ventilation	Environmental Control, Energy Performance Urban Morphology	1- Generation of 1600 urban alternatives 2- Validating the simulation 3- Calculation of the cooling load and wind flow 4-Choosing 16 urban forms having the lowest cooling load,high ventilation rate	Autodesk Inventor - Autodesk CFD,Grasshop per (Archsim) EnergyPlus
[49]	Gros et al.	2016	Building energy simulation, District design, Urban heat island, Urban microclimate	Environmental Control, Energy Performance Urban Morphology	1- Choosing the case area 2- Generating 3 urban alternatives 3- Analyzing solar radiance and air flow 4- Calculating the energy load	EnviBatE, SOLENE-Microclimate, SATURNE (CFD)

2.4 State of Art Related to The Impacts of Urban/District Morphology on Comfort Level

With the impact of foreseen climate change, the concept of urban climate design shares the significance of mitigating the adverse atmospheric effect of urban growth since, to tackle the current problems, the form and function of cities are rediscussed by relating urban heat islands, energy, and unpleased urban conditions for people both for indoor and outdoor of the houses [51,52]. The series of parameters of a city can depend on physiological, psychological, meteorological, and morphological factors since the impact of urban climate is correlated with human health and the quality of life through the sensation of thermal comfort [53]. Thus, from season to season, person to person, the needs, and preferences for achieving thermal comfort level can differ among the parameters like activity level, clothing, body shape, and psychological aspects [25].

Lau et al. [54] stated that most studies about outdoor thermal comfort mentioned pedestrian thermal comfort as static; however, in high-density cities, urban geometry has an important influence on dynamic changes in pedestrian thermal comfort throughout the walking route. Also, according to the meteorological variables, the study shows that the spatial pattern of thermal sensation impacts the pedestrians' short-term thermal experience even in 2-3 min. The research findings contribute to the influence of urban design to mitigate the thermal discomfort of pedestrians and improve the pedestrian environment in high-density cities properly [54].

Mouada et al. [55] highlight the relationship between urban morphology and walking behavior to provide a walkable environment for the hot, dry city of Sidi Okba, Algeria. The research finding proves that urban morphology strongly links outdoor thermal conditions and potential pedestrians for short distances. The critical parameters of urban form to ensure a comfortable environment are building density, height-street width ratio, and tree density [55].

2.4.1 Hot Climates

Othman and Alshboul [56] aim to investigate the role of urban morphology on urban microclimate and its impact on outdoor comfort. Four different urban alternatives are organized for the hot climatic region of Al-Sharq City regarding courtyard configurations. To evaluate the urban alternatives, Envi-met and Rayman simulation tools are used. The urban forms are compared based on the air temperature, wind speed, mean radiant temperature, humidity, and physiologically equivalent temperature for outdoor thermal comfort. The results demonstrate that the dominant variables for outdoor comfort are wind speed and mean radiant temperature. Mean radiant temperature has a strong correlation with shade situation. The mean radiant temperature can vary from 20C to 30C for shaded areas and the ones exposed to sunlight. However, air temperature behavior is a weak indicator of outdoor thermal comfort since there are a few changes within the different urban forms [56]. Similar research to investigate the outdoor comfort of the mean radiant temperature, the physiological equivalent temperature in Egypt as the hot-arid climate, is studied by Galal et al. [57].

Sözen and Oral [58] propose to analyze outdoor thermal comfort regarding the urban canyon and courtyard concepts in Mardin, which has a hat arid climate in Turkey. The urban canyon concept is evaluated by the geometrical parameters of aspect ratio, orientation, asymmetry, and additional galleries in the street. For the courtyards, the geometric parameters of plan ratio, openings, materials, use of *eyvan*, and specific heat mitigation strategies like integration of vegetation and water are studied. The parameters are decided after evaluating the vernacular urban morphology of Mardin. The Envi-met simulation considers outdoor thermal comfort in streets and courtyards as the urban alternative. There are three building height-street width ratios 1,2,4. There are four orientations southeast-northwest, southwest-northeast, east-west, and north-south. There are two street types asymmetrical and galleries. They are shown in Figure 10. For the courtyard alternatives, 12 building forms are organized. The urban configurations are represented in Figure 11.

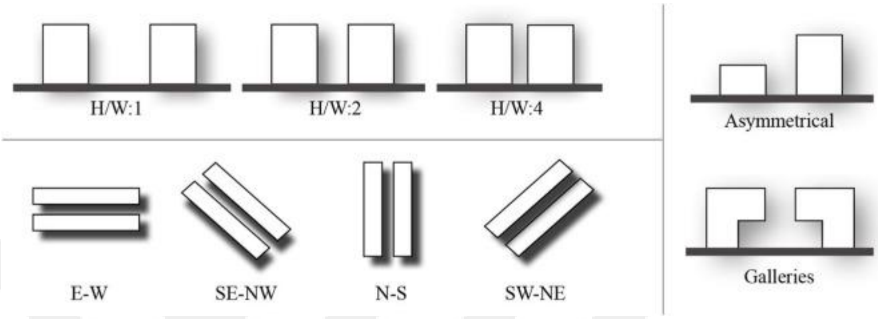

Figure 10: Urban configurations of the article [58] *(Sözen and Oral, 2019, p.4)*

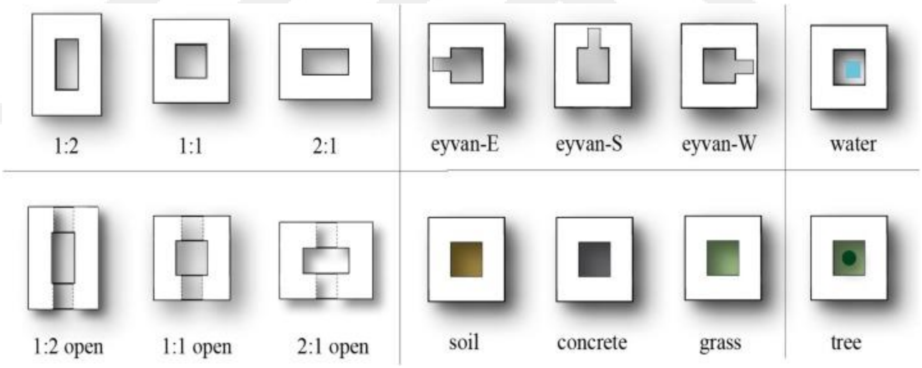

Figure 11: Vernacular forms by the article [58] *(Sözen and Oral, 2019, p.5)*

The main results are that the lower building height-street with ratio and N-S orientation has the lowest physiological equivalent temperature values. It results in the highest thermal comfort for streets. However, the east-west direction is the least comfortable one. Asymmetry does not impact the comfort level, but the usage of galleries improves the comfort conditions. For the courtyard results, the north-south oriented courtyard with a 1:2 ratio provides the highest comfort. If the *eyvan* is oriented to the south, improve the comfort level. The most dominant heat mitigation strategy for the courtyards has been determined using trees and water by reducing the air temperatures through evaporation [58].

2.4.2 Sub-Tropical Climates

Sabrin et al. [59] analyze the benefit of a tree for an existing urban area in Philadelphia. Nine neighborhoods are selected based on residential, commercial, and mixed-use categories. The Rayman model calculated the mean radiant temperature, physiological equivalent temperature, surface temperature, and global radiation based on five urban scenarios. These scenarios include a built environment without vegetation, a built environment with existing vegetation, a built environment with additional vegetation after one year, a built environment after 5-years, and a built environment after a 10-years growth period. The scenarios of integrating trees in the streets of residential and mixed-used sites provide a higher sky view factor by improving pedestrian comfort for the long-term period thanks to reducing mean radiant temperature and physiological equivalent temperature. The reduction is mainly recorded for the mixed-use site with the highest thermal comfort value [59].

Krüger et al. [60] evaluate the relations between urban morphology and changes in microclimate and air quality in downtown Curitiba, Brazil. The research analyzed the impact of street geometry, sky-view factor, and ambient temperature on pedestrian comfort using Envi-met simulation. The existing sky view factor is calculated between Santos Andrade Square and General Osório Square by determining 18 points in the street using Rayman. 4 wind scenarios were decided according to various wind directions. The main result of the research is that there is a high correlation between the mean radiant temperature of solar radiation and determining human comfort levels [60].

Wai et al. [61] analyze the impact of urban form on outdoor thermal comfort at the pedestrian level by evaluating five representative urban forms in Hong Kong. The alternatives are examined with Computational Fluid Dynamics by the FLUENT tool and Rayman model. The results of pedestrian-level air temperatures for the five alternatives are represented in Figure 12. The main result of the research is that to have a better design in the subtropical climate, there needs to reduce to physiological equivalent temperature. Reducing the building length and increasing the low-level porosity is the most effective way to diminish pedestrian heat stresses [61].

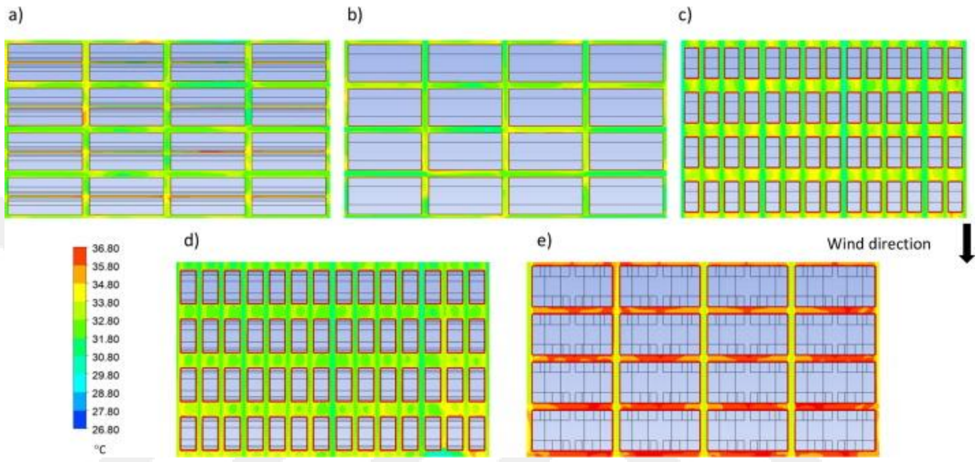

Figure 12: Pedestrian level air temperature of the research [61] *(Wai et al., 2020, p.5)*

2.4.3 Temperate Climates

Ghaffour et al. [62] stated that the critical parameters for external microclimate are urban morphology and building geometry to offer positive thermal comfort to pedestrians. The objective of the research is to evaluate the impact of the urban morphology on the external microclimate to understand the relationship between user perception and the calculation of the thermal environment by focusing on the City of Tlemcen in Algeria. The city has a Mediterranean climate. The Envi-met 4.1 model completes the simulation during the coldest month of the winter and the hottest month of the summer. The urban morphology is evaluated by the variability of the sky view factor, predicted mean vote, solar access, and air temperature. The study's findings show that outdoor thermal comfort is directly correlated with the sky view factor, height/width ratio, and the orientation of the urban canyon. The choosing points from the north-south direction perform in the comfort level. Trees in the street provide heat stress reduction in outdoors for the height/width ratio between 1.18 and 1.70 [62].

Song and Jeong [63] analyze the impact of the sky view factor on urban microclimate based on the human thermal responses in Korea. The body temperatures of the test subjects and their psychological responses were compared in the different urban areas. The results show that 95 % of subjects were satisfied with the road that was covered with trees in the summer season. Therefore, urban morphology impacts the thermal stress that can be optimized thanks to the improvements in urban greening to ensure thermal comfort [63]. The urban wind environment is a significant feature for populated areas like London since increasing building heights change the behavior of urban configuration, which affects the local wind environment, especially for the layer of lower urban canyon [64]. Pedestrian-level wind patterns are also critical for ensuring the air quality of the city by decreasing the pollutants due to traffic and industrial activities [64].

Tsichritzis and Nikolopoulou [64] evaluated the pedestrian wind comfort level on different urban textures in London. The urban configuration of London is evaluated by ArcGIS software with Python scripts. Computer fluid dynamic simulation examined twenty case studies with different configurations. The urban alternatives are tested through 8 wind directions. Four main features are discussed for evaluating pedestrian-level wind environment: mean building height and maximum building height standard deviation of the building height façade area ratio. The findings show a strong connection between the ground-level mean wind speed ratio and tolerable wind conditions for pedestrians. The most influencing factor is the façade area ratio on mean wind speed ratio and the percentage of outdoor space for increasing values of plan area ratio [64].

Chatzidimitriou and Yannas [64] present research on the impact of urban morphology and its parameters like street dimensions and building geometry, landscape elements indicating vegetation and water, also material properties to understand their relations on pedestrian thermal comfort for temperate climates. The base case is chosen from Greece. The design parameters are two aspect ratios for square type, two aspect ratios for courtyard type, three alternatives for shading canopy, six variations for pavement surface albedo, five alternatives for pavement surface emissivity, four types of pavement thermal capacity, three alternatives for solid humidity, tree cover, grass cover, and water cover. By the combination of single parameters, 35 variations of urban configuration are arranged. For the calculations, Envi-met software simulates microclimate solutions, Fluent characterizes the air movement and RadTherm analyses the surface and mean radiant temperatures.

The output of these simulations is used as the input of RayMan to examine the Physiological Equivalent Temperature. The findings of the research can be summarized as; the aspect ratio has the strongest impact on physiological equivalent temperature, especially for the courtyard urban form. Trees have more influence on square type urban texture on the microclimate. Water, soil, and grass have a similar impact on the comfort both for square and courtyard while considering the daily cycle their square urban form has a sustainable comfort level thanks to the exposure of solar radiation [65].

The research shows that there is a strong correlation between urban morphology and comfort level especially based on wind and solar radiation. The main parameters that impact the pedestrian comfort to reduce thermal stress are mean radiant temperature, physiologically equivalent temperature, sky view factor, the orientation of the urban block, integration of trees on the streets, building height-street width ratio. The summary of the section is in Table 4.

Table 4: Impacts of urban morphology on comfort level

No	*Authors*	*Year*	*Keywords*	*Main Features*	*Method*	*Tools*
[56]	Abdel and Othman	2021	Outdoor thermal comfort Urban microclimate, Urban forms, PET, ENVI-met software	Outdoor Thermal Comfort Urban Morphology	1- Selecting a neighborhood in Al-Sharq City 2- Arrangement of 4 different urban forms 2- Evaluation of the alternatives	Envi-met Rayman
[58]	Sözen and Oral	2015	-	Outdoor Thermal Comfort Urban Morphology	1- Evaluation of vernacular urban pattern of Mardin 2- Determining urban canyon and courtyard parameters 3-Simulating outdoor comfort	ENVI-met
[59]	Sabrin et al.	2021	Heat mitigation Human-biometeorological indices; Thermal comfort, Urban canopy, Urban planning	Outdoor Thermal Comfort Urban Morphology	1- Selecting 9 neighborhoods in the categories of residential, commercial, and mixed-use 2- Decision of the 5 urban scenarios 3- Simulating the outdoor thermal comfort	Rayman
[60]	Krüger et al.	2011	Air quality, ENVI-met, Sky-view factor, Thermal comfort, Urban planning	Outdoor Thermal Comfort Urban Morphology	1- Calculation of Sky view factor on 18 points between Santos Andrade Square and General Osório Square 2- Calculation of outdoor comport 3- Determining 4 wind speed scenarios	ENVI-met, Rayman
[61]	Wai et al.	2020	Computational fluid dynamics, Heat stress, Urban climate modeling, etc.	Outdoor Thermal Comfort Urban Morphology	1-Choosing different urban forms in Hong Kong 2- Simulating the outdoor thermal comfort on mean radiant temperature and physiological equivalent temperature	FLUENT (CFD) Rayman

No	*Authors*	*Year*	*Keywords*	*Main Features*	*Method*	*Tools*
[62]	Ghaffour et al.	2020	Microclimate, Thermal comfort outside, Tlemcen, Urban shape	Outdoor Thermal Comfort Urban Morphology	1- Choosing the case study area 2- Calculating the sky view factor, predicted mean vote, solar access, and air	ENVI-met
[63]	Song and Jeong	2016	Core temperature, Skin temperature, Sky view factor, Thermal comfort, Urban morphology	Outdoor Thermal Comfort Urban Morphology	1- Choosing different urban forms in Korea 2- Calculation of skin temperatures and psychological responses 3- Evaluating the results	Experimental human test
[64]	Tsichritzis and Nikolopoulou	2019	Building height CFD, Façade area ratio, London, Pedestrians Urban morphology, Wind comfort, assessment, Wind speed ratio	Outdoor Thermal Comfort Urban Morphology	1- Evaluation of the existing urban form of London 2- Choosing 20 case study areas 3- Analyzing the pedestrian level wind environment by 4 main features	ArchGIS, Python, CFD
[65]	Chatzidimitrious and Yannas	2016	Microclimate, Pedestrian thermal comfort, Simulation of urban microclimates, Urban design	Outdoor Thermal Comfort Urban Morphology	1- Choosing the base case 2- Deciding the 10 single urban parameters 3- Generation of 35 scenarios of urban texture 4- Conducting the simulations 5- Finding the results	ENVI-met RadTherm Fluent RayMan

2.5 State of Art Related to Urban Heat Island

Recently, with the impact of global warming, the urban heat island is one of the most critical problems on the urban scale [66,67,68]. The increase in urbanization impacts both the indoor and outdoor environments of buildings since it has a mutual impact of increasing the heat generation from people, vehicles, appliances, and other human activities in urban areas [51,66,67,68]. The increase in outdoor air temperature causes urban heat generation which is also related to the thermal comfort of the place. Unpleasant outdoor air conditions have also resulted in the usage of air conditioning systems and increasing energy consumption [51]. Urban heat island is the interaction of buildings and microclimate since it is the phenomenon that can increase the cooling load by influencing urban morphology, urban landscaping, and the thermal properties of buildings, also soil [49,66,69]. Gros et al. [49] categorize the six urban heat island factors as mentioned below.

- Urban street canyon geometry [70,71] indicates radiation trapping. Short wave radiation diminishes the impact of albedo [66], increases the solar radiation trapping.
- The urban greenhouse effect, increase the polluted warm urban atmosphere [72].
- Thermal properties of the building, store the sensible heat of the city [73].
- Anthropogenic heat [74] results from human activities like traffic.
- Diminution of evapotranspiration is due to the reduction of the evaporation surface of the city.
- Wind shelters diminish the turbulent heat transfer because of the urban form [70,71,74,75,76].

Before deciding the urban morphology of the city all the topics have careful attention. To improve the microclimate in high-density cities finding solutions to mitigate the intense urban heat island effect is essential in Hong Kong since the city suffers from an urban heat island impact of up to 4°C due to the compact urbanized landform [25]. Lau et al. (2022) conducted simulation-based research to investigate wind-path design strategies based on urban greenery on the neighborhood scale. The analysis is made for different urban morphologies in two-climate sensitive urban areas in Hong Kong. The research results show that the vegetation arrangement in wind corridors has a twice positive impact on the cooling of air temperature and sensible heat. Therefore, planting trees with a proper urban form effectively mitigates daytime urban heat island impact [75].

Apreda et al. [71] researched the influence of outdoor thermal comfort on different housing urban blocks in the Euro-Mediterranean climate. They were modeled in Envi-met v4.4 model with the Computer Fluid Dynamic analysis to calculate the air temperature at the pedestrian level. The simulation inputs are hourly air temperature, hourly relative humidity, wind speed, and wind directions as west, south-west, and south. The typologies are categorized as a detached block, attached block, linear block, U-shaped block, block with a courtyard, block with multiple courtyards, and tower urban block. The urban morphology descriptors are surface coverage, density, and canyon geometry. The three surface coverages are 0%, 20%, and 60% of the previous cover. Three alternatives of floor area ratio related with a density as low (0.5), mid (0.5-1), high (1-3), and very high (3). Canyon geometry has three height-to-width ratios 0.5, between 0.5 and 2.0, and more than 2.0. The seven urban morphologies combined with urban morphology descriptors and 21 configurations are achieved.

The results show that optimal urban configurations are U-shaped blocks, blocks with a courtyard, and blocks with multiple courtyards. One of the microclimate results is that the wind direction impacts the thermal behavior of the urban block. If the wind direction is from the south, the daytime temperature is enhanced with a ratio of 2.0 for height-to-width. However, in the nighttime, that increases air temperature at the pedestrian level [71].

Gülten [70] analyses the impact of the urban heat island effect in Elazığ, Turkey, using a computational fluid dynamics program. The densest urban area is chosen as a case study in the city, which has a temperate dry climate. The variables of the study are traffic, tree, and the building height-street width ratio, orientation, and urban form alternatives. The building height-street width ratio is taken at 0.5, 1, and 2. Urban alternatives are decided as adjacent and detached housing units. The result of the study is that the wind velocity on heat island potential for midnight on 1st, 11th, and 21 of June, July, and August is increased by about 2m/s for all the scenarios of building height-street width ratios [70].

Yuan et al. [74] stated that anthropogenic heat is one of the critical factors for intensive urban heat islands. The research aims to investigate the effect of urban morphology on anthropogenic heat dispersion to diminish urban heat island intensity for extreme weather scenarios like having meager wind speed and high heat emission. While organizing urban forms, site area, the number of buildings, and building lengths are the constant parameters. The changing ones are building width, height, floor footprint area, site coverage ratio, and frontal area density. Ten parametric cases are designed as representative urban areas using a Geographic Information System (GIS)-based modeling tool and analyzing the results with CFD. There are two alternatives for anthropogenic heat on air temperature annually averaged incoming wind and minimum incoming wind between 2009 and 2020. If the incoming wind speed is minimal, it is hard to distribute the anthropogenic heat. Therefore, the possibility of heat stress risk is higher at the low wind speed since the rise in the temperature for minimum wind speed is six times more than the average wind speed [74].

He et al. [76] investigate the relationship between urban morphology, ventilation performance, urban heat island impact, and outdoor thermal comfort in Sydney, Australia. The case study focuses on compact, high-rise urban blocks. By using sensors, the precinct ventilation performance, precinct urban heat islands, precinct relative humidity, and precinct outdoor thermal comfort is calculated in the case study area under different combination of external meteorological conditions. The study proves that the precinct morphological characteristics of compact high-rise blocks have a critical role in precinct ventilation. The precinct ventilation performance dominated by sea breeze makes a significant change to reduce urban heat island impact and improve thermal comfort. The orientation of the street does not have a dominant factor in ventilation performance, urban heat island, and outdoor thermal comfort [76].

Liu et al. [77] investigate the impact of climate conditions on canopy layer urban heat islands according to urban morphology. The graphical abstract of the study is given in Figure 13.

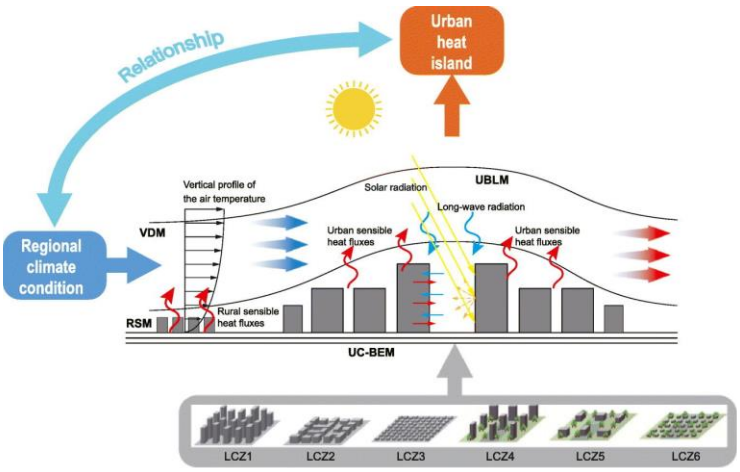

Figure 13: Graphical abstract of the research [77] *(Liu et al., 2020, p.1)*

Five typical cities in China were chosen as Harbin, Xi'an, Nanjing, Guangzhou, and Kunming. Their climatic zone is severe cold, cold, hot summer-cold winter, hot summer-warm winter, and mild respectively. In different climatic conditions, six urban morphologies are designed with the variables of built types, aspect ratio, horizontal building density, and average building height. There are six built types of compact high-rise, compact midrise, compact low-rise, open high-rise, open midrise, and open low-rise. The aspect ratio ranges between 0.5 and 2. The horizontal building density variables are 0.3, 0.5, and 0.55. The average building height is 25m, 17.5m, and 6.5m. The envelope properties are managed according to the condition of the climate. The climate model is developed by Urban Weather Generator which is related to the Energy Plus. The main conclusion of the study is the urban heat island is strongly correlated with the wind speed and air temperature during daytime and nighttime. The city of Kunming has the most critical urban heat island impact due to having low wind speed and strong solar radiation. Generally, reducing urban density is more effective than reducing building height to mitigate urban heat island impact in Kunming. Among the six urban morphologies in different climates, the average urban heat island impact of the first scenario (LCZ1) is about 1-2.3 °C which means 1.5 times higher than the fourth scenario (LCZ4) [77].

Rajan and Amirtham [73] conducted research in Chennai, İndia to assess urban heat island intensity and evaluate the outdoor thermal comfort. Eight hot spot points were determined to measure air temperature and relative humidity in the city. The outdoor comfort level in the defined hotspots is measured with Envi-met simulation. The study shows that the urban heat island intensity is 4.5°C in winter and 2.5°C in summer in the tropic climate of the chosen city. The study also proved that changes in the urban form result from a maximum 22°C physiological equivalent temperature difference for the decided locations [73]. Ekinci [66] conducted a study in Istanbul, Aksaray to understand the relationship of albedo value and temperature changes for an urban block. The albedo value which is affected to urban canopy through urban morphology and solar radiation is defined as the most critical feature in the formation of urban heat island is urban scale. The study proves that when the albedo value changes to 0.1, it causes a temperature increase between 0,3 °C and 0.5°C. Another significant parameter mentioned is the vegetation to reduce the urban heat island impact. Therefore, the green roof implementation to the case study urban block diminishes the urban heat island impact in the range of 50% and 90% [66]. In addition, Tabanoğlu [72] conducted research in Antalya on climate change adaptation strategies by including urban streams, water, urban heat island, public health, green spaces, biodiversity, and planning approach. By surveying 40 participants the impact of climate change is aimed to be identified from the vision of citizens [72].

Santos et al. [78] analyze the impact of different urban morphologies on urban heat islands regarding energy costs in Singapore. The case study area has a hot, humid climate typical of tropical regions. Nine urban forms are organized by evaluating Singapore's generic urban typologies. There are three alternatives for building site coverage 30%,40%, and 50%. The average building heights are 49m, 65m, and 81m. Other parameters include the mean urban heat island, the mean density of productivity and population per site area, and the operational energy cost. The Urban Weather Generator tool generates the weather file, which mainly evaluates the relationship between urban morphology and weather, especially for the wind. The calculation of the operational cost of energy is calculated by using specific formulations. The study's main result is that if the highest building height (81 m) is combined with a medium and low-density urban area, the optimal consequence is achieved according to minimum urban heat islands impact and maximum energy cost efficiency [78].

One of the consequences of climate change is overheating in urban areas, impacts comfort level of living environments. The main factors are urban canyon geometry, solar radiation, the greenhouse effect, building envelope properties, androgenic heat, and wind behavior. The studies related to urban heat island impacts proved a strong correlation with urban form. The articles associated with the topic are displayed in Table 5.

Table 5: Urban heat islands and urban morphology

No	*Authors*	*Year*	*Keywords*	*Main Features*	*Method*	*Tools*
[70]	Ayça Gülten	2014	Urban Heat Island, Computational Fluid Dynamics, Surface Temperature, Urban Areas	Urban Heat Island Urban Morpholog	1- Determining the densest area in Elazığ 2- Determining 5 main urban form variables 3- Analyzing the wind velocity on urban heat island 4- Discussion of the results	CFD
[71]	Apreda et al.	2020	Air temperature, Housing blocks, Microclimate, Urban morphology, Urban parameterization	Urban Heat Island Urban Morpholog	1- Determination of most recurrent urban blocks in Euro-Mediterranean cities 2- Modelling 7 urban blocks 3- Measurement of air temperature at pedestrian level 4- Evaluation of the measurements with different block types	CFD by ENVI-met simulation
[73]	Rajan and Amirtha m	2021	Thermal comfort, Urban climate, Urban heat island, Urban morphology	Urban Heat Island Urban Morpholog	1-Measurement of air temperature and relative humidity on 8 points in the city 2- Simulation the outdoor comfort by Envi-met Simulation 3- Analyzing the relationship between urban heat island and outdoor comfort	ENVI-met
[74]	Yuan et al.	2009	Anthropogenic heat dispersion, Semi-empirical model, CFD simulation, Urban planning, GIS mapping	Urban Heat Island Urban Morpholog	1- Decision of urban morphology parameters 2- Designing 10 urban forms 3- Estimation of the impact of anthropogenic heat dispersion on ambient air temperature	CFD Geographic Information System

No	*Authors*	*Year*	*Keywords*	*Main Features*	*Method*	*Tools*
[76]	He at al.	2020	Precinct ventilation performance, Urban heat island, Outdoor thermal comfort, Precinct ventilation zone, Coastal cities	Urban Heat Island Urban Morpholog	1- Implementation of the environmental sensor to the selected points of the case study area 2- Calculation of ventilation performance, Precinct urban heat island impact, relative humidity, and outdoor thermal comfort 3- Comparison of the results	Environmental Sensors
[77]	Lui et al.	2020	Canopy layer urban heat islands, Numerical model, regional climate condition, Urban morphology	Urban Heat Island Urban Morpholog	1- Choosing 5 cities from different climatic zones 2- Arranging the 4 variables for urban configurations 3- Organizing 6 urban forms	Urban Weather Generator Energy Plus
[78]	Santos et al.	2021	Decision support systems, Urban overheating, Climate-informed design, Damage function, Data processing	Urban Heat Island Urban Morpholog	1- Analyzing the generic urban forms in Singapore 2- Designing 9 urban alternatives 3- Creating weather file by Urban weather generator 4- Calculation of energy cost by formulations	Urban Weather Generator Formulations

2.6 State of Art Related to Environmental Control, Energy Performance, Indoor Comfort and Outdoor Comfort Relating Urban Morphology

The morphology of settlements has continued to exist for a long time without any changes [15]. The changes in urban texture can be possible during the redevelopment process after demolishment [15]. By the current increase in population and urbanization rate, it is calculated that the global urban areas will rise three times compared to the number at the beginning of the 20^{th} century; by 2050, two-thirds of the world population will be living in urban areas [31, 15, 45,26,48,79]. Mangan et al. [15] stated that the fast growth in urban areas causes the failure to establish an efficient plan by considering energy, environmental, and pedestrian level problems. With this purpose, evaluating the existing and new settlements by conducting a multi-scale approach is essential for building scale and urban scale [15].

Only a few studies examine the impact of urban morphologies on energy performance, outdoor comfort level, and indoor comfort level by including environmental control parameters [15,79,80,81]; recently, these aspects started to interconnect [81].

Mangan et al. [15] analyze the residential reference building in 30 urban textures to examine the building energy performance, outdoor thermal comfort, and economic performance in İstanbul, which has a temperate humid climate [15,79]. The 30 urban textures are shown in Figure 14. A reference building is designed based on the national regulation of the Housing Development Administration of Turkey (TOKİ). Regarding the regulation, the reference building is designed to be 100m² with square and rectangular plans.

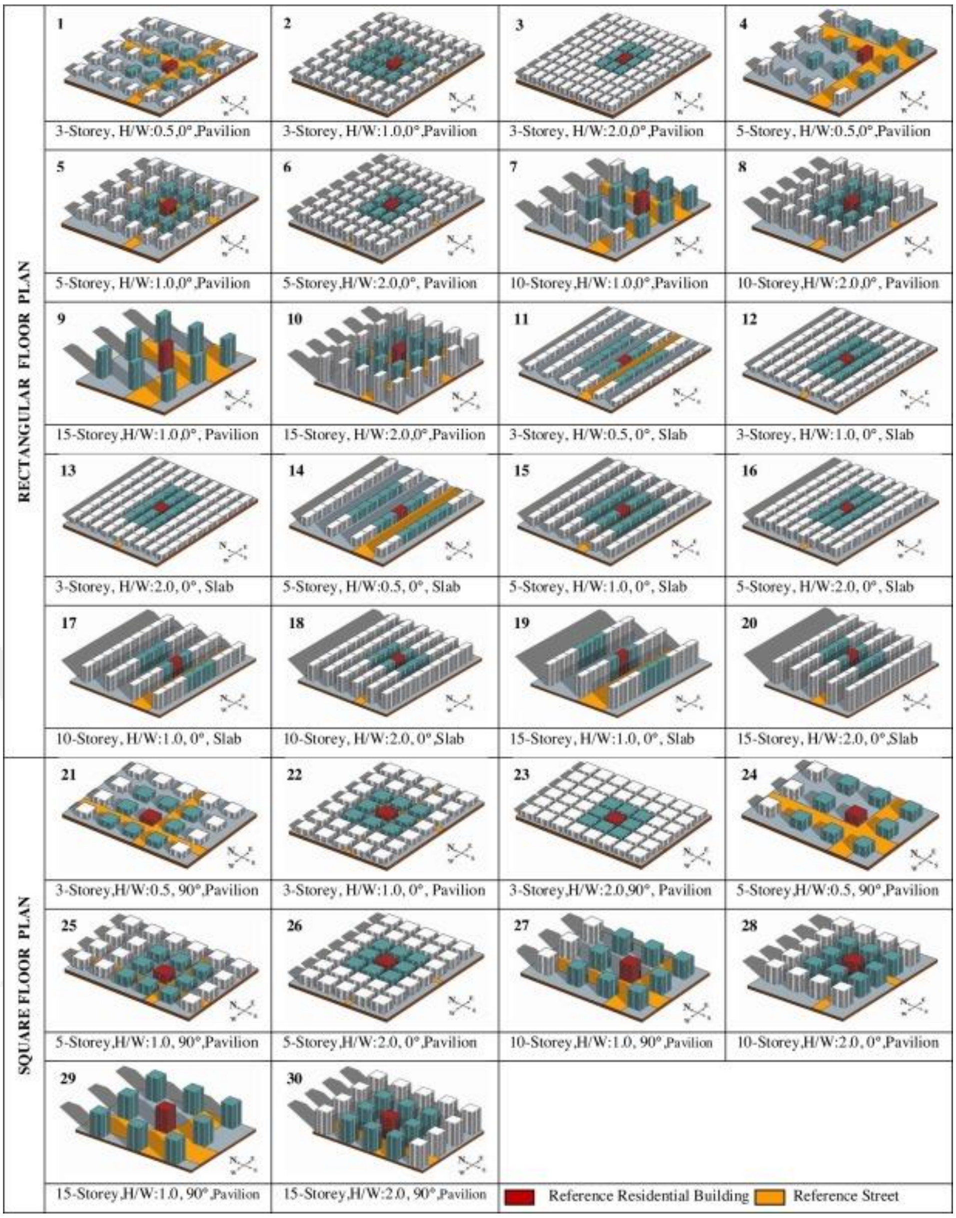

Figure 14: Thirty urban scenarios of [15] *(Mangan et al., 2020, p.5)*

The urban design parameters are settlement scale, building scale, and building component scale. The settlement scale parameters are settlement type, aspect ratio, and street section. The building scale parameters are plan type, number of floors, and construction detail related to the component scale. The building component scale parameter is about six variables for the thermal properties of the exterior wall. The building number of floor variables is 3,5,10, and 15, with 3.00m floor-to-floor height. The building height-street width ratio alternatives are decided according to the shadow analysis on the 21st of July since the day is the longest and the shortest night of the year on the summer solstice. The optimum space between buildings is calculated as 1.8m, which does not cast a shadow on surrounding buildings. Therefore, the aspect ratios are 0.50, 1.00, and 2.00. For the calculation of heating, cooling, and the final energy consumption Design Builder program is used. The annual carbon dioxide emission of the reference building is calculated by the Tier 2 method. To examine thermal comfort, the Envi-met V4 simulation model is used.

The analysis results on 30 different settlement textures demonstrate that the most critical parameter that affects outdoor thermal comfort conditions is the building height-street width ratio. The best aspect ratio for İstanbul is determined at 2.00 to provide the best thermal comfort conditions in the summer. The shading effect thanks to trees significantly improves the outdoor thermal comfort level. The findings of the energy and cost analyses show that the heating energy consumption takes a larger percentage of both total energy consumption and cost since the heating period is longer than the cooling period. Among the six alternatives for 30 urban forms, the best performance is noted by increasing the thickness of the insulation layer by 8cm [15].

Mirzabeigi and Razkenari [79] stated that there is a lack of research on the relationship between urban morphology, outdoor thermal comfort, and building energy performance in cold climates. The study explores the effectiveness of urban geometry and building envelope characteristics in multiple scenarios by evaluating Syracuse's building energy performance and outdoor microclimate. The case study area is in the cold climate region. This study has six urban typologies, including low-rise, mid-rise, and high-rise scenarios. The floor area ratio for the low-rise scenario is 3; the mid-rise scenario is 8, and the high-rise is 13. The six urban alternatives with different floor ratios are given in Figure 15.

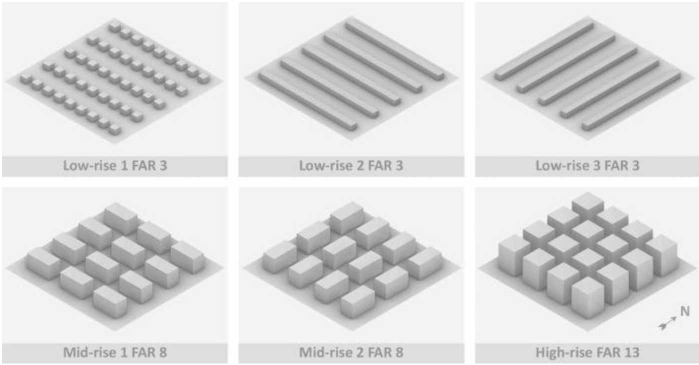

Figure 15: Six urban alternatives with different floor area ratios [79] *(Mirzabeigi and Razkenari, 2022, p.6)*

The window-to-wall ratio and thermal mass are considered for the building envelope properties variables. For all scenarios, window-to-wall ratios are 0.3,0.5 and 0.7; thermal mall alternatives are two construction materials, low mass, and high mass. By the combination of urban typology, floor area ratio, window-to-wall ratio, and thermal mass, 72 design scenarios were tested.

Urban Weather Generator and Dragonfly tools are used to generate weather files. Energy simulations are conducted by Energy Plus software by including Ladybug and Honeybee plugins in Rhino and Grasshopper. Moreover, the urban scenarios were tested in Eddy3d, a Grasshopper plugin for computational fluid dynamics. The main result of the research is that the most energy-efficient form is M2_HM_F08_W30 (mid-rise with north-south orientation, high mass, floor area ratio of 8, and the window-to-wall ratio of 0.3) by improving energy performance by about 55.8% compared to the baseline. The hot season outdoor comfort satisfaction for mid-rise scenarios was between 92.9 and 98.5%, but the satisfaction in the cold season was between 8.4 and 11.6% [79].

De Luca et al. [80] mentioned that there is little research focusing on indoor, outdoor comfort and associated building energy consumption in tall buildings. This research aims to examine the high-rise office buildings to understand the impact of different urban forms on indoor comfort, outdoor comfort, and energy performance by the combination of wind analysis in Tallin, Estonia which is in Nordic climate. The office buildings have 25 floors with 4m in height. The distance between buildings varies from 12m to 30m. Figure 16 shows the main ideology of the study to organize cluster variations.

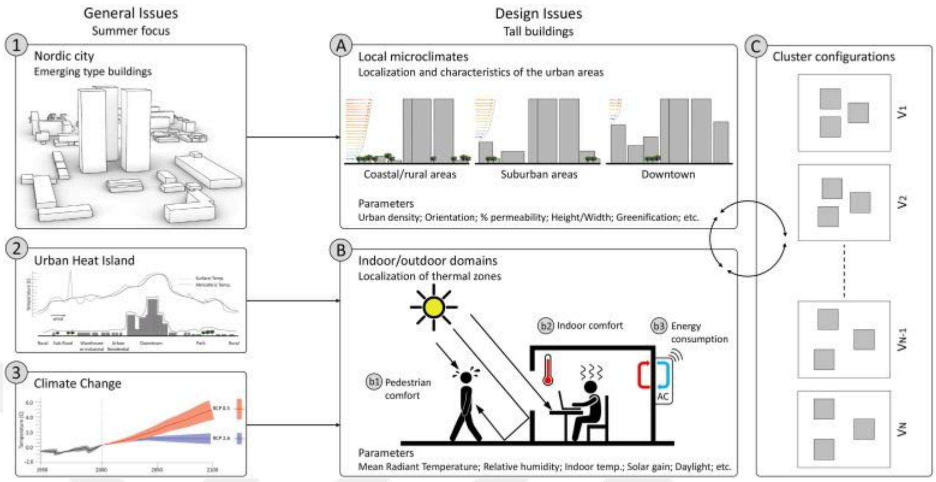

Figure 16: Design issues by the article [80] *(De Luca et al., 2021, p.3)*

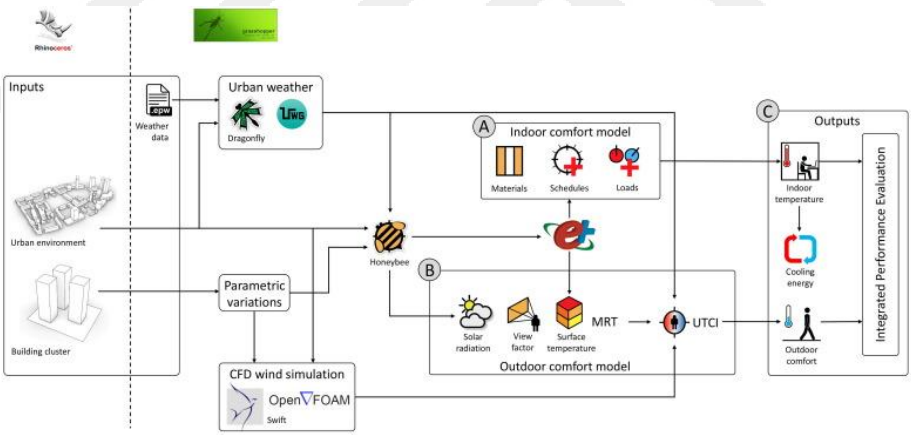

Figure 17: Methodology diagram of the study [80] *(De Luca et al., 2021, p.5)*

There are nine building cluster variations which are given in Figure 18. The energy and comfort analysis are tested for the period between 1st June to 31st August. The thermal and energy calculations are completed by using Energy Plus by the Grasshopper plug-in of Honeybee. A Computational Fluid dynamic model is conducted by Swift through Open FOAM, Grasshopper. Dragonfly plugin which is based on Urban Weather Generator is used to account for urban microclimate. For the thermal comfort simulations, Ladybug tools were used to calculate mean radiant temperature and wind velocity. The general workflow is shown in Figure 17.

The main result of the study is that the proper distance, orientation, and position are obtained, it is possible to reduce the indoor temperature by 12%, overheating by 56%, and cooling energy consumption by 14%. in Nordic city of Tallinn. Also, the maximum ratio of the pedestrian area in a state of thermal comfort can be increased by up to 34% by considering the solar radiation and wind pattern [80].

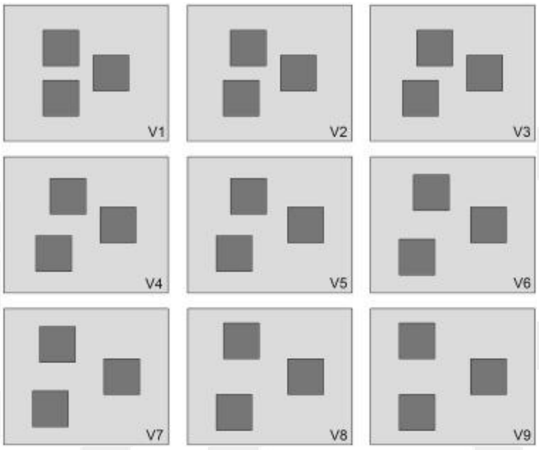

Figure 18: Nine district forms of the study [80] *(De Luca et al., 2021, p.5)*

It is mentioned that cities mainly have an irregular building pattern; the recent studies by Sharmin et al. [82] and Sharmin et al. [83] proved that the variability in aspect ratio and urban form could reduce the air temperature with the range of 1.0 °C and 4.0 °C. That provides a huge benefit for pedestrian-level comfort.

Evola et al. [81] evaluate mutual connections of the building environment, indoor and outdoor comfort, and urban microclimate in Catania, southern Italy, by testing the reliability of parametric tools. The urban block includes six buildings. The case study is modeled in Rhinoceros software. The weather file is generated by Urban Weather Generator with the Dragonfly plugin by Grasshopper. EnergyPlus calculates the energy demand of the buildings via OpenStudio. Ladybug Honeybee conducts the comfort analysis. The results of the calculations are compared with the existing condition by a

Testo 480 data logger. The result proved that the difference between the simulation results and calculations in the real environment is below 0.6 °C for the outdoor mean radiant temperature distribution. The paper concludes the reliability of parametric investigation, especially on the measurements of indoor and outdoor thermal fields [81].

Tsoka et al. [84] analyze the impact of urban trees on the cooling load of buildings in an urban area of Thessaloniki, Greece. The case study area has a Mediterranean climate. The vegetation scenarios are defined with the three-leaf area density alternatives 1.5 m^2/m^3, 2.0 m^2/m^3, and 2.5 m^2/m^3. The energy calculations are conducted by EnergyPlus, and the ENVİ-met v4 model completes the simulation scenarios. The maximum energy saving was recorded up to 54% with the 2.5 m^2/m^3 of the leaf area density [84].

The literature review's main inferences highlight the research's significance and originality and systematize the methodology. Table 6 indicates the study that examines the impact of urban/district morphology on environmental control, energy performance thermal comfort of humans, which is the focal point of the thesis. These studies refer that there is a knowledge gap about the relationship of three between district morphology, energy performance, and comfort level for both indoor and outdoor [15,79,80,81]. The research details in Table 6 are demonstrated in Table 7.

Table 6: Comparison of five research includes three key features

Number of the article	*Type of the Case Study*	*Type of the Climate*	*Whether have an actual site (Yes/No)*	*Whether have an irregular building texture (Yes/No)*	*Environmental Control*		*Energy Performance*	*Thermal Comfort*	
					Solar Radiation	*Wind*		*Indoor Comfort*	*Outdoor Comfort*
[15]	Residential	Temperate humid	No	No	✓		✓		✓
[79]	Residential	Cold	Yes	No		✓	✓		✓
[80]	High-rise office	Cold	Yes	No		✓	✓	✓	✓
[81]	Residential	Mediterranean	Yes	No	✓		✓	✓	✓
[84]	Residential	Mediterranean	Yes	No	✓		✓		✓

Table 6 shows that;

- There is only little research that have a comprehensive approach by integrating environmental control parameters, energy performance and thermal comfort as a key feature of the study. Therefore, this thesis will make a good contribution to fill the knowledge gap in the literature.
- According to environmental control integration, some studies include solar radiation analysis during the determination of urban morphology, while some of them consider the wind pattern. None of them consider both solar and wind potential at the same study, although both critical for the urban design.
- While designing new urban scenarios, all of them include regular building forms without integrating heterogeneity for urban morphology. However, Shareef [36]

mentioned that irregular form of urban morphology can have an advantage for urban energy performance, that is detailly mentioned in Table 2.

- Most of them include residential urban blocks with different climates.
- Except one, they include an existing case study is to compare the design scenarios with the base case.
- For the thermal comfort categories, just two articles include both indoor and outdoor comfort.

The thesis focuses on the impact of district morphology on environmental control both considering sun and wind potential, energy performance, and thermal comfort for indoor and outdoor. In Chapter III, the methodology of the thesis is explained.

Table 7: Articles include the three key features of the thesis

No	*Authors*	*Year*	*Keywords*	*Main Features*	*Method*	*Tools*
[15]	Mangan et al.	2020	Settlement Texture, Residential Building Performance, Energy Efficiency, Cost Efficiency,etc.	Environmental ControlEnergy Performance ComfortUrban Morphology	1-Developing 30 urban alternatives 2-Calculation of shadow on 21 Jan. 3- Calculating final energy consumption 4- Evaluation of 6 envelope properties 5-Analysing cost, and outdoor comfort	Design Builder Envi-Met V4
[79]	Mirzabeigi and Razkenari	2022	Urban design, Energy simulation, Outdoor thermal comfort, Energy efficiency, etc.	Environmental ControlEnergy Performance ComfortUrban Morphology	1-Defining 6 variables 2- Determining72 urban alternatives 3-Conducting energy performance analysis 5- Analyzing outdoor comfort, wind behavior	EnergyPlus, Grashopper (Ladybug, Eddy3D, Dragonfly, UWG)
[80]	De Luca et al.	2021	Climate change, Tall commercial buildings, Performance-driven design, etc.	Environmental ControlEnergy Performance ComfortUrban Morphology	1- Designing 9 building clusters 2- Analysis of energy, outdoor comfort, and wind 3- Discussion of the results	EnergyPlus, Grashopper (Ladybug, Swift,Dragonfly , UWG)
[81]	Evola et al.	2020	Mean radiant temperature, Universal thermal climate, Outdoor comfort, etc.	Environmental ControlEnergy Performance ComfortUrban Morphology	1- Modelling the case study area 2- Conducting climate analysis 3- Replacement of data logger in the area 4- Conduction the energy and comfort analysis datalogger is placed to the area	Grasshopper, Ladybug Tools and Urban Weather Generator
[84]	Tsoka et al.	2021	Vegetation, Foliage density, LAD, Cooling energy needs, Coupling, etc.	Environmental ControlEnergy Performance ComfortUrban Morphology	1- Choosing the case study area 2- Modelling in the software 3- Defining the 3 leaf density area alternatives	Envi Met EnergyPlus

CHAPTER III

METHODOLOGY

Having an appropriate methodology is one of the essential parts of research. Inappropriate method or misleading process cause incorrect results and wrong discussions. This negatively affects the research quality and reliability. The systematization of the methodology has critical points like having a comprehensive knowledge of the literature, making a qualified data collection, managing the analysis tools properly, making calculations carefully, etc. In general, the methodology of the thesis has the following steps:

- Step 1: Determination of the case study urban block
- Step 2: Establishment of the physical and thermo-physical properties of the case study
- Step 3: Development of the alternative district morphologies
- Step 4: Achievement of the Grasshopper algorithms
- Step 5: Conducting simulations and saving results in an Excel document
- Step 6: Determination of the best urban block alternatives

Figure 19 explains the workflow of the thesis methodology with a particular diagram. The methodology systematized with the three main points: Parametric Modelling, Performance Simulations and Comparative Assessment.

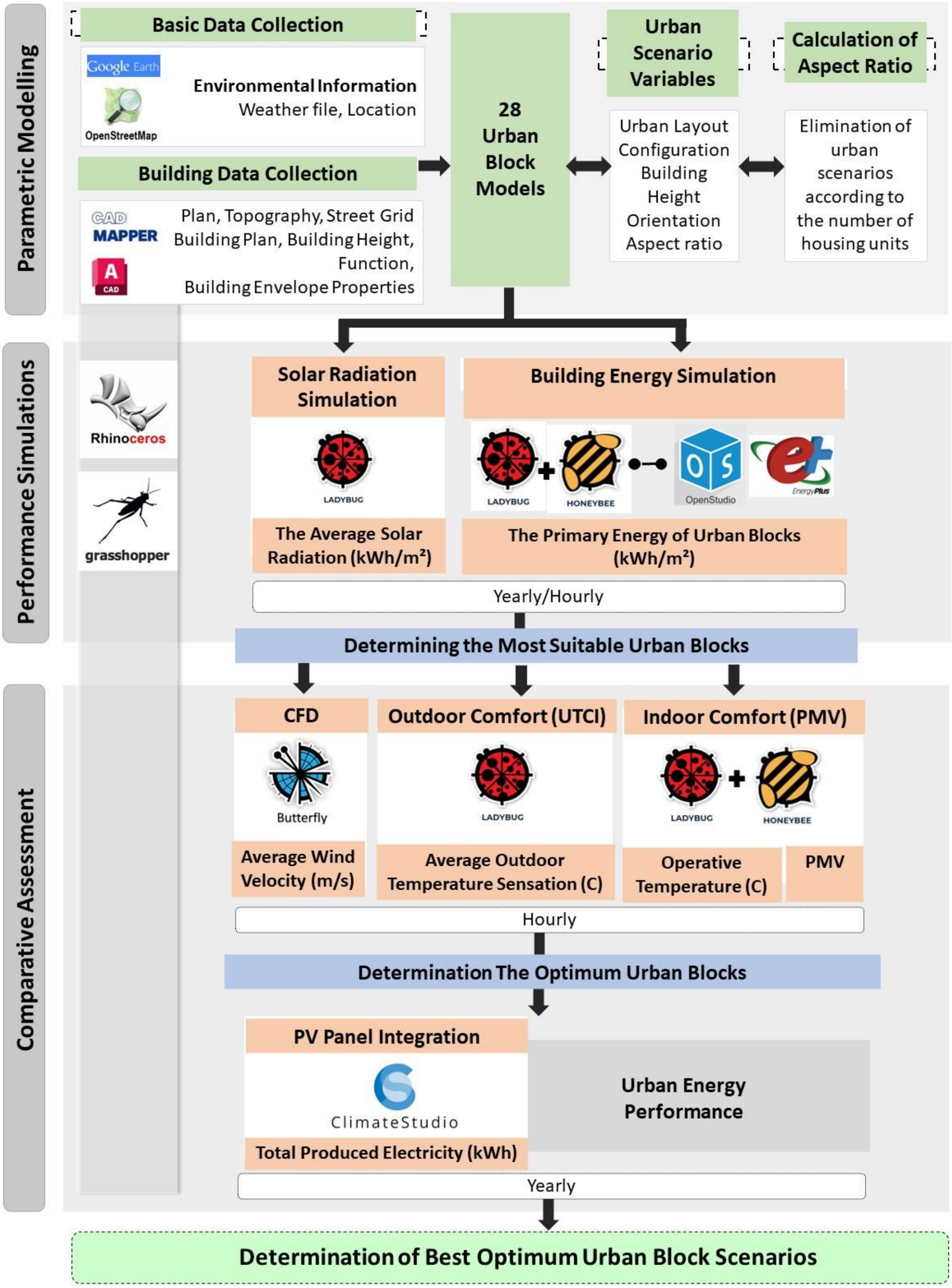

Figure 19: Workflow of the thesis methodology

3.1 Data Collection and Organization for Parametric Modelling

3.1.1 Investigation of Climate Zones in Turkey

In Turkey, there are five climatical zones. These are temperate-humid, temperate-dry, cold, hot-humid, and hot-dry. Mostly, the Marmara Region and the northern part of the Black Sea Region have a temperate humid climate. The cold climate prevails in the east part of Turkey and some parts of central Anatolia. South-Eastern Anatolia has a hot-dry climate. Central Anatolia, partly the black sea region, and the western side of Turkey are dominated by a temperate-dry climate. In the western side of Turkey, mostly the seaside region has a hot-humid climate.

Figure 20: Climate zones of Turkey

For this research, the location of the case study urban area is determined in the temperate-dry climatic zone since it is dominated in central Anatolia. Also, the size of dominance is one of the largest climatic zones in Turkey. Therefore, Ankara, Turkey's capital city, is determined as the representative city of a temperate-dry climate. Hence, the case study urban block is in Ankara. The hot-humid climate is determined to make a comparison with the temperate-dry climate. The weather data of İzmir will be used as the representative city of this climatical zone. Figure 20 shows the climatic regions of Turkey, the location of Ankara, and İzmir. After figuring out the study climatic zones and the representative cities, the case study urban block is determined.

3.1.2 Determination of The Case Study Urban Block

Selecting an appropriate case study for an urban block is one of the critical subjects. Thus, some boundary conditions are assigned to choose the most proper urban block in Ankara. These boundary conditions are mentioned below.

- All buildings in the urban block will have the same purpose usage since it impacts the user profile, occupancy schedule, lighting, and equipment types and schedules. Therefore, all the buildings have a residential purpose of having homogeneous building load data.
- The case study urban block will be close to the city center and have a context in the surrounding.
- It is advantageous to be close to the meteorological station since the climate data should represent the selected case study area most appropriately. This provides more consistent climate data of the case urban block.
- The physical and thermo-physical properties of the building in the urban block need to be similar to have a common data.
- The case study urban block should have an extensive area with buildings to enable new planning for urban model alternatives.

According to requirements mentioned above, an urban block is determined using Google Earth [85] which is a tool to represent earth in 2D and 3D by using satellite images. Figure 21 shows the case study urban block.

Figure 21: Case study district in Ankara

The case study district is in Etimesgut, Ankara. The site coordinates are 39°, 59’ 54’ N, 32°37’27 E. It has 76,183 m². The district is on Bozhöyük Avenue, one of the main avenues in Etimesgut, Ankara. It is at the intersection of Bozhöyük Avenue,13th Street, 579th Street, and 583rd Street, called the Özahikent site.

The site plan of the selected district is taken by using CADMAPPER [86] online website and upgraded by superimposing the satellite images from Google Earth [85] on AutoCAD 2023 [87]. To clarify, CADMAPPER [86] includes worldwide data by transforming it from public resources like OpenStreetMap [88]. The downloaded map is coherent with AutoCAD [87] and Rhinoceros [89] software.

In the Özahikent site, all buildings are residential apartments with the same plan organization. They were constructed approximately in 1999. The number of floors is between 9 and 12. Each floor has 578,43m² and four dwelling units. One dwelling unit has 118,65m² with a kitchen, a living room, three bedrooms, and three toilets. The height of each floor is 3m, and it is estimated that there are four people in every dwelling unit. Approximately, the case study urban block generally includes 600 dwelling units and 2,400 dwellers.

The 2D plan of the buildings is figured out from the investigation of real estate websites [90]. Figure 22 shows the 2D and 3D organization of buildings in the case study district. The plan belongs to the Burçak Apartment, A1 Block on 598th Street. Also, it can be seen that there is a same plan organization with the Akasya Apartment, B1 Block on 583rd Street. In the right-bottom, the view from the case study urban model is represented. The details of the physical and thermos-physical properties are mentioned in the following section.

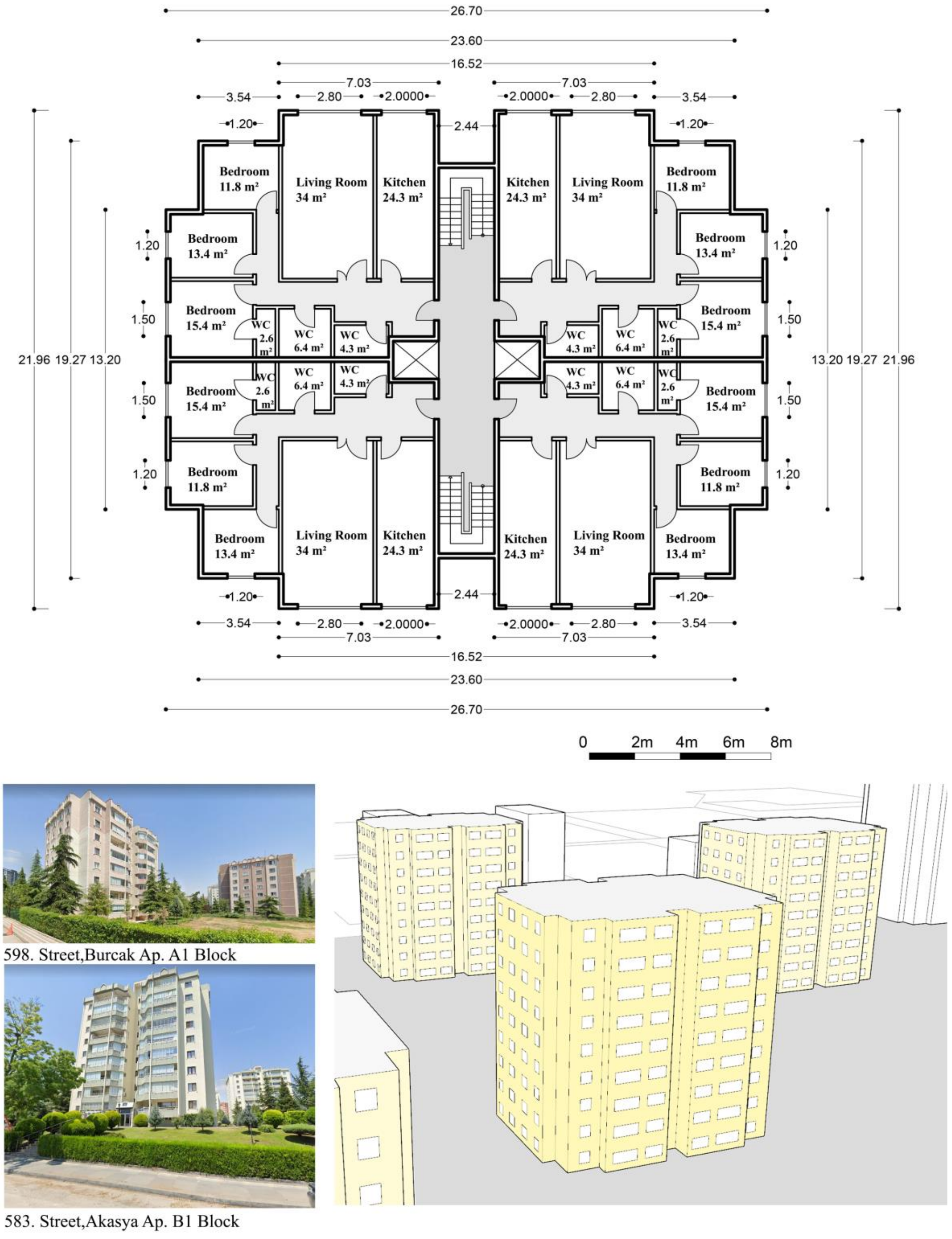

Figure 22: 2D and 3D organization of buildings in the case study district

3.1.3 Determination of the Physical and Thermo-Physical Properties of Case Study Urban Block

The physical and thermo-physical properties of the building include the architectural, mechanical, and occupancy characteristics. Building material characteristics are arranged based on TS-825 Standard [88]. It consists of detailed data from the Turkish Standard Institution. According to the standard, Ankara is in the III. Region. The standard ensures the limit values of U (W/m^2K), the thermal conductivity value. Moreover, the material layers are organized thanks to the articles [9] and [15]. Table 8 shows the general building materials layering system and the U-Value ($W/m^2°K$) of construction.

Table 8: Building material characteristics

Construction	*Material Layers (From outside to inside)*	*U-Value ($W/m^2°K$)*	*The Limit for U-Value ($W/m^2°K$)*
Exterior	plaster+ XPS+ cement rendering+ brick+ gypsum plaster	0,40	0,48
Roof	tile+ roofing sheet+ XPS+ concrete+ plaster	0,26	0,28
Ground Floor	reinforced concrete+ concrete+ XPS+ concrete+ screed+ PVC flooring	0,40	0,43
Glazing	Isıcam synergy	1,6	1,8
Interior Wall	plaster+ brick+ plaster	3,12	-
Floor	plaster+ concrete+ XPS+ screed+ PVC flooring	0,97	-

The glazing system is determined as *ISICAM Synergy* [91], a glazing technology that provides thermal insulation thanks to the heat control coating layer. Solar Heat Gain Coefficient (SHGC) of the glazing system is 0,56, and Visible Transmittance (t-vis) is 0,79. These data of the glazing system is investigated from the website [92] of the company. Table 9 indicates the details of material properties. The thickness of the materials is generally taken from the article [15]. The conductivity data and density values are based on the standard TS-825 Standard [93]. The missing values in the standard and the values for the specific heat of the material are figured out from Honeybee Material Library. Its interface is represented in Figure 23.

Table 9: Detail of material properties

Name	*Thickness (m)*	*Conductivity (W/m²K)*	*Density (kg/m3)*	*Specific Heat of the Material (J/kgK)*
Plaster	0,02	0,7	1400	1089
XPS	0,1 (roof) 0,06(external wall, ground floor) 0,03 (floor)	0,035	25	1209
Cement Rendering	0,03	1,65	2000	1089
Brick	0,2	0,38	750	790
Tile	0,03	2,5	2400	1209
Roofing Sheet	0,02	0,16	1121	1460
Concrete	0,2(roof, ground floor) 0,1(floor)	1,65	2200	832
Reinforced Concrete	1	2,5	2322	832
Screed	0,02	12	2100	2100
PVC flooring	0,02	0,2,	1500	1209

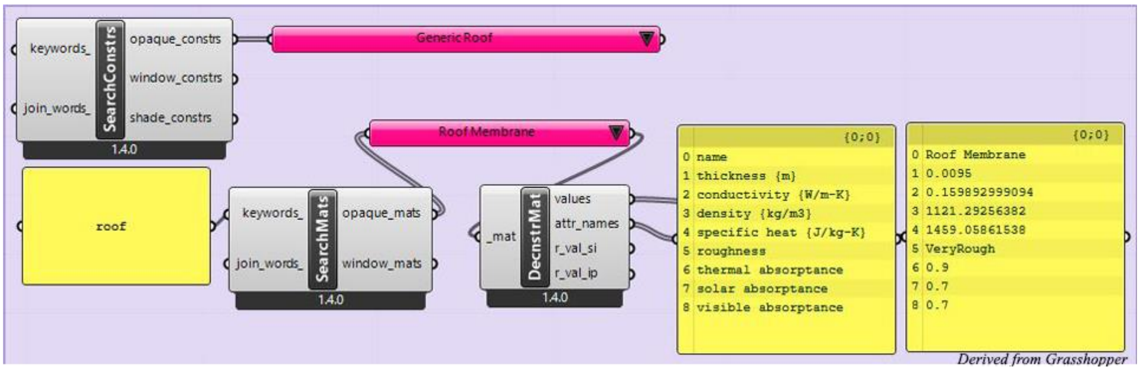

Figure 23: Honeybee Material Library interface

Table 10 indicates the mechanical system properties. The heating set point is 21 C°, while the cooling set point is 26 C° with the reference of the articles [9,15]. There are nine HVAC types for residential buildings in Honeybee HVAC Template. These HVAC templates are residential AC with baseboard electric, residential AC with baseboard gas boiler, residential AC with baseboard central air source heat pump, residential AC with baseboard district hot water, residential AC with baseboard residential forced air furnace, residential AC with no heat, residential heat pump, residential heat pump with no cooling, and residential forced air furnace. In these HVAC templates, the most appropriate type is determined as a Residential AC Boiler baseboard.

There is an explanation for the Honeybee infiltration component. The infiltration rate for a tight building should be 0,0001 (m^3/s per m^2 façade); the rate is 0,0003 (m^3/s per m^2 façade) for an average building; it should be 0,0006 (m^3/s per m^2 façade) for a leaky building. For this research, the infiltration rate is 0,0003 (m^3/s per m^2 façade) according to the average number. The ventilation rate is a numerical value for the design level of ventilation in air changes per hour (ACH) for the selected zones. Therefore, the value is 0,5 ach for living rooms, kitchens, and bedrooms, while 0,1 ach for corridors and toilets.

Table 10: Mechanical properties

Data	*Value*	*Reference*
Heating Set Point	21 C°	[9,15]
Cooling Set Point	26 C°	[9,15]
HVAC Type	Residential AC with baseboard gas boiler	Honeybee HVAC Templates
Infiltration Rate	0,0003 m^3/s per m^2 facade	Honeybee Average Building Infiltration
Ventilation Rate	0,5 ach (for rooms) 0,1 (for toilets, corridors)	[9,15]

The building loads can be categorized as people, lighting and equipment which are represented in Table 11. The Honeybee Load Library provides data for midrise apartments as a building program. There are three generics for the zone programs apartment, office, and corridor. The values include equipment load per area, infiltration rate per area, lighting density per area, number of people per area, ventilation per area, ventilation per person. Figure 24 shows the interface of Honeybee Load Library.

A numerical value for the number of people per square meter of floor area is 0,02 for frequently used spaces like living rooms, kitchens, and bedrooms. Toilets and corridors do not have people loads since the spaces are used rarely. It is estimated that there can be four people in every dwelling unit. The articles [9] and [15] that make an investigation from the Housing Development Association of Turkey, ensure the numerical values.

The equipment loads per area for living rooms, kitchens, and bedrooms is 3,87 W/m^2. The explanation of the Honeybee Load Library equipment load is the desired load per square meter of the floor. The value can range from 2 W/m^2 to 15 W/m^2. 2 W/m^2 can use enough space with one or two computers. 15 W/m^2 represents an office area full of computers. In the research, the equipment load is taken as 3,87 W/m^2 for a residential building, and there is no equipment load for toilets and corridors according to the template of Honeybee.

Table 11: Loads for spaces

Data	*Value*	*Spaces*
People	0,02 people per area (Total: 4 people)	living rooms, kitchens, bedrooms
	0	corridors and toilets
Lighting	10,60 W/m²	living rooms, kitchen, bedrooms, corridors, and toilets
Equipment	3,87 W/m²	living rooms, kitchens, bedrooms
	0	corridors and toilets

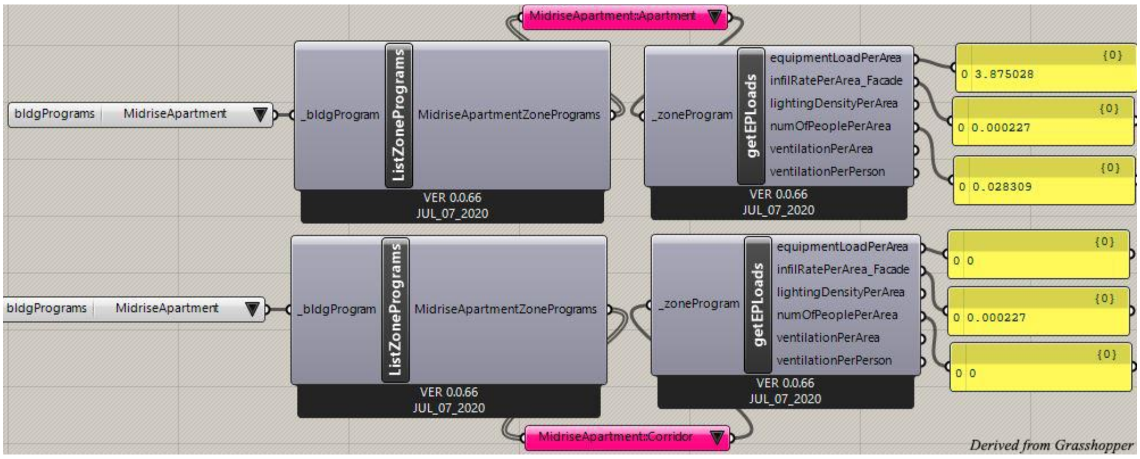

Figure 24: Honeybee Load Library interface

Figure 25 shows the Honeybee Lighting Density Calculator component. The Honeybee Lighting Density Calculator component defines the spaces' lighting load. The input data are lighting level, luminous efficacy, maintenance factor, and coefficient of utilization.

The lighting level represents the value for the required lighting level in the space. 500 lux can be for a typical office area, and 300 lux is for a typical residential space. Therefore, the lighting level is determined as 300 lux. Luminous efficacy is defined in the component as a value between 0 and 100. This represents how well a light source produces visible light in lumens/watt. The component defines the six common options: fluorescent (T5 tube), led screw base lamp, fluorescent (T8 tube), compact fluorescent, incandescent, and candle. Their values are 92, 81, 80, 52, 13.8, 0.3 respectively. For this study, compact fluorescent is selected with a value of 52. A maintenance factor is a number between 0 and 1, representing the frequency of cleaning and repairing. 0,7 is good; 0,65 is the medium value, and 0,55 is poor. The default is set as the medium value. The last input is the coefficient of utilization. It is taken 0,84 for a basic fluorescent strip.

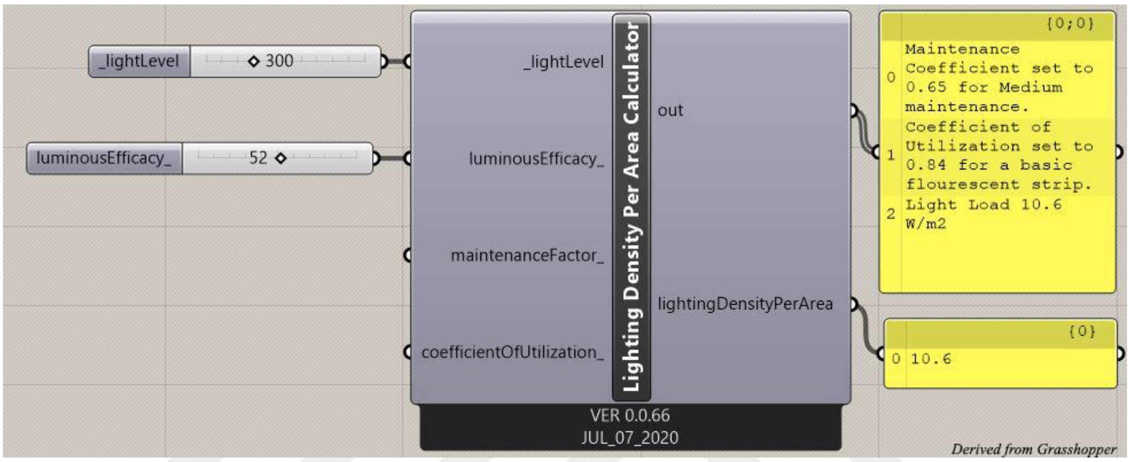

Figure 25: Calculation of lighting load

After determining the building loads, their schedules are developed using the Honeybee Weekly Component, which lists daily values for each day of the week. The schedules are set by considering a general daily routine of a human being—also the overall relationship with each other. Living rooms, kitchens, and bedrooms are frequently used areas. They have people, lighting, and equipment schedules. The corridors and toilets are used rarely in a general daily routine.

For frequently used spaces, there are two separate occupancy schedules for weekends and weekdays. During weekends and summer design days, the occupancy rate is 1.00 between 00.00 a.m.-09.00 a.m., 14.00 p.m.-17.00 p.m., 21.00 p.m.-23.59 p.m. The rate is 0.25 between 10.00 a.m. -13.00 p.m., and 18.00 p.m.-20.00 p.m.. During weekdays and winter design days, the occupancy rate is 1.00 between 0.00 a.m.-08.00a.m., and 18.00 p.m.-23.59 p.m.. The rate is 0.25 between 08.00 a.m. and 17.00 p.m. regarding the possible working hours are considered. For holidays in the year, the occupancy rate is 0.5.

Lighting schedules for the living rooms, kitchens, and bedrooms are identified. During weekends and summer design days, the lighting systems are off until 18.00 p.m. thanks to the sun's movement. At 19.00 p.m. the lighting rate is 0.20. The value is 0.30 and 0.40 at 20.00 p.m., and 21.00 p.m. The lighting rate is 0.50 between 22.00 p.m.- 23.59 p.m.. During weekdays and winter design days, the lighting value is 0.50 between 06.00 a.m.-07.00 a.m. The rate is 0.20, 0.30, 0.40 at 19.00 p.m., 20.00 p.m., 21.00 p.m. respectively. The lighting rate is 0.50 between 22.00 p.m.- 23.59 p.m.. For the other time periods, it is 0.00. During holidays of the year, they are using with the degree of 0,3.

There is a schedule to define usage of equipment for frequently used spaces in a week. The equipment usage value is 0.00 between 0.00 a.m.-05.00 a.m., and 08.00 a.m.-11.00 a.m. The rate is 0.25 between 06.00 a.m.-07.00 a.m., 12.00 p.m.-16.00 p.m., and 22.00 p.m.-23.59 p.m.. It is 0.70 between 17.00 p.m.-21.00 p.m. For holidays, the usage degree of equipment is 0,3.

For corridors and toilets, a lighting schedule is identified. Between 06.00 a.m.-07.00 a.m., and 16.00 p.m.-20.00 p.m. the lighting usage rate is 0.25. For the other time periods, it is 0.00. During holidays of a year, the degree of usage decreases by 0,1. After the physical and thermo-physical properties of the case study urban block, alternative urban block models are developed.

3.1.4 Arrangement of Alternative Urban Block Models

To develop alternative urban block models, the constant parameters are building form, physical-thermophysical properties, number of dwellers, and dwelling units. The four variables are urban morphology, aspect ratio, number of floors, and orientation, which is displayed in Figure 26.

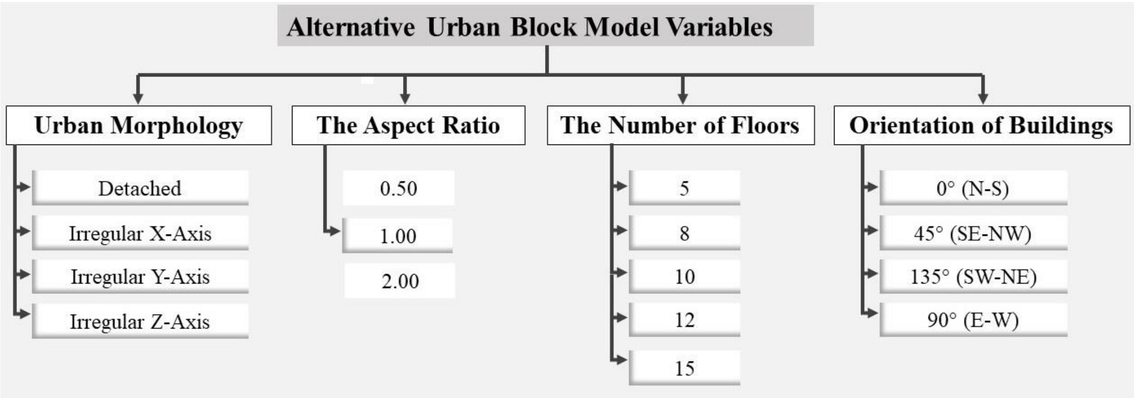

Figure 26: Urban block model variables

Urban morphology is the architectural pattern of the urban block. This research includes two urban morphology patterns: detached form and irregular form. The detached form means that the building in the urban block has the same height. Irregular form means a height diversity in the urban block to provide heterogeneity. The irregular urban pattern has three categories: height diversity along X-Axis, height diversity along Y-Axis, and height diversity along Z-Axis. The buildings in Irregular X-Axis and Irregular Y-Axis are sorted according to the hierarchy of building heights. However, there is not any hierarchical order for Irregular Z-Axis. The only consideration for Irregular Z-Axis is that the same floor heights do not come side by side; they are sorted in a mixed order.

In the research, there are five alternatives for the number of floors: 5 floors, 8- floors, 10- floors, 12- floors, and 15- floors. The aspect ratio is the ratio of height of the building and the distance between buildings. There are three alternatives for aspect ratio: 0.5, 1.00, and 2.00, which is explained in Table 12. The last category is the orientation of buildings. It has four alternatives: 0°,45°,135°, and 90°. Figure 27 shows the diagrammatic explanation of district morphology variables.

Table 12: Calculation of the aspect ratio

Number of floors	*Height (m)*	*Aspect Ratio*		
		0.5	*1.00*	*2.00*
		Space Between Buildings (m)		
5	15	30	15	7,5
8	24	48	24	12
10	30	60	30	15
12	36	72	36	18
15	45	90	45	22.5

While developing the alternative urban block models, there are some critical points to explain.

- The alternative models have a setback distance of 20 m from all directions.
- One of the constant parameters is the number of dwelling units which is 600. The aspect ratio directly impacts the density of the buildings. When the aspect ratio is 0.5, the number of dwelling units does not meet the required number. When it is 2.00, it exceeds the dwelling unit's limit. Therefore, all alternatives need to have an aspect ratio of 1.00, which provides an equal number of dwelling units with the existing situation.
- The placement of the buildings in the parcel needs to have an equal distribution. Aspect ratio is assigned 1.00 for the North and South direction. The buildings are fitted in the parcel for the West and East direction by considering the setback distance.
- The distance between buildings is taken at 30m for irregular urban patterns, which is the mode and the median value according to the numbers in Table 12.

Figure 28 includes the 28 alternative models. In the figure, red shows the 5-floors, green represents 8-floors, blue is 10-story buildings, purple is 12-story buildings, and orange shows the buildings with 15-floors.

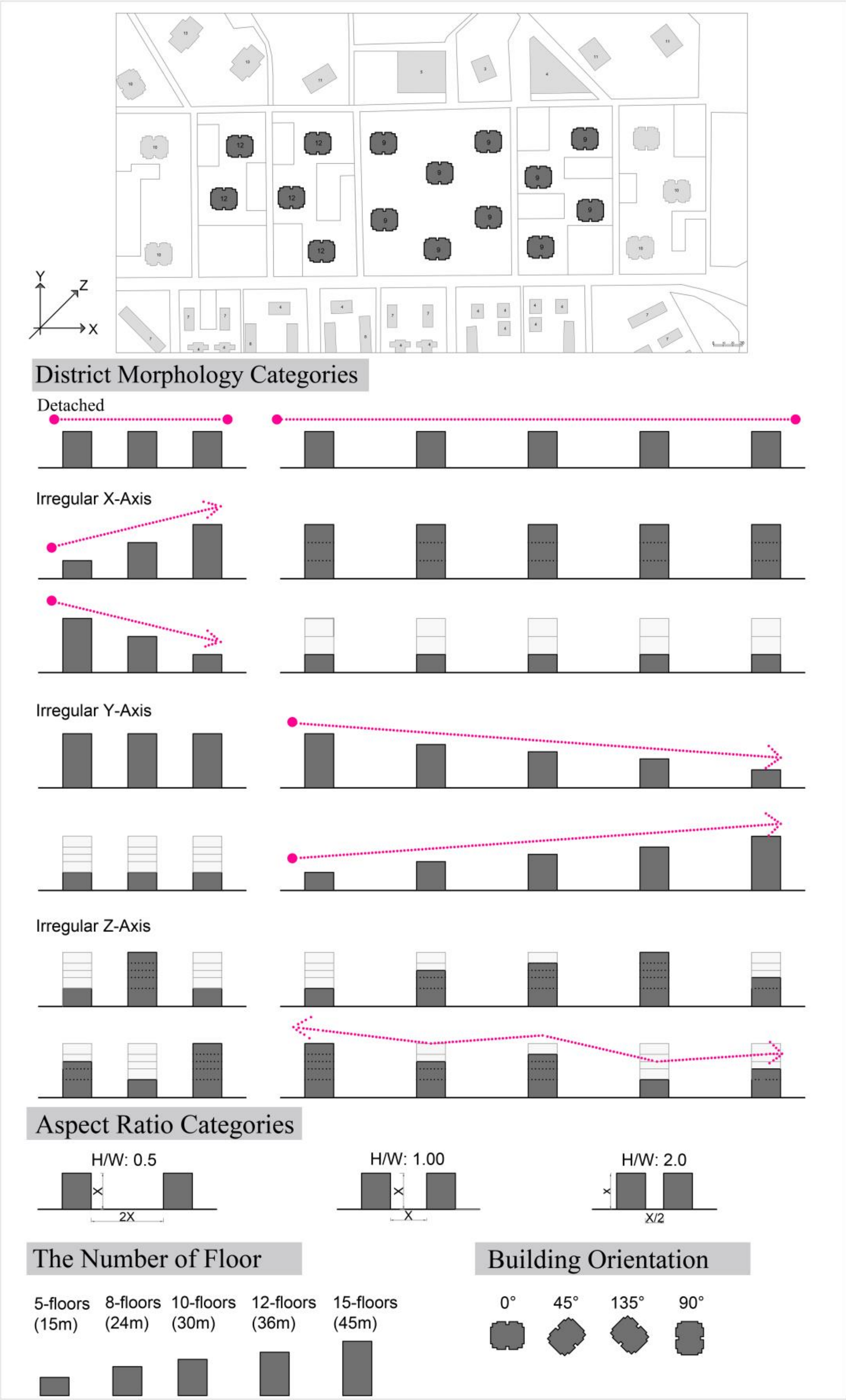

Figure 27: Diagrammatic explanation of district model variables

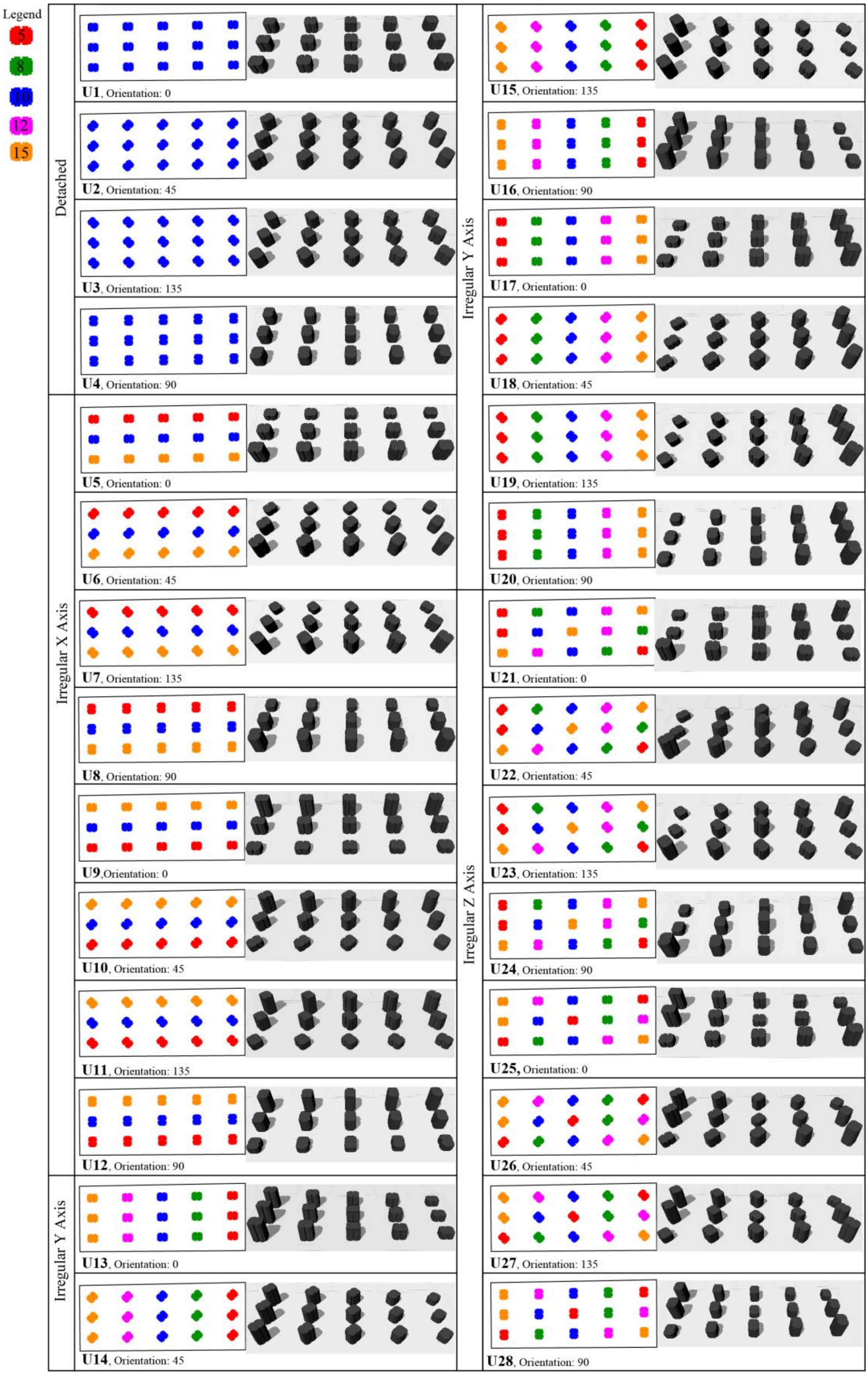

Figure 28: 28 urban block models

3.2 Arrangement of Grasshopper Algorithms

After data collection and organization, the second phase of the thesis methodology is conducting performance simulations. This section includes preparation of simulations scripts in Grasshopper/Rhinoceros Software.

3.2.1 Determination of The Analysis Periods

The weather file is provided form epw.map [94] whose data works with climate.onebuilding.org. The weather file of Ankara is from the meteorological station of 171290 in Etimesgut. It includes 69 years typical meteorological year (TMY) data. The period of record is between 1950 and 2019. The weather file of İzmir belong to 172180 meteorological station in Çiğli. The TMY data includes 71 years period of record which is between 1950 and 2021. The weather file of Ankara and İzmir is downloaded with Ladybug Download Weather component in Grasshopper. It relates to LB Import Stat component to determine the hourly analysis periods. Appendix A1 shows the outputs of LB Import Stat. The component enables to determine extreme cold week, extreme hot week, and typical weeks from weather file.

- For Ankara, the extreme cold week is between 22 December and 5 January; the extreme hot week is 24- 30 August. There are four typical weeks; 22-28 December, 5-11 April, 17-23 August, and 13-19 October.
- For İzmir, the extreme cold week is between 1-7 December; the extreme hot week is 20-26 July. Typical weeks are between 22 December and 5 January, 26 April and 2 May, 8-14 June, 29 September, and 5 October.

To determine a specific day and hour in these weeks, dry bulb temperature is examined for a time interval based on people's active hours. For extreme cold weeks in Ankara and İzmir, the minimum dry bulb temperature is examined between 09.00 and 18.00. The maximum dry bulb temperature is figured out for extreme hot weeks between 08.00 and 21.00. The average value is examined for the typical weeks between 09.00 and 20.00. Table 13 shows the determined hourly periods to ensure the hourly simulations.

Table 13: Determination of hourly analysis periods

Data		*Week*	*Time İnterval*	*Day/Hour*	*Dry Bulb Temperature (C°)*	*Wind Speed (m/s)*	*Wind Direction*
Ankara	Extreme Cold	22 Dec- 5 Jan	09.00-18.00	2 Jan/ 11.00	-8.0	2.6	260
	Extreme Hot	24 -30 Aug	08.00-21.00	26 Aug/ 10.00	35.3	4.1	45
	Typical	13-19 Oct	09.00-20.00	15 Oct/ 10.00	14.0	3.1	340
İzmir	Extreme Cold	1-7 Dec	09.00-18.00	5 Dec/ 10.00	1.0	1.0	350
	Extreme Hot	20-26 Jul	08.00-21.00	22 July/ 16.00	36.8	9.3	338
	Typical	29 Sep-5 Oct	09.00-20.00	1 Oct/ 10.00	22.0	0.5	50

- For Ankara, the minimum dry bulb temperature is -8.00 C° on 2 January at 11.00 a.m. for the extremely cold week. The maximum dry bulb temperature for the extremely hot week is 35.3 C° on 26 August at 10.00. The average value is about 14 C° on 15 October at 10.00 a.m.

- For İzmir, the minimum dry bulb temperature is 1.00 C° on 5 December at 11.00 a.m. for the extremely cold week. The maximum dry bulb temperature for the extremely hot week is 36.8 C° on 22 July at 16.00 p.m. The average value is about 22 C° on 1 October at 10.00 a.m.

3.2.2 Achievement of Solar Radiation Simulation Script

To achieve the solar radiation algorithm, Ladybug Tools is utilized in Grasshopper. The tool, which is written in Python, visualizes and analyzes weather data to develop radiation, shadow, and view analysis. Ladybug 1.4.0 is used to conduct solar radiation analysis. There are five steps to developing a solar radiation script: identifying weather data and analysis period, providing the input data of sky matrix and incident radiation, and reading the simulation results. Appendix A2 shows the solar radiation script from the Grasshopper interface.

- To define weather data in the Grasshopper interface LB Download Weather is used by a supported component of LB EPWmap. LB Import EPW components provide the data of location, direct normal radiation, and diffuse horizontal radiation. These are the inputs of the Sky Matrix component.
- LB Cumulative Sky Matrix calculates radiation for each patch of the sky dome. The output of the component is the first input of incident radiation.
- LB Incident Radiation component calculates the radiation on a specified geometry based on sky matrix data in kWh/m². Therefore, the inputs are geometry study, the geometry of surroundings, and the grid size of the test surface, which is 5 m. The analysis output is read using the LB Special Heat map with a mesh surface. Also, the arithmetic mean of the results is calculated using the Average component for yearly and hourly results.

3.2.3 Development of Energy Performance Simulation and Indoor Comfort Algorithm

Ladybug Tools includes Honeybee which supports detailed daylighting and thermodynamic modelling by integrating different simulation engines like using Radiance for daylight simulations and using EnergyPlus and OpenStudio for energy models. The algorithm of energy performance simulation and indoor comfort simulation are developed simultaneously using Honeybee 1.4.0 in Grasshopper.

There are six steps: defining zones in the Grasshopper interface, defining construction properties, determining zone loads and their schedules, creating the Honeybee Model, identifying weather data, and organizing the inputs of the Honeybee Simulation Parameter.

Honeybee Simulation Parameter and Honeybee Model are combined with OpenStudio Model using the Honeybee Energy plug-in to read the energy performance results. The results of energy performance simulation enable with the unit of kWh/m² and kWh. The analysis is taken both yearly and hourly.

Honeybee Simulation Parameter and Honeybee Model are combined with HB PMV Comfort Map to read the indoor comfort results. The simulation output enables the results of operative temperature and predicted mean vote (PMV) with a 7-point Likert rating system which is cold, cool, slightly cool, neutral, slightly warm, warm, and hot. The indoor comfort analysis is taken for hourly periods with extreme cold, extremely hot, and typical.

The steps are mentioned below. Figure 29 shows the organization of energy performance and indoor comfort scripts.

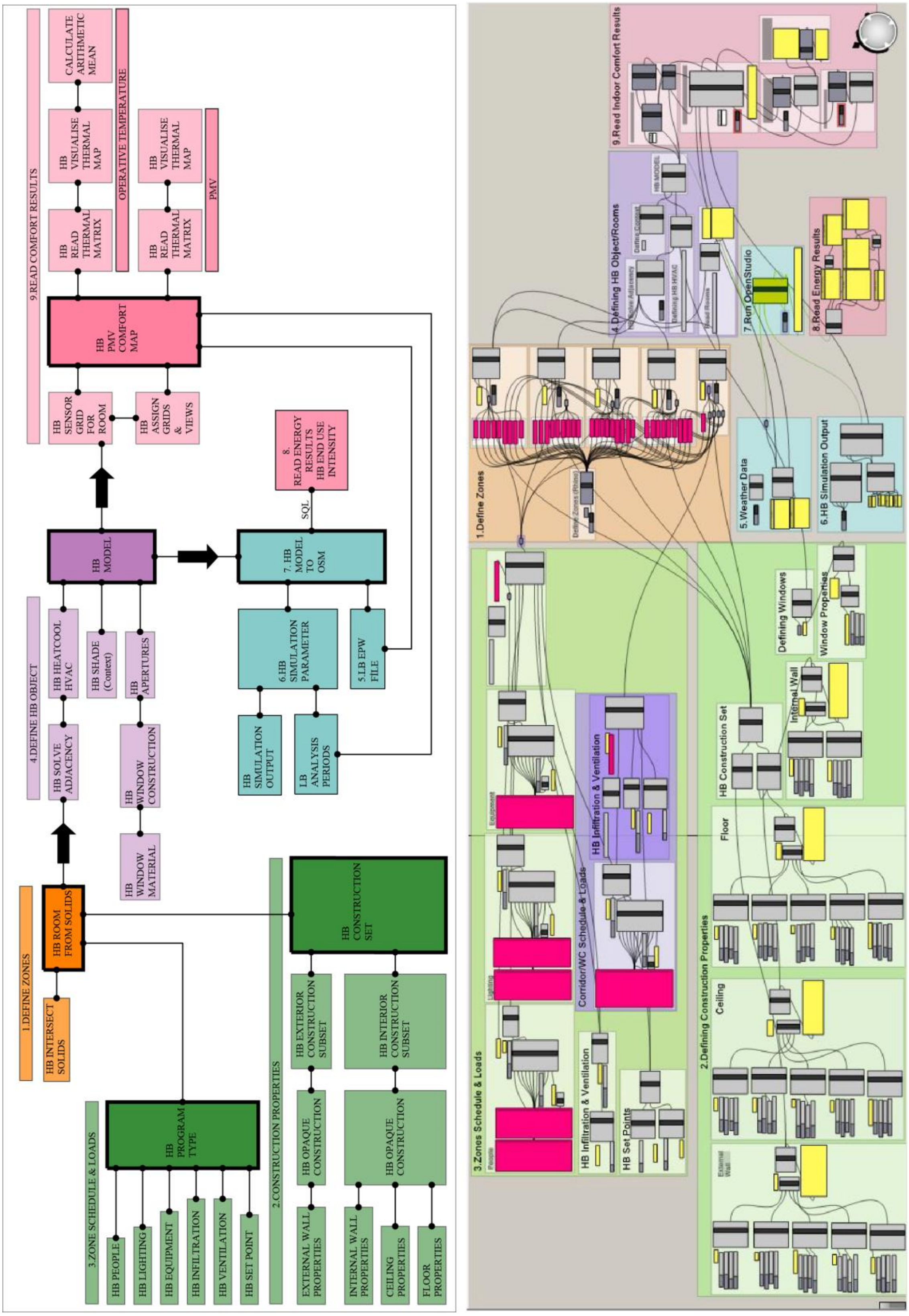

Figure 29: Algorithm of energy performance and indoor comfort simulation

- 1- Define Zones: The zones are determined based on the floor plan of buildings which was mentioned in Figure 25. The zones are living rooms, bedrooms, kitchens, toilets, and an apartment corridor. They are modeled in Rhinoceros 6.0. The zones are imported to the Grasshopper interface using HB Intersects Solids component. The HB Room from Solid component creates Honeybee rooms from solid. Each zone is mapped in EnergyPlus 9.4.0 and OpenStudio 3.5.1. The input data of the Room Solid component is the geometry of the zones, the construction set of building materials, the program of the zones, and the data of conditioned or unconditioned with a Boolean toggle. Appendix A3 shows the Grasshopper organization of the first phase.
- 2- Determination of Construction Properties: The building material characteristics and the material properties was organized in Table 8 and Table 9. The data of opaque materials are organized based on the tables. The Honeybee Construction Set includes two main inputs: Exterior Subset and Interior Subset. The Honeybee Exterior Construction Subset has the thermophysical properties of the exterior wall. The Honeybee Interior Construction Subset consists of the thermophysical properties of the interior wall, ceiling, and interior floor. They have organized thanks to the component of HB Opaque Construction. Appendix A4 shows the visual explanation to define construction properties in Grasshopper.
- 3-Development of Zone Loads and Schedules: the input data of the Honeybee Program Type component is the base program of zones, HB People, HB Lighting, HB Electric equipment, HB Infiltration, HB Ventilation, and HB Setpoints. Their values are taken from Table 12. A detailed explanation of load values and their schedules are detailly mentioned in Section 3.1.3. The base program of frequently

used zones is "*Midrise Apartment: Apartment"*, the base program of corridors and toilets are *"Midrise Apartment: Corridors".* Appendix A5 shows the organization of zone loads and their schedule in Grasshopper.

- 4-Definition of Honeybee Object: The inputs of the HB Model are rooms, shades, and apertures. The Honeybee Solve Adjacency brings the series of zones together. They are combined with HB HeatCool HVAC. The type of HVAC is mentioned in Table 10. Honeybee Shade is the component to define surrounding buildings. HB Aperture includes the data of the glazing system. The data in HB Window Construction component is based on the explanation in the Section 3.1.3.. Appendix A6 shows the organization of the phase in Grasshopper.
- 5- Organization of Weather Data: the epw file of Ankara and İzmir is downloaded using LB Download Weather.
- 6-Organisation of Simulation Output: HB Simulation Parameter carries a set of Energy Plus simulation settings. The input data of components are the simulation output and run period. The simulation outputs are zone energy use, HVAC energy use, gains and losses, comfort metrics, and surface temperature. The run period is organized with LB Analysis Period component. Appendix A7 shows the organization of steps five and six.
- 7-Running Open Studio for Energy Performance Simulation: The HB Model to OSM component translates the script data into an IDF file to run Energy Plus.
- 8-Reading Energy Results: HB End Use Intensity provides information from the Energy Plus SQL file. The values are in kWh/m² and kWh. Appendix A8 shows the interface of steps seven and eight.

- 9-Reading Indoor Comfort Results: The HB Sensor Grid from Rooms generates a sensor grid on the floor of honeybee rooms. The grid size is determined as 0.5 m. The sensors have a 0.8 m height from floor level. It is connected to HB Assign Grids and Views to add radiance sensor grids to Honeybee Model. HB PMV Comfort Map computes operative temperature and predicted mean vote thermal comfort. It uses the data of Energy Plus to obtain surface temperature, indoor air temperature, and humidity value. The outdoor air temperature, relative humidity, and airspeed data are taken from the weather file. The inputs of the components are HB Model, weather file, analysis period, metabolic rate, and clothing level. The usage of curtains is ignored while developing HB Model. The default value in the component for metabolic rate is 1.1 for seated and typing.

  The clothing level is 0.7 for pants and a long sleeve shirt as a default value. Therefore, 0.7 is taken for typical weeks, 0.5 for extremely hot weeks, and 0.9 for extreme cold weeks.

  The outputs of the HB PMV Map are operative temperature and PMV, which HB Read Thermal Matrix and HB Visualize Thermal Map can read. For the operative temperature results, the average number is also calculated. The indoor comfort simulation was run with Python and Queenbee. Appendix A9 shows the structure of the step for reading indoor comfort results.

3.2.4 Development of Computational Fluid Dynamic Simulation Script

The computational fluid dynamic (CFD) script is developed in Butterfly 0.0.05, in Grasshopper. The tool includes an object-oriented python library that creates and runs air flow simulations using OpenFOAM. There are eight phases to develop computational fluid dynamic simulation; importing weather data and organizing the analysis period, defining geometry to simulate, creating a wind tunnel, connecting the butterfly solution component by indicating the test surface and probes, visualizing the results, and calculating the average wind velocity. Appendix A10 shows the structure of the CFD script.

- 1- Importing weather data and organization of run period: The weather data is imported using LB Download Weather. The output of the component is the input of LB Import EPW. According to the EPW file, the component provides the necessary data on wind speed and wind direction. The run period is organized using LB Analysis Periods. Appendix A11 shows the interface in the software.

- 2-Definition of geometry and creation of wind tunnel: Create Butterfly Geometry defines test objects in Grasshopper. The Butterfly Object is the input of the Butterfly Create Case from Tunnel. The other inputs are wind vector, landscape, and tunnel params. The wind vector relates to Butterfly Wind Vector, whose inputs are wind speed and direction. To define the landscape, there are seven options: sea, smooth, open, roughly open, rough, very rough, skimming, and chaotic. Also, there is an integer between 0 and 7 for each alternative. For this research, the landscape is defined as rough, 0.25. The tunnel params are the output of Butterfly Wind Tunnel Parameters. The created wind tunnel is the input of Butterfly wind Tunnel Grading which obtains a 3D grading system. The cell size is 5m. To define a mesh, Butterfly Block Mesh, and Butterfly SnappyHexMesh components are used by specifying the global refine level (1,1). Appendix A12 shows the organization of components for the second step.

- 3-Definition of Butterfly Solution: The outputs of Butterfly SnappyHexMesh connected with Butterfly Solution, which runs the CFD simulation with OpenFOAM. The other inputs are recipe and solution parameters. The data for the recipe is provided by Butterfly Steady Incompressible Recipe, whose output is a script variable Python. The data for the solution parameter is obtained using Butterfly Solution Parameters and Butterfly ControlDict. The output of the Butterfly Solution relates to Butterfly Load Probes Value and Butterfly plot Residuals. Appendix A13 shows the structure of step 3.
- 3-Creating Test Surface and Probes: To define the probes for Butterfly Solution Parameters, the test surface is defined in Rhinoceros and imported to Grasshopper using LB Generate Point Grid. The grid size is 5m. The test surface is 1.50m above the ground. The inputs of Butterfly probes are points and the field value. The points are taken from LB Generate Point Grid. The field is "U" which means the measurement of wind velocity. Appendix A14 displays the components' interface.
- 4-Reading Results: It is possible to read results on vectoral visualization using the Gradient component. It is the output of the Butterfly Load Probes Value. According to the wind velocity (m/s) results, the limits are between 0 and 10. Also, a calculation of average wind velocity (m/s) is conducted to discuss the general wind velocity in the district. Appendix A15 shows the organization of the components.

3.2.5 Achievement of Outdoor Comfort Script

The outdoor comfort script is developed by following five steps using Ladybug 1.4.0 plug-in. The steps are importing weather data and defining the analysis period, defining test surface area, developing LB Human to Sky Relation, calculating outdoor solar Mean Radiant Temperature (MRT), and calculating Universal Thermal Climate Index (UTCI). The result of the analyses is discussed with the average temperature value whose unit is C°. Also, LB Spatial Heat Map component visualizes the result with a mesh surface on site. Appendix A16 shows the outdoor comfort script.

- The weather file is imported with LB Import EPW, and LB Analysis Period is used to ensure the run period.
- The test surface is determined around the district parcel. It is 1.5m above the ground level. The test points are ensured with LB Generate Point Grid which is 5m.
- LB Human to Sky Relation provides a calculation by using input parameters to ensure the relationship between human geometry and the sky. The input parameters are the test surface, site location, and context buildings. The output of the component is the input of LB Outdoor Solar MRT.
- LB Outdoor Solar MRT calculates Mean Radiant Temperature by estimating the impact of shortwave solar to determine longwave radiant exchange. It is defined that the component uses SolarCal, which is the model ASHRAE-55, for calculations. The inputs are location data, surface temperature, direct normal radiation, diffuse horizontal radiation, and horizontal infrared radiation, which are the outputs of LB Import EPW. The two inputs are fraction body exposure and sky exposure. These are the outputs of LB Human to Sky Relation. The last input is the ground reference which is between 0 and 1 to represent the reflectance of the floor. The average number is considered (0.5). The output of the calculation is MRT.

- LB UTCI Comfort calculates Universal Thermal Climate Index. It is an outdoor thermal comfort model to define outdoor temperature sensation (C°). The input for the calculation is air temperature, MRT, relative humidity, and wind velocity.

3.2.6 Development of Renewable Energy Integration Script

ClimateStudio which is a new parametric workflow in Grasshopper, supports daylight simulation, energy modelling toolkit, visual and thermal comport analysis. The renewable energy integration algorithm using ClimateStudio 1.1.9 is represented in Appendix A17. There are four steps to establish the script.

- 1-Definition of Geometry: There are two geometries like the surface of photovoltaics and the geometry of context buildings.
- 2-Runing Climate Studio PV panel component: The inputs are PV panels, Shade, Working Directory, Location, and Run. PV panels include the panel geometry, efficiency, and area. The efficiency is the default value (0,15). The area means the effective area covered with PV cells. It is the default value with 0,80. Shade relates with the context geometry. The location is connected to the LB Download Weather component. The output of ClimateStudio PV is the Model.
- 3-Loading CS PV Results: The Load CS PV Result needs Model,Normalize and Run. The model is to the output of the ClimateStudio PV component. Normalize works with Boolean Toggle. True means the result is kWh/m². False means the unit of the results is kWh. The component’s output provides results for panel-produced electricity. The simulation run with SOLEMMA and EnergyPlus9.4.0.
- 4-Reading Results: The results are readable as text thanks to the connection with the Panel. By using ClimateStudio XY Plot, the results are displayed with a graph.

CHAPTER IV

RESULTS and DISCUSSION

In Chapter III, the methodology of the thesis is mentioned in a detailed way. This section includes the results of performance simulations and comparative assessment process. The performance simulation results consist of analyzing the existing situation and 28 alternative district models about solar radiation and energy performance. Their analysis periods are both yearly and hourly.

After determining the most efficient urban block models based on the results of performance analysis, the comparative assessment process results are discussed. This process tests the district models regarding CFD simulations and outdoor and indoor comfort performances. Their analysis period is hourly. This analysis determines the optimum district models for Ankara and Izmir to integrate photovoltaic panels to enhance district energy performance. Therefore, yearly simulations are conducted to analyze the performance of photovoltaic panels. The results show the best optimum urban block model for different climatic zones.

4.1 Performance Simulations

The results of performance simulations have two primary analyses: solar radiation and energy performance. Their results are discussed below.

4.1.1 Solar Radiation

4.1.1.1 Yearly

Table 14 shows the yearly results of average solar radiation for Ankara, and İzmir. For Ankara,the existing case study district has an average of 1196.47 kWh/m² solar radiation. When the climatic property of Ankara is considered, the maximum solar radiation is beneficial. For detached models, the maximum solar radiation is 1197.19 kWh/m² with the U1 alternative. For Irregular X-Axis, the maximum result is 1214.58 kWh/m² with the U9 scenario. For Irregular Y-Axis, the maximum result is 1206.18 kWh/m² with the U17 block model. The maximum yearly solar radiation for Irregular Z-Axis is 1207.72 kWh/m². All the maximum results have a 0° orientation. When buildings in the parcel have 0° orientation, the solar radiation has the highest results. It has minimum results when the orientation of buildings has 90° orientation. Among all results, the yearly solar radiation is minimum for the U3 block model, and the maximum annual solar radiation belongs to the U9 model. Appendix A18 shows the yearly solar radiation results for Ankara.

Since Izmir has a warmer climate than Ankara, the solar radiation results are higher than Ankara's. According to the climatic conditions of İzmir as a hot-humid climate, the minimum solar radiation is advantageous for İzmir. The result of the yearly solar radiation simulation is 1279.63 kWh/m² for the existing case study. The minimum result for detached alternatives is the U3 alternative with 1272.47 kWh/m². The building orientation of the U3 alternative is 135°. For Irregular X-Axis, the minimum result is 1277.81 kWh/m² with the U8 alternative. The buildings have a 90° orientation. For Irregular Y-Axis, the minimum result is 1281.09 kWh/m² with U18 and U19 alternatives. The orientation of buildings 45 and 135, respectively. For

Irregular Z-Axis, the minimum result is 1279.60 kWh/m² with the U24 alternative. The direction of buildings is 90°. Among the 28 urban options, the maximum yearly solar radiation is 1298.55 kWh/m² with the U9 district model. The minimum annual solar radiation is 1272.55 kWh/m² with the U3 scenario. Appendix A19 shows all results with a heat map in İzmir.

Table 14: Yearly solar radiation results for Ankara, and İzmir

Average Solar Radiation(kWh/m²) Yearly Results			
Urban Scenario		*Ankara*	*İzmir*
Existing	**U0**	**1196.47**	**1279.63**
Detached	U1	1197.19	1280.12
	U2	1190.96	1272.55
	U3	1190.87	1272.55
	U4	1192.46	1274.36
Irregular X-Axis	U5	1212.71	1285.52
	U6	1196.93	1278.58
	U7	1196.32	1277.88
	U8	1196.00	1277.81
	U9	1214.58	1298.55
	U10	1208.15	1290.75
	U11	1207.88	1290.60
	U12	1208.70	1291.50
Irregular Y-Axis	U13	1205.69	1289.28
	U14	1200.02	1282.12
	U15	1199.85	1281.93
	U16	1199.44	1281.56
	U17	1206.18	1289.14
	U18	1199.33	1281.09
	U19	1199.34	1281.09
	U20	1199.36	1281.37
Irregular Z-Axis	U21	1203.45	1286.56
	U22	1197.97	1279.81
	U23	1197.56	1279.35
	U24	1197.62	1279.60
	U25	1207.72	1291.07
	U26	1200.70	1282.74
	U27	1200.94	1283.00
	U28	1201.36	1283.59

4.1.1.2 Hourly

Table 15 shows the hourly simulation results for Ankara. The maximum solar radiation is beneficial.

Table 15: Hourly solar radiation results for Ankara

ANKARA Average Solar Radiation (kWh/m²)				
Urban Scenario		*Hourly Results*		
		Extreme Cold (2 Jan. 11.00)	*Extreme Hot (26 Aug. 10.00)*	*Typical (15 Oct. 10.00)*
Existing	**U0**	**0.1396**	**0.5132**	**0.3244**
Detached	U1	0.1404	0.5096	0.3240
	U2	0.1401	0.5130	0.3306
	U3	0.1405	0.5229	0.3409
	U4	0.1406	0.5085	0.3262
Irregular X-Axis	U5	0.1409	0.5131	0.3227
	U6	0.1407	0.5171	0.3295
	U7	0.1410	0.5267	0.3383
	U8	0.1408	0.5106	0.3234
	U9	0.1427	0.5118	0.3386
	U10	0.1424	0.5159	0.3446
	U11	0.1427	0.5259	0.3539
	U12	0.1427	0.5117	0.3401
Irregular Y-Axis	U13	0.1417	0.5145	0.3302
	U14	0.1414	0.5181	0.3366
	U15	0.1418	0.5280	0.3462
	U16	0.1417	0.5127	0.3319
	U17	0.1414	0.5113	0.3275
	U18	0.1411	0.5142	0.3331
	U19	0.1413	0.5247	0.3430
	U20	0.1413	0.5093	0.3282
Irregular Z-Axis	U21	0.1413	0.5127	0.3286
	U22	0.1411	0.5156	0.3348
	U23	0.1414	0.5259	0.3448
	U24	0.1413	0.5101	0.3301
	U25	0.1417	0.5141	0.3283
	U26	0.1413	0.5164	0.3352
	U27	0.1417	0.5267	0.3444
	U28	0.1417	0.5112	0.3304

The existing urban district has 0.1396 kWh/m² solar radiation for the extreme cold hour. The maximum result is 0.1427 kWh/m² with U9 urban model. The case study has 0.5132 kWh/m² solar radiation for extremely hot periods, while the maximum result is 0.5267 kWh/m² with U7 and U27 models. For a typical hour, the case model has 0.3244 kWh/m². The maximum result belongs to U11 with 0.3559 kWh/m². Appendix A20-A23 represent the hourly solar radiation maps. These figures highlight the solar radiation change through the impact of the district's morphology character. The effect of height diversity on a district's solar radiation is also readable, especially for extremely hot and typical periods.

Table 16 gives the hourly simulation results for İzmir. For the existing situation, the extreme cold, extremely hot, and typical hour results are 0.0734 kWh/m², 0.4794 kWh/m², and 0.3587 kWh/m², respectively. The proper result of this climate is taking the minimum result for the extremely hot hour, the maximum for extreme cold, and the typical hour. The maximum result for extreme cold and typical hours are 0.0782 kWh/m² and 0.3884 kWh/m² with the U11 alternative. The minimum result for the extremely hot hour is 0.4605 kWh/m² with the U3 alternative. Appendix A24-A27 represent the hourly solar radiation maps of the alternatives regarding detached, Irregular X-Axis, Irregular Y-Axis, and Irregular Z-Axis respectively.

Table 16: Hourly solar radiation results for Izmir

IZMIR Average Solar Radiation (kWh/m²)				
Urban Scenario		*Hourly Results*		
		Extreme Cold (5 Dec. 09.00)	*Extreme Hot (22 Jul. 16.00)*	*Typical (1 Oct. 10.00)*
Existing	**U0**	**0.0734**	**0.4794**	**0.3587**
Detached	U1	0.0693	0.4771	0.3542
	U2	0.0707	0.4635	0.3771
	U3	0.0742	0.4605	0.3771
	U4	0.0686	0.4662	0.3533
Irregular X-Axis	U5	0.0686	0.4799	0.3567
	U6	0.0701	0.4680	0.3559
	U7	0.0734	0.4642	0.3784
	U8	0.0681	0.4702	0.3540
	U9	0.0737	0.4799	0.3672
	U10	0.0750	0.4679	0.3757
	U11	0.0782	0.4643	0.3884
	U12	0.073	0.4697	0.3664
Irregular Y-Axis	U13	0.0718	0.4782	0.3638
	U14	00733	0.4654	0.3727
	U15	0.0765	0.4627	0.3855
	U16	0.0711	0.4675	0.3626
	U17	0.0691	0.4850	0.3564
	U18	0.0704	0.4714	0.3648
	U19	0.0738	0.4686	0.3780
	U20	0.0683	0.4734	0.3546
Irregular Z-Axis	U21	0.705	0.4790	0.3594
	U22	0.0719	0.4671	0.3682
	U23	0.0751	0.4642	0.3817
	U24	0.0697	0.4691	0.3580
	U25	0.0705	0.4817	0.3602
	U26	0.0719	0.4677	0.3696
	U27	0.0751	0.4650	0.3819
	U28	0.0700	0.4699	0.3594

4.1.2 Energy Performance

The energy performance results are compared by calculating primary energy. The formula for total primary energy calculation is shown in equation (1) which is below. Total end uses of electricity include loads of cooling, interior lighting, electric equipment, residential HVAC fans, and pumps. The total end uses of natural gas include the load of heating.

$$\begin{aligned} &Total\ Primary\ Energy \\ &\quad = \left(Total\ End\ Uses\ Electricity\ \left(\frac{kWh}{m^2}\right) x(2{,}36)\right) \\ &\quad + Total\ End\ Uses\ Natural\ Gas\ (kWh/m^2) \end{aligned} \tag{1}$$

When building energy simulation was performed, two ways were tried to determine the most accurate representation. Firstly, the middle floor of the building in the center of the parcel is taking reference to determine the energy performance of the case district. The second way is a mixed approach. The energy results in the parcel were obtained by referring to the buildings' top-right, top-left, bottom-right, bottom-left, and middle floor. In the calculation for the second approach, the representation of the same accepted buildings is shown in Figure 30. The two approaches' total primary energy (T.P.E) results are compared. The unit of the simulation result is kWh/m². To find the Total District Primary Energy, the value is converted to kWh by multiplying the area of one floor, which has 578.43m². The number is multiplied by the total number of housing units, which is 150.

Figure 30: Determination of reference building

Table 17 shows the calculation of the district's total primary energy in Ankara based on Approach 1 which is taking the middle floor of the building which is in the middle of the parcel. The district's total primary energy is 18,023,398.7 kWh. Table 18 shows the result of the district's total primary energy for Ankara based on approach 2. The result is 18,030,493.12 kWh. The difference between Approach 1 and Approach 2 is 0,036%.

Table 17: Calculation of district total primary energy according to Approach1 for Ankara

Approach 1 Reference of middle building	*Ankara (yearly)*	*T.P.E. (kWh/m²)*	*T.P.E. (kWh)*	*Total Number of Floor*	*District T.P.E. (kWh)*
	U0	207.727	120,155.99	150	18,023,398.7

Table 18: District total primary energy according to Approach 2 for Ankara

<table>
<tr><td rowspan="7">Approach 2- Mixed Reference

Ankara (yearly) U0</td><td>Reference Building</td><td>T.P.E. (kWh/m²)</td><td>T.P.E. (kWh)</td><td>Total Number of Floor</td><td>Reference Buildings T.P.E. (kWh)</td></tr>
<tr><td>Top-Right</td><td>207.7934</td><td>120,193.93</td><td>27</td><td>3,245,236.28</td></tr>
<tr><td>Bottom-Right</td><td>207.2490</td><td>119,879.06</td><td>27</td><td>3,236,734.68</td></tr>
<tr><td>Top-Left</td><td>208.4879</td><td>120,595.69</td><td>36</td><td>4,323,126.03</td></tr>
<tr><td>Bottom-Left</td><td>207.608</td><td>120,086.83</td><td>33</td><td>3,962,865.53</td></tr>
<tr><td>Middle</td><td>207.7278</td><td>120,155.99</td><td>27</td><td>3,244,211.78</td></tr>
<tr><td colspan="3">District Total Primary Energy</td><td>150</td><td>18,030,493.12</td></tr>
</table>

Table 19 shows the district's total primary energy calculation in İzmir based on Approach 1. The district's total primary energy is 12,819,270.93 kWh. Table 20 shows the result of the district's total primary energy for İzmir based on approach 2. The result is 12,825,387.07 kWh. Approach 2 is 0,05% more than the difference between Approach 1.

According to the comparison of the two approaches for Ankara and İzmir, the results are very close. Therefore, it is determined that the energy calculations are conducted based on Approach 1 by taking the middle building as the reference of the district since there can be advantages in time efficiency.

Table 19: Calculation of district total primary energy according to Approach1 for İzmir

<table>
<tr><td rowspan="2">Approach 1 Reference of middle building</td><td>Izmir (yearly)</td><td>T.P.E. (kWh/m²)</td><td>T.P.E. (kWh)</td><td>Total Number of Floor</td><td>District T.P.E. (kWh)</td></tr>
<tr><td>U0</td><td>147.747</td><td>85,461.80</td><td>150</td><td>12,819,270.93</td></tr>
</table>

Table 20: District total primary energy according to Approach 2 for İzmir

Approach 2- Mixed Reference Izmir (yearly) U0	*Reference Building*	*T.P.E. (kWh/m²)*	*T.P.E. (kWh)*	*Total Number of Floor*	*Reference Buildings T.P.E. (kWh)*
	Top-Right	147.7231	85,447.50	27	2,307,082.70
	Bottom-Right	147.4055	85,263.77	27	2,302,121.92
	Top-Left	148.2634	85,760.04	36	3,087,361.61
	Bottom-Left	147.8061	85,495.51	33	2,821,352.07
	Middle	147.7478	85,461.80	27	2,307,468.77
	District Total Primary Energy			150	12,825,387.07

4.1.2.1 Yearly

Table 21 displays the yearly energy performance for the middle floor of the central building in the parcel in Ankara. For the current case study, the primary energy for electricity (P.E.E) is 35.234 kWh/m². The primary energy for natural gas (P.E.N.) is 172.493 kWh/m². The total primary energy (T.P.E.) is 207.727 kWh/m². Among the results, the minimum P.E.E. is 34.99 kWh/m² with the alternative of U2. The minimum P.E.N. is 170.183 kWh/m² with U28 model. The minimum T.P.E. belongs to U9 with 207.504 kWh/m².

Table 22 shows the yearly energy performance results for Izmir. For the existing situation, the P.E.E is 46.510 kWh/m², and the P.E.N is 101.237 kWh/m². The T.P.E is 147.747 kWh/m². When the results of the existing case block in Ankara are compared with those in Izmir, the result of P.E.E. in Izmir is more than that in Ankara. However, the results for P.E.N. and T.P.E for Izmir are lower than the results for Ankara. Therefore, it can be said that the necessity of electricity in İzmir is more critical than in Ankara. Still, the heating load in Ankara is crucial because of the climatical differences between the cities.

Among the urban model alternatives, the minimum P.E.E. is the U3 alternative with

30.568 kWh/m². The minimum P.E.N. is 99.309 kWh/m² with U28. According to T.P.E., the minimum result is 132.120 kWh/m² with the U3 alternative.

Table 21: Yearly energy performance results for Ankara

ANKARA Energy Performance (kWh/m²)							
Urban Scenario		*Yearly Results*					
		Heating (kWh/m²)	*Electricity (kWh/m²)*	***P.E.E. (kWh/m²x2,36)***	***P.E.N. (kWh/m²)***	***T.P.E. (kWh/m²)***
Existing	**U0**	172.493	14.930	**35.234**	**172.493**	**207.727**
Detached	U1	172.795	14.910	35.187	172.795	207.982
	U2	172.949	14.830	34.998	172.949	207.947
	U3	172.78	14.944	35.267	172.78	208.047
	U4	172.867	14.925	35.233	172.867	208.090
Irregular X-Axis	U5	171.936	18.383	43.383	171.936	215.319
	U6	174.582	14.940	35.258	174.582	209.840
	U7	174.443	14.963	35.312	174.443	209.755
	U8	176.486	14.934	35.244	176.486	211.730
	U9	172.281	14.925	35.223	172.281	207.504
	U10	172.469	14.944	35.267	172.469	207.736
	U11	172.248	14.968	35.324	172.248	207.572
	U12	172.291	14.939	35.256	172.291	207.547
Irregular Y-Axis	U13	172.839	14.910	35.187	172.839	208.026
	U14	172.978	14.900	35.164	172.978	208.142
	U15	172.829	14.944	35.267	172.829	208.096
	U16	172.887	14.925	35.233	172.887	208.110
	U17	172.824	14.906	35.178	172.824	208.002
	U18	173.007	14.930	35.234	173.007	208.241
	U19	170.250	18.407	43.440	170.250	213.690
	U20	172.882	14.925	35.223	172.882	208.105
Irregular Z-Axis	U21	173.597	14.853	35.053	173.597	208.650
	U22	173.756	14.867	35.086	173.756	208.842
	U23	170.985	18.341	43.284	170.985	214.369
	U24	173.602	14.867	35.086	173.602	208.688
	U25	172.608	14.963	35.312	172.608	207.920
	U26	172.781	14.987	35.369	172.781	208.150
	U27	172.608	15.002	35.404	172.608	208.012
	U28	170.183	18.441	43.520	170.183	213.703

Table 22: Annual energy performance results for İzmir

IZMIR Energy Performance (kWh/m²)							
Urban Scenario		*Yearly Results*					
		Heating (kWh/m²)	*Electricity (kWh/m²)*	***P.E.E. (kWh/m²x2,36)***	***P.E.N. (kWh/m²)***	***T.P.E. (kWh/m²)***
Existing	**U0**	101.237	19.708	**46.510**	**101.237**	**147.747**
Detached	U1	101.525	19.651	46.376	101.525	147.901
	U2	101.650	19.699	46.489	101.650	148.139
	U3	101.552	12.952	30.568	101.552	132.120
	U4	101.592	19.675	46.433	101.592	148.025
Irregular X-Axis	U5	100.939	23.253	54.877	100.939	155.816
	U6	102.999	19.718	46.534	102.999	149.533
	U7	102.889	19.742	46.591	102.889	149.480
	U8	102.922	19.699	46.489	102.922	149.411
	U9	101.155	19.675	46.433	101.155	147.588
	U10	101.304	19.708	46.510	101.304	147.814
	U11	101.145	19.747	46.602	101.145	147.747
	U12	101.184	19.704	46.501	101.184	147.934
Irregular Y-Axis	U13	101.558	19.651	46.376	101.558	147.934
	U14	101.669	19.699	46.489	101.669	148.158
	U15	101.563	19.723	46.546	101.563	148.109
	U16	101.606	19.679	46.442	101.606	148.048
	U17	101.544	19.651	46.376	101.544	147.920
	U18	101.688	19.686	46.458	101.688	148.146
	U19	99.546	23.296	54.978	99.546	154.524
	U20	101.597	19.675	46.433	101.597	148.030
Irregular Z-Axis	U21	102.216	20.506	48.394	102.216	150.610
	U22	102.341	19.540	46.114	102.341	148.455
	U23	100.199	22.953	54.170	100.199	154.369
	U24	102.240	20.530	48.450	102.240	150.690
	U25	101.136	19.654	46.385	101.136	147.521
	U26	101.29	19.901	46966	101.29	148.256
	U27	101.155	19.93	47.034	101.155	148.189
	U28	99.306	23.468	55.384	99.306	154.690

4.1.2.2 Hourly

The hourly results for the extremely cold period in Ankara on 2 January at 11.00 a.m. are explained in this section. The current situation results for the P.E.E, P.E.N., and T.P.E is 0.08968 kWh/m², 1.59 kWh/m², and 1.67968 kWh/m², respectively. Among the results for the alternative models, P.E.E. does not have any change, it is 0.08968 kWh/m² which is also same as the existing situation. For P.E.N, there is a small reduction with 1.585 kWh/m² for U1, U9, U10, U11, U12, U13, U16, U25, U26, U27, and U28 models. Therefore, the T.P.E decreases for these alternatives by 1.67468 kWh/m². Other alternatives' P.E.N. and T.P.E. results are almost same as the U0 model's results. Therefore, the T.P.E decreases for these alternatives by 1.67468 kWh/m².

The energy results for the extremely cold period in İzmir ia on 5 December 09.00 a.m.. The U0 model has 0.08968 kWh/m² of P.E.E., 0.893 kWh/m² of P.E.N, and 0.98268 kWh/m² of T.P.E. Among the district alternative models' results, the P.E.E. is the same as the existing case result. However, for the alternatives U9, U10, U11, and U12, the P.E.N. decreases to 0.888 kWh/m². Hence, their T.P.E. is 0.97768 kWh/m². Other alternatives' P.E.N. and T.P.E. results are almost same with the U0 models.

The energy performance results for the extremely hot period in Ankara are analyzed on 26 August 10.00 a.m . The P.E.E for the existing case study is 0.39648 kWh/m². The P.E.N is 0.077 kWh/m² and the T.P.E. is 0.47348 kWh/m². The results for the alternative models are the same, and they are below the existing results. The P.E.E., P.E.N., and T.P.E. results are 0.21476 kWh/m², 0.077 kWh/m², and 0.29176 kWh/m² respectively.

The energy performance results during the extremely hot period in İzmir is analyzed on 22 July 16.00 p.m.. The results for the existing situation for P.E.E., P.E.N., and T.P.E are 1.96588 kWh/m², 0.067 kWh/m², and 2.03288 kWh/m², respectively. The minimum result for P.E.E is 0.37288 kWh/m² with U21, U22, and U24 district models. The minimum P.E.N and T.P.E belong to U24 with 0.037 kWh/m² and 0.40988 kWh/m². The alter alternative's P.E.E. is 0.38468 kWh/m², P.E.N. is 0.067 kWh/m², and T.P.E. is 0.45168 kWh/m².

The energy performance results for the typical period of Ankara which is on 15 October at 10.00 a.m. is explained. The P.E.E, P.E.N, and T.P.E results are 0.08968 kWh/m², 0.331 kWh/m², and 0.42068 kWh/m² respectively for the U0 model. Among the alternative models' results, U9, U11, U12, U25, U27, and U28 have the same energy performance as the existing situation. Although the other alternatives modes' results are same for P.E.E. like the U0 model, the P.E.N. results are between 0.336 kWh/m² and 0.346 kWh/m². Thus, the other alternatives' T.P.E. is between 0.43068 kWh/m² and 0.43568 kWh/m².

The energy performance results for the typical hour in İzmir is analyzed on 1 October 10.00 a.m.. The energy performance results for the U0 model are 0.08968 kWh/m², 0.072 kWh/m², 0.16168 kWh/m² regarding P.E.E., P.E.N. and T.P.E. respectively. Among the alternatives, except U21, U22, and U23 models' results, the P.E.E., P.E.N. and T.P.E. are same as the results of the existing situation. These three models have 0.08968 kWh/m², 0.077 kWh/m², 0.16668 kWh/m² results of P.E.E., P.E.N. and T.P.E. respectively.

It is necessary to mention that the energy performance results which are the same or similar are also analyzed by taking the first floor and the top floor of the building in the center of the parcel as a reference in addition to referencing the middle floor. When the first floor of the building in the center of the parcel is considered as the reference the P.E.E. results are around 0.08968 kWh/m²; the P.E.N results are generally between 0.072 kWh/m² and 0.077 kWh/m²; the T.P.E. results are between 0.16168 kWh/m² and 0.16668 kWh/m² for the typical periods. Therefore, referencing the middle floor or the first floor and top floor or not does not cause a considerable difference in results. They are almost same. It can be related with the aspect ratio since it impacts the density of buildings in the parcel; also has a relation with the shadow, and daylighting which directly impact the heating and cooling loads in the building.

4.1.3 Discussion of The Most Suitable Urban Block Models

Comparing the yearly and hourly results about solar radiation and energy performance highlights the most suitable urban block models regarding 28 district models and the condition of the existing situation among the alternatives.

Figure 31 indicates the positive points tables for Ankara and İzmir. U0 represents the existing situation. The maximum solar radiation results gain the positive point by considering Ankara's climatical condition, which is temperate-dry.

ANKARA

Scenarios			U0	U1	U2	U3	U4	U5	U6	U7	U8	U9	U10	U11	U12	U13	U14	U15	U16	U17	U18	U19	U20	U21	U22	U23	U24	U25	U26	U27	U28
Solar Radiation	Yearly											max																			
Solar Radiation	Hourly	Ext.Cold										max																			
Solar Radiation	Hourly	Ext.Hot								max																				max	
Solar Radiation	Hourly	Typical												max																	
Energy Performance	Yearly	PEE			min																										
Energy Performance	Yearly	PEN																													min
Energy Performance	Yearly	TPE										min																			
Energy Performance	Ext.Cold	PEE	same results with existing																												
Energy Performance	Ext.Cold	PEN		min								min	min	min	min	min			min									min	min	min	min
Energy Performance	Ext.Cold	TPE		min								min	min	min	min	min			min									min	min	min	min
Energy Performance	Ext.Hot	PEE		min	min	min	min	min	min	min	min	min	min	min	min	min	min	min	min	min	min	min	min	min	min	min	min	min	min	min	min
Energy Performance	Ext.Hot	PEN	same results with existing																												
Energy Performance	Ext.Hot	TPE		min	min	min	min	min	min	min	min	min	min	min	min	min	min	min	min	min	min	min	min	min	min	min	min	min	min	min	min
Energy Performance	Typical	PEE	same results with existing																												
Energy Performance	Typical	PEN																													
Energy Performance	Typical	TPE																													
Positive Point.1			0	4	3	2	2	2	2	3	2	7	4	5	4	4	2	2	4	2	2	2	2	2	2	2	2	4	4	5	5

İZMİR

Scenarios			U0	U1	U2	U3	U4	U5	U6	U7	U8	U9	U10	U11	U12	U13	U14	U15	U16	U17	U18	U19	U20	U21	U22	U23	U24	U25	U26	U27	U28
Solar Radiation	Yearly					min																									
Solar Radiation	Hourly	Ext.Cold												max																	
Solar Radiation	Hourly	Ext.Hot				min																									
Solar Radiation	Hourly	Typical												max																	
Energy Performance	Yearly	PEE				min																									
Energy Performance	Yearly	PEN																													min
Energy Performance	Yearly	TPE				min																									
Energy Performance	Ext.Cold	PEE	same results with existing																												
Energy Performance	Ext.Cold	PEN										min	min	min	min																
Energy Performance	Ext.Cold	TPE										min	min	min	min																
Energy Performance	Ext.Hot	PEE																						min	min		min				
Energy Performance	Ext.Hot	PEN																									min				
Energy Performance	Ext.Hot	TPE																									min				
Energy Performance	Typical	PEE	same results with existing																								same results with existing				
Energy Performance	Typical	PEN																													
Energy Performance	Typical	TPE																													
Positive Point.1			0	0	0	4	0	0	0	0	0	2	2	4	2	0	0	0	0	0	0	0	0	1	1	0	3	0	0	0	0

Figure 31: First positive point table for Ankara and İzmir

For Ankara, U9 takes the positive remark for the yearly and extremely cold period. U7 and U11 gain a positive response from extremely hot and the typical period, respectively. According to annual energy performance, the positive points are for U2, U28, and U9 thanks to providing minimum results for P.E.E, P.E.N., and T.P.E. Consistent with hourly results, most of the alternatives offer a positive remark which are U1, U9, U10, U11, U12, U13, U16, U25, U26, U27, and U28. The general outcomes of solar radiation and energy performance analysis are mentioned below.

- U9 district model achieves seven positive points, the best response among the models. The model belongs to the category of Irregular X-Axis.
- U11, U27, and U28 gets 5 positive points. These share the second placement among the models.
- About solar radiation and energy performance, the existing situation does not acquire any positive point.

For İzmir, having minimum solar radiation about the yearly and extremely hot period is advantageous since the climate is hot-humid. Hence, U3 gains positive points. U11 gains positive remarks for the extreme cold and the typical period by providing maximum solar radiation. Regarding energy performance results, U3 provides minimum results for P.E.E, and T.P.E. U28 gains a positive point by having minimum result for P.E.N.. According to the extremely cold period results, U9, U10, U11, and U12 achieve positive points by having a minimum result. For the extremely hot period, U24 has minimum P.E.E., P.E.N., and T.P.E.. The other results are the same as the existing case, and some of them exceed the existing result. The main outcomes of solar radiation and energy performance analysis for İzmir are summarized below.

- U3 and U11 succeed in 4 positive points. These are the best responses for İzmir. The U3 model is under the category of Detached, the U11 model belongs to the category of Irregular X-Axis.

- U24 gains three positive points. This model acquires the second placement.

- The other models have 2,1 and 0 positive remarks. The U0 model does not have any positive points.

Consequently, the models that achieve the best positive points are included in the comparative assessment process.

4.2 Comparative Assessment Process

The most suitable district model alternatives for Ankara and İzmir are determined in Section 4.1.3 regarding yearly and hourly results of solar radiation and energy performance. The models that acquire the best positive points are analyzed with CFD simulation, outdoor comfort, and indoor comfort for hourly periods.

4.2.1 CFD

The results of the CFD simulation are discussed according to average wind velocity. Table 23 shows the hourly results for Ankara. Because of having a temperate-dry climate, the advantageous situation is when the wind velocity is minimum for the extremely cold, and the typical hours, maximum for the extremely hot period. For the existing situation, the average wind velocity for extreme cold, extremely hot, and typical periods are 2.0578 m/s, 1.7462 m/s, and 1.4479 m/s respectively. The minimum result for the extreme cold period is 1.1773m/s, and the maximum wind velocity for the extremely hot period is

1.8079 m/s with the U11 alternative. For the typical period, U27 the alternative has the minimum result of 1.3765m/s.

Table 23: CDF simulation results for Ankara

ANKARA Average Wind Velocity (m/s)				
Urban Scenario		*Hourly Results*		
		Extreme Cold (2 Jan. 11.00)	*Extreme Hot (26 Aug. 10.00)*	*Typical (15 Oct. 10.00)*
Existing	**U0**	**2.0578**	**1.7462**	**1.4479**
Irregular X-Axis	U9	2.2812	1.6265	1.5716
	U11	1.1773	1.8079	1.4959
Irregular Z-Axis	U27	2.1641	1.7280	1.3765
	U28	2.1817	1.5652	1.6672

Figure 32, Figure 33, and Figure 34 show the CFD simulation results for the hourly periods in Ankara. This shows the wind movement in the district. The wind movement is affected by the buildings, their heights and orientation, and the wind direction during the run period. In the visuals, both vector length and color change according to the wind velocity from purple to red. The purple vectors show the low wind velocity, the blue represents the middle value, and the red shows the high wind velocity.

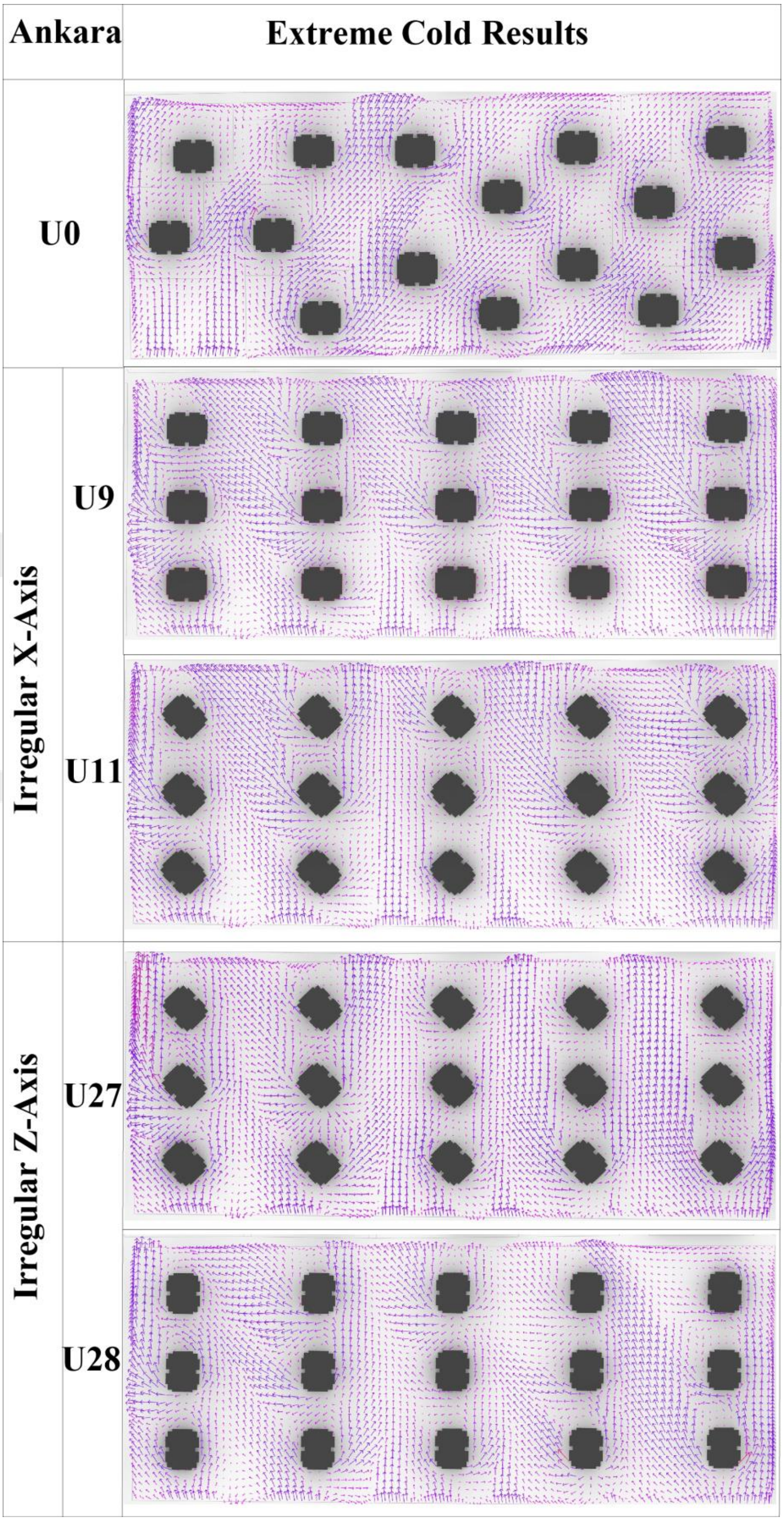

Figure 32: Wind velocity results for the extremely cold period in Ankara

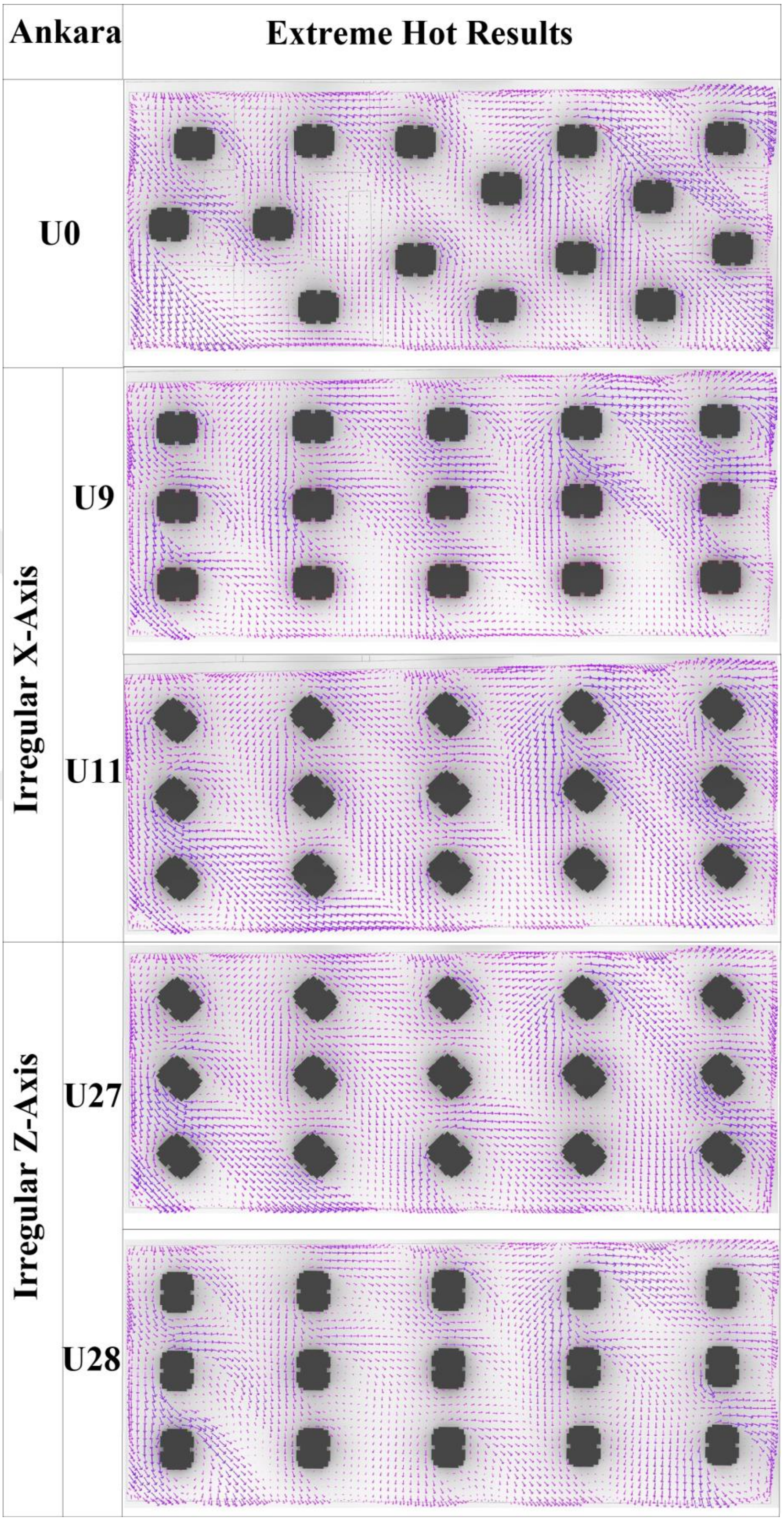

Figure 33: CFD results for the extreme hot period in Ankara

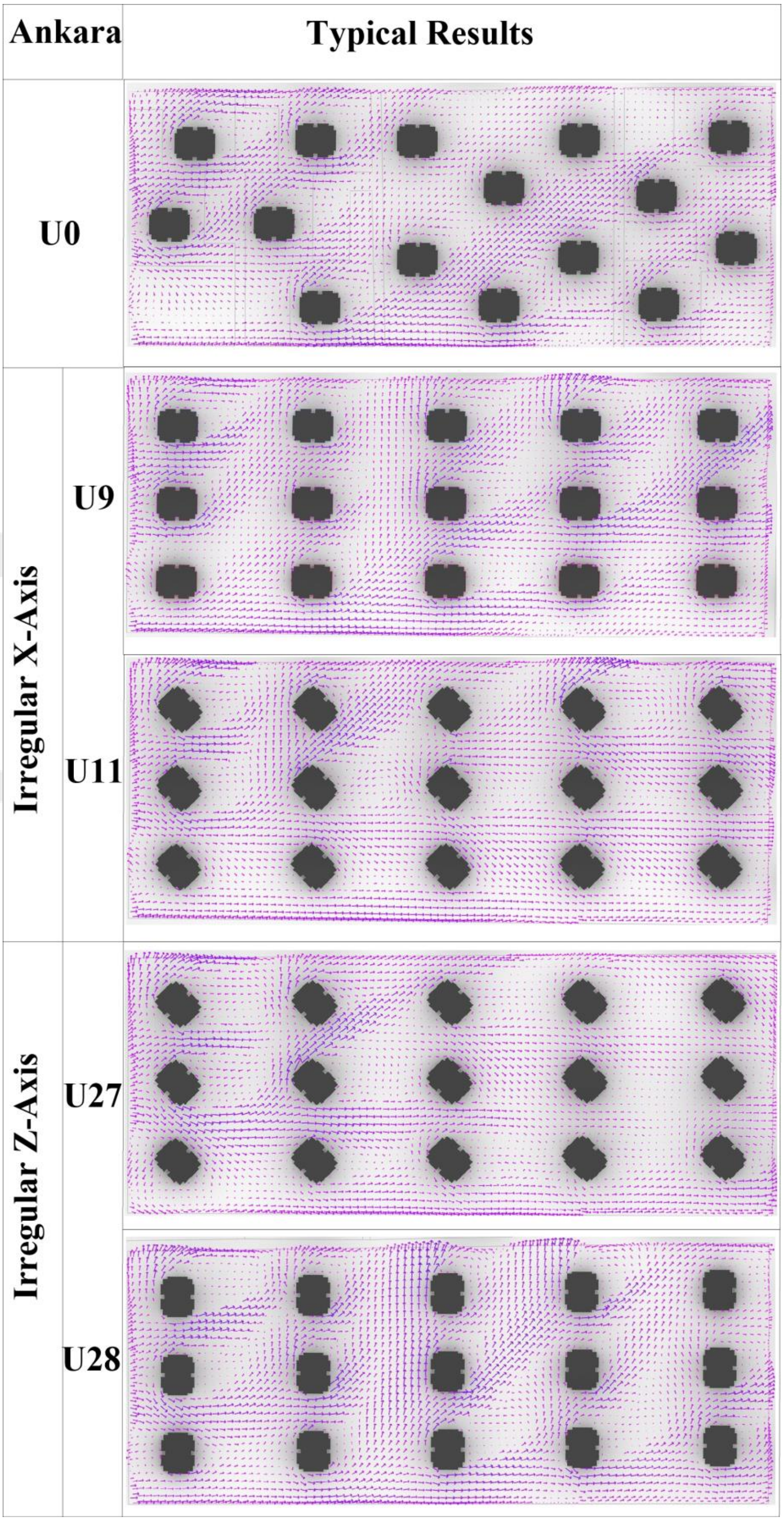

Figure 34: Typical period CFD results in Ankara

Table 24 displays the average wind velocity results for İzmir. Since having hot-humid climate, the minimum wind velocity is beneficial for the extremely cold period, while the maximum wind velocity is beneficial for the extremely hot, and typical periods. The results for the existing situation about the extreme cold, the extremely hot, and the typical period are 1.0046 m/s, 4 .2961 m/s, and 2.0491 m/s, respectively. Among the results, the minimum wind velocity for the extremely cold period is 0.7839 m/s, and the maximum wind velocity for the extremely hot period is 4.5954 m/s with the U11 model. The wind velocity of the U3 model is 2.2311 m/s, the maximum result for the typical period in İzmir.

Table 24: CFD results for İzmir

Izmir Average Wind Velocity (m/s)				
Urban Scenario		*Hourly Results*		
		Extreme Cold (5 Dec. 09.00)	*Extreme Hot (22 Jul. 16.00)*	*Typical (1 Oct. 10.00)*
Existing	**U0**	**1.0046**	**4.2961**	**2.0491**
Detached	U3	0.7881	4.2451	2.2311
Irregular Y-Axis	U11	0.7839	4.5954	1.1937
Irregular Z-Axis	U24	0.9526	4.3314	2.0778

Figure 35, Figure 36, and Figure 37 show the CFD simulation results for the hourly periods in İzmir. The maximum wind velocity difference is during the extremely hot period in İzmir.

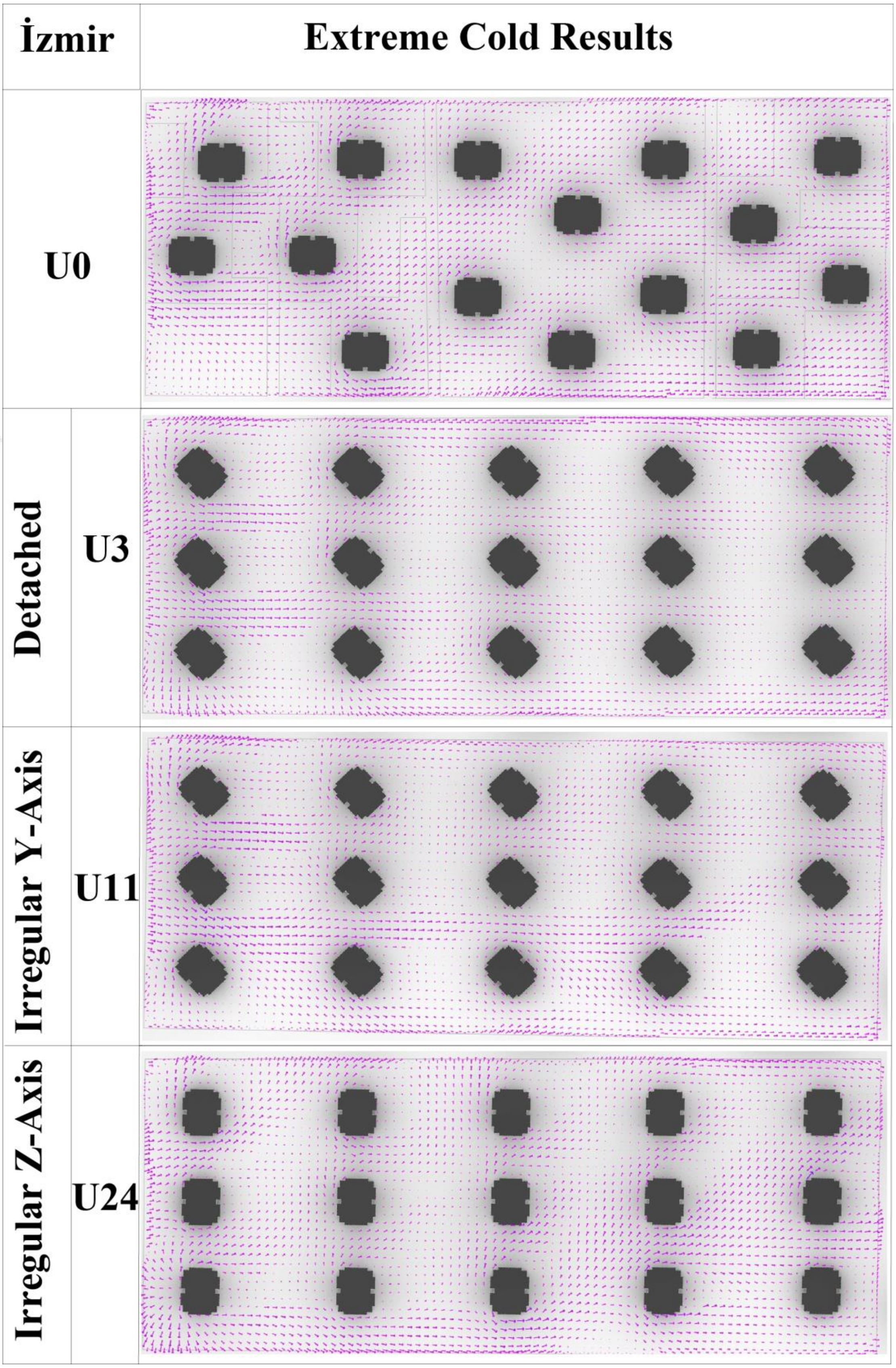

Figure 35: Extremely cold period CFD simulation in İzmir

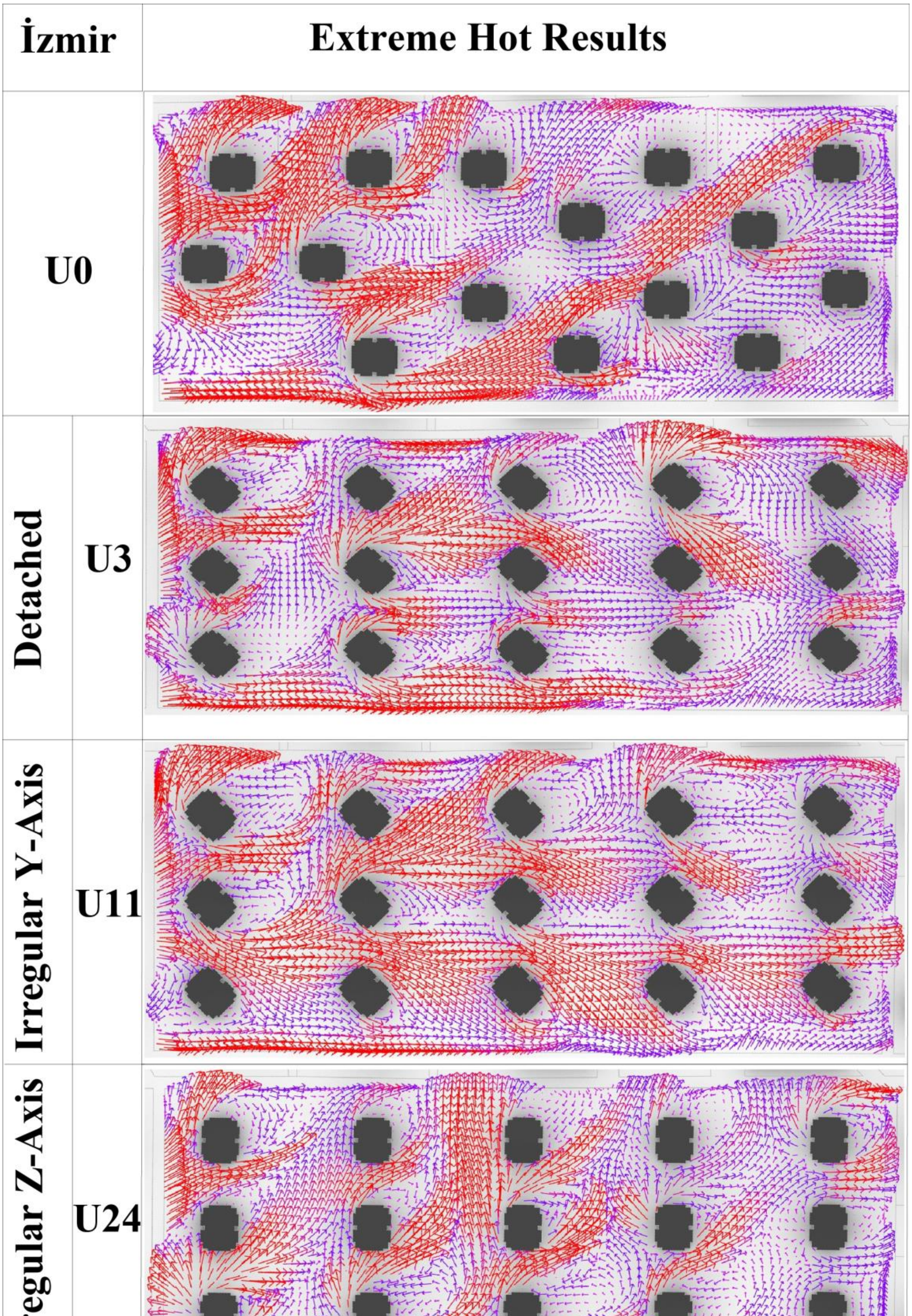

Figure 36: Extremely hot period CFD analysis in İzmir

İzmir		Typical Results
U0		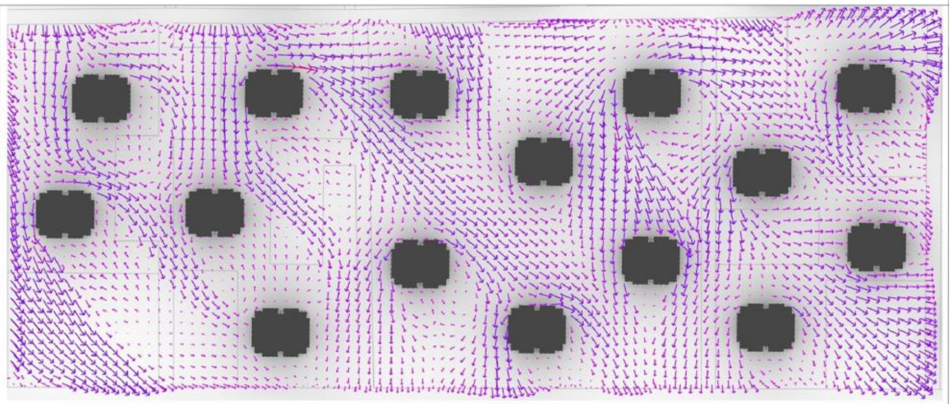
Detached	U3	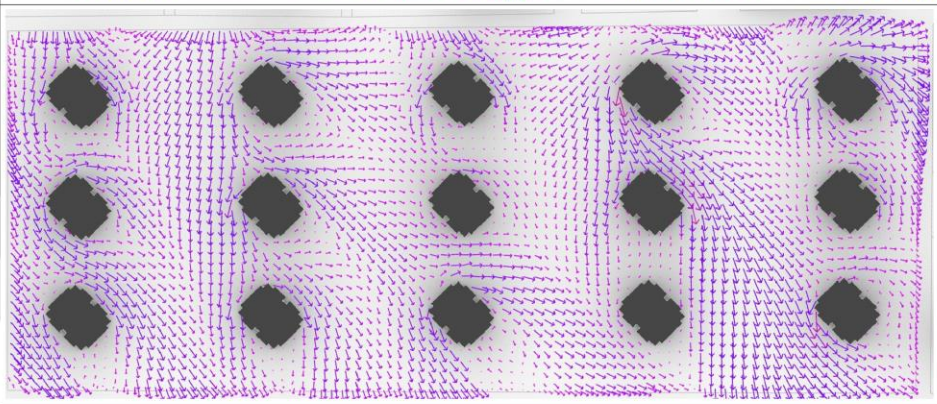
Irregular Y-Axis	U11	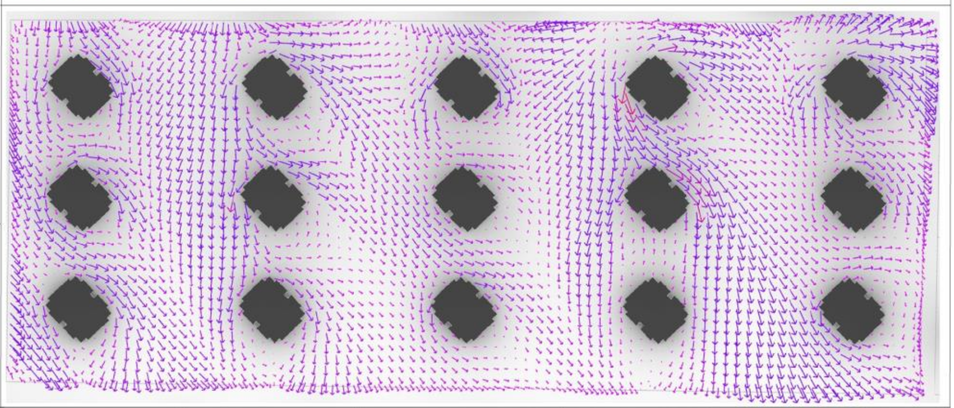
Irregular Z-Axis	U24	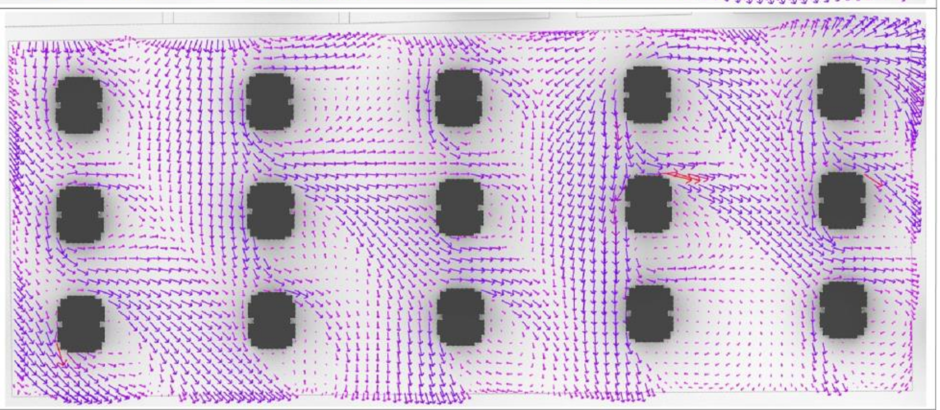

Figure 37: CFD results for the typical period in İzmir

4.2.2 Outdoor Comfort

Table 25 includes the results of the average outdoor temperature sensation for Ankara. Having maximum outdoor temperature sensation for the extremely cold period and the typical hour is beneficial. Having minimum outdoor temperature sensation for the extremely hot period is advantageous. The results for the existing situation are -13.8062 C°, 30.8297 C°, and 16.7039 C° during extreme cold, extremely hot, and typical hours respectively. The maximum outdoor temperature sensations for the extreme cold and the typical hours are -13.73 C° and 17.4196 C° with the U11 model. The minimum result is measured for the existing situation during the extremely hot period.

Table 25: Outdoor comfort results for Ankara

ANKARA *Average Outdoor Temperature Sensation (C°)*				
Urban Scenario		*Hourly Results*		
		Extreme Cold *(2 Jan. 11.00)*	*Extreme Hot* *(26 Aug. 10.00)*	*Typical* *(15 Oct. 10.00)*
Existing	**U0**	**-13.8062**	**30.8297**	**16.7039**
Irregular X-Axis	U9	-13.7380	30.8370	17.0159
	U11	-13.7328	30.9179	17.4196
Irregular Z-Axis	U27	-13.7601	30.9577	17.2498
	U28	-13.7695	30.8595	16.7941

Figure 38, Figure 39, and Figure 40 show the outdoor comfort simulation results for the hourly periods in Ankara. During the extremely cold period, the outdoor temperature sensation is approximately between -15.96 C° and -12.79 C°. It is generally between 21.96 C° and 33.96 C° for the extremely hot period. For the typical period, the value is between 8.84 C° and 20.69 C°.

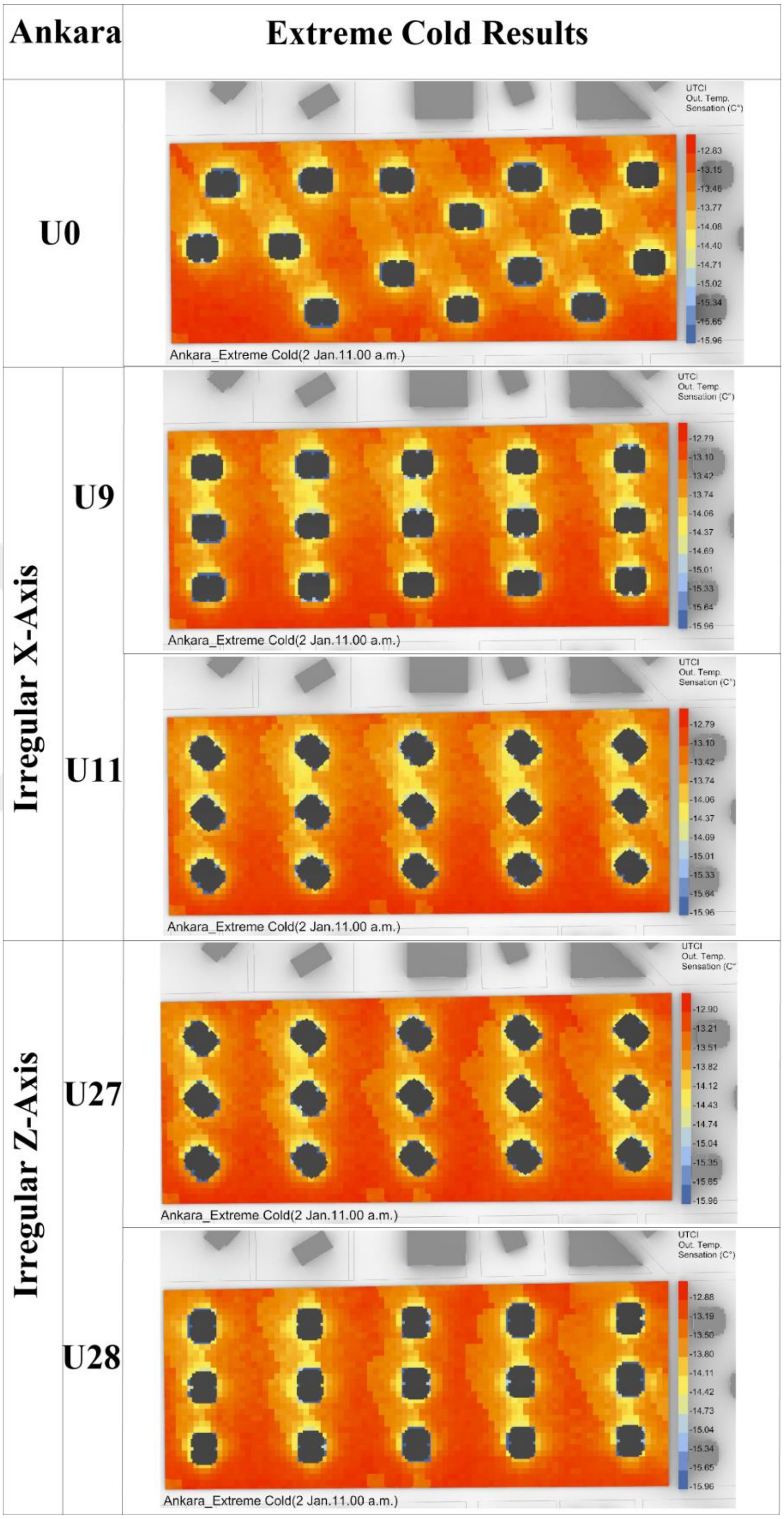

Figure 38: Outdoor comfort during the extremely cold period in Ankara

<table>
<tr><th colspan="2">Ankara</th><th>Extreme Hot Results</th></tr>
<tr><td colspan="2">U0</td><td>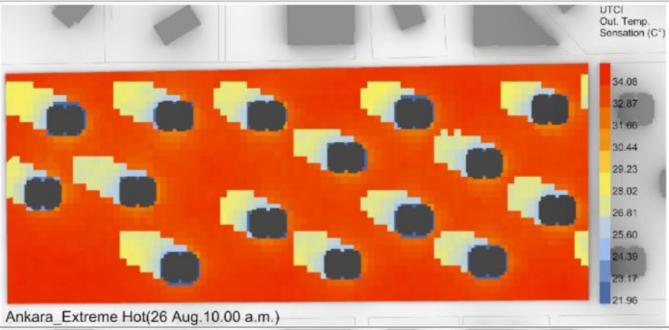
</td></tr>
<tr><td rowspan="2">Irregular X-Axis</td><td>U9</td><td>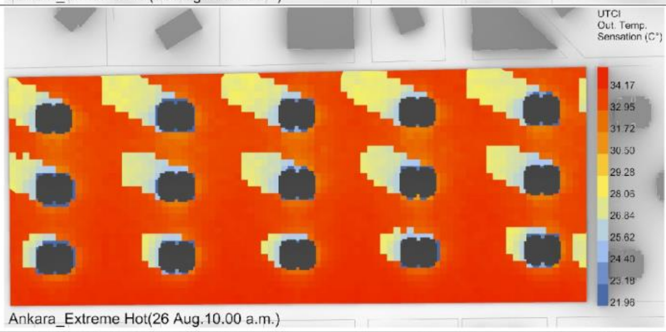
</td></tr>
<tr><td>U11</td><td>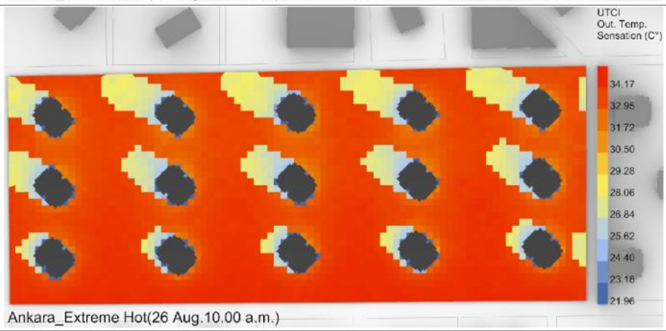
</td></tr>
<tr><td rowspan="2">Irregular Z-Axis</td><td>U27</td><td>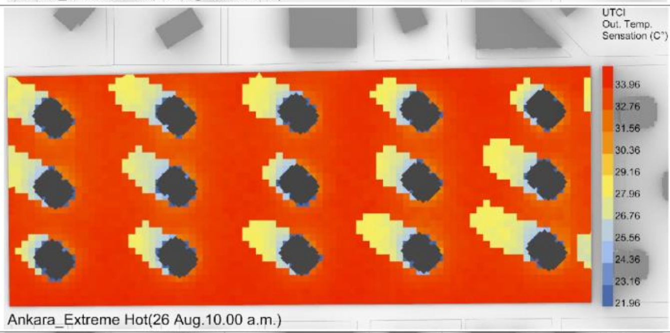
</td></tr>
<tr><td>U28</td><td>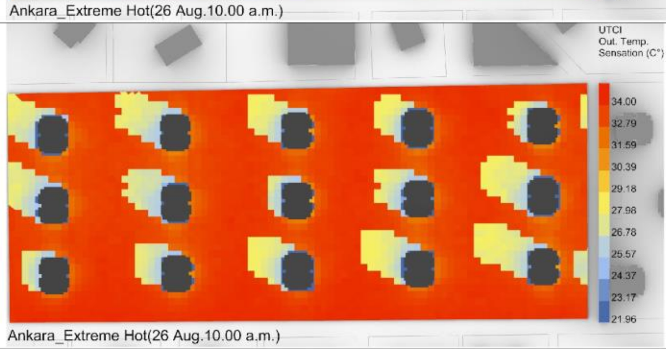
</td></tr>
</table>

Figure 39: Outdoor comfort for the extremely hot period in Ankara

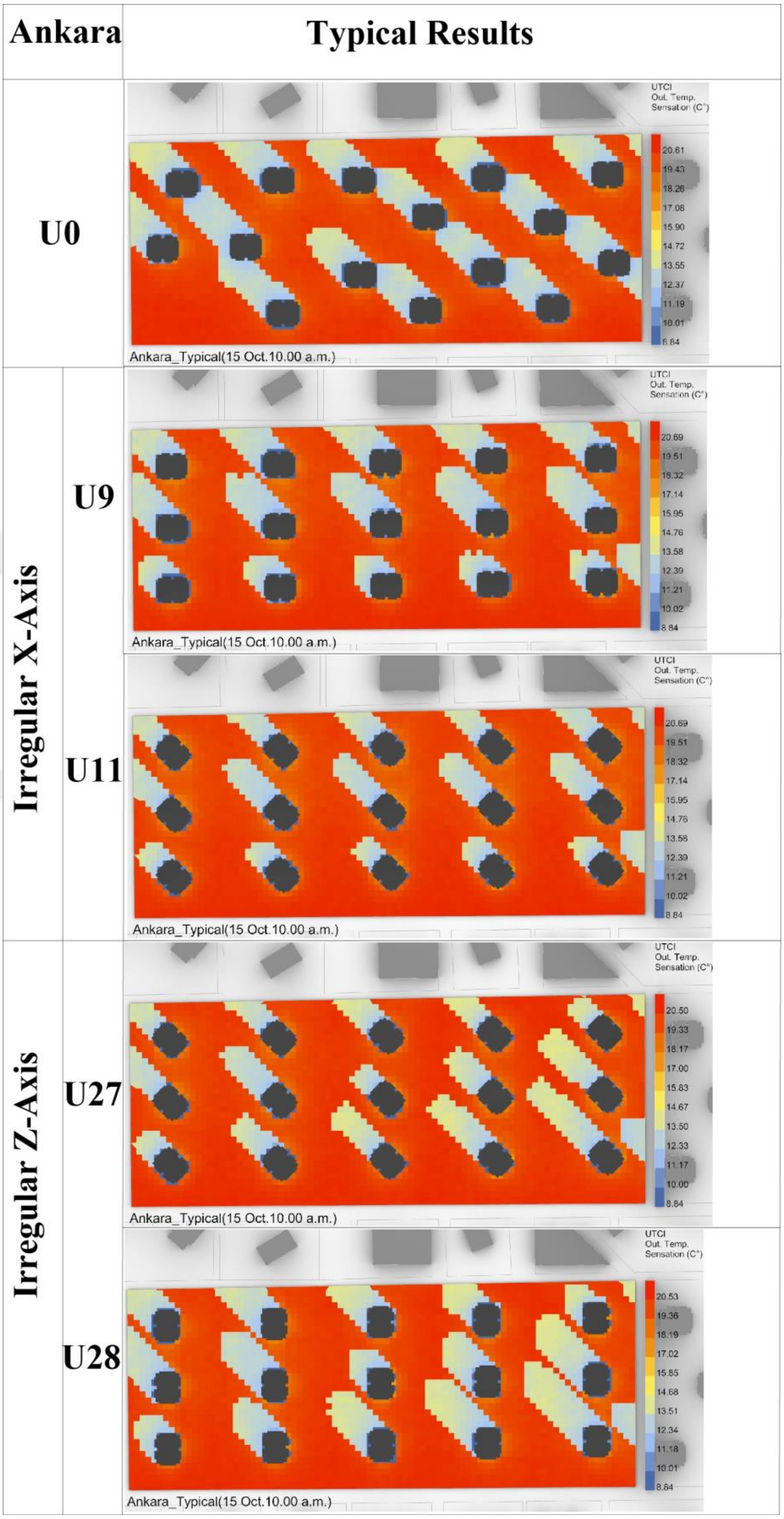

Figure 40: Typical period outdoor comfort results in Ankara

Table 26 shows the average outdoor temperature sensation results for İzmir. It is beneficial to have a maximum result for the extremely cold hour, the minimum for the extremely hot hour, and the typical period. The results for the existing situation are 1.9953 C°, 42.3588 C, and 28.5626 C° regarding extreme cold, extremely hot, and typical periods. The result for the extreme cold hour is the maximum outdoor temperature sensation among the alternatives. The minimum result for the extremely hot hour is 42.3002 C° with the U3 model. The U24 alternative has a minimum result of 28.5215, about the typical hour.

Table 26: Outdoor comfort results for İzmir

Izmir Average Outdoor Temperature Sensation (C°)				
Urban Scenario		*Hourly Results*		
		Extreme Cold (5 Dec. 09.00)	*Extreme Hot (22 Jul. 16.00)*	*Typical (1 Oct. 10.00)*
Existing	**U0**	**1.9953**	**42.3588**	**28.5626**
Detached	U3	1.6821	42.3002	28.7759
Irregular Y-Axis	U11	1.9578	42.3723	28.9964
Irregular Z-Axis	U24	1.4811	42.3312	28.5215

Figure 41, Figure 42, and Figure 43 show the outdoor comfort simulation results for the hourly periods in İzmir. The outdoor temperature sensation is approximately between 0.13 C° and 5.08 C° during the extremely cold period. It is generally between 36.58 C° and 44.55 C° for the extremely hot period. For the typical period, the value is between 21.00 C° and 32.30 C°.

<table>
<tr><th colspan="2">İzmir</th><th>Extreme Cold Results</th></tr>
<tr><td colspan="2">U0</td><td>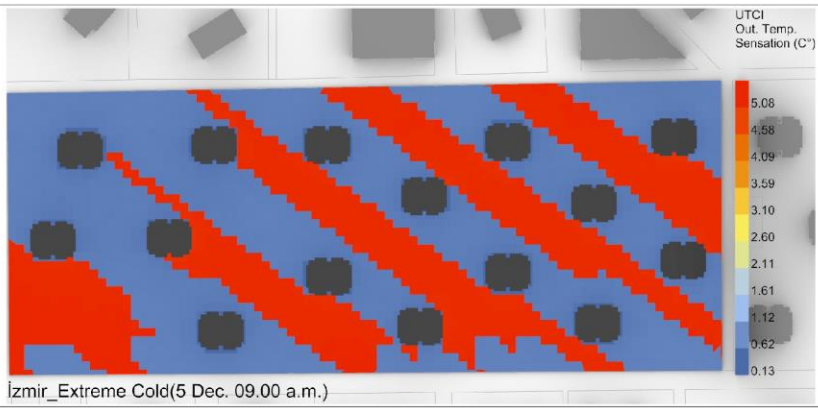
</td></tr>
<tr><td>Detached</td><td>U3</td><td>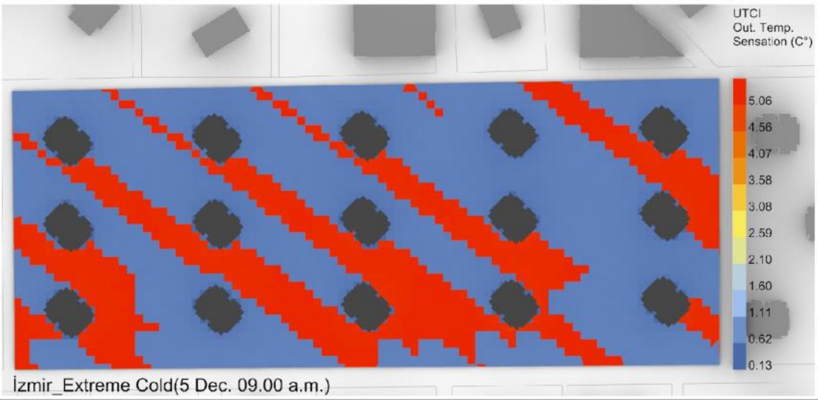
</td></tr>
<tr><td>Irregular Y-Axis</td><td>U11</td><td>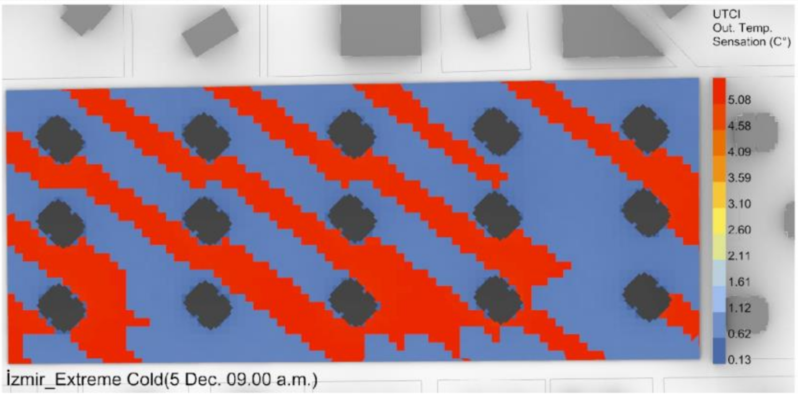
</td></tr>
<tr><td>Irregular Z-Axis</td><td>U24</td><td>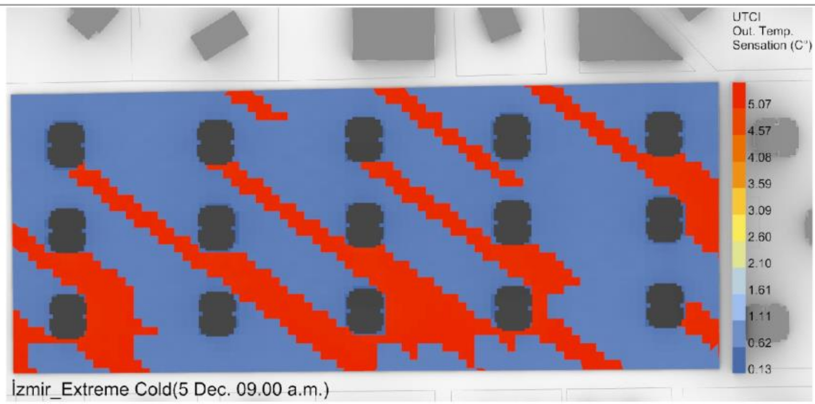
</td></tr>
</table>

Figure 41: Extremely cold period outdoor comfort results in İzmir

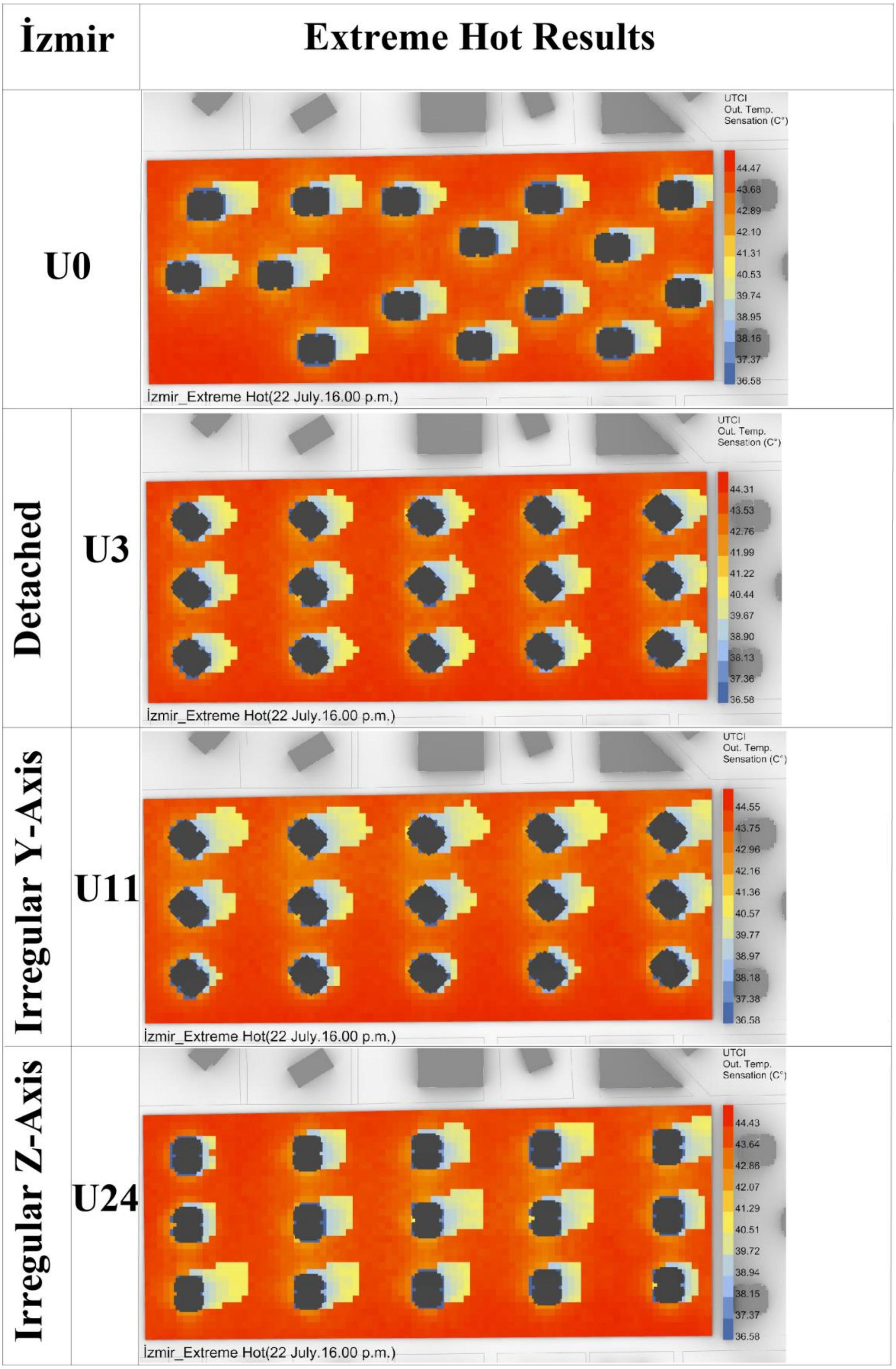

Figure 42: Outdoor comfort during the extremely hot period in İzmir

<table>
<tr><th colspan="2">İzmir</th><th>Typical Results</th></tr>
<tr><td colspan="2">U0</td><td>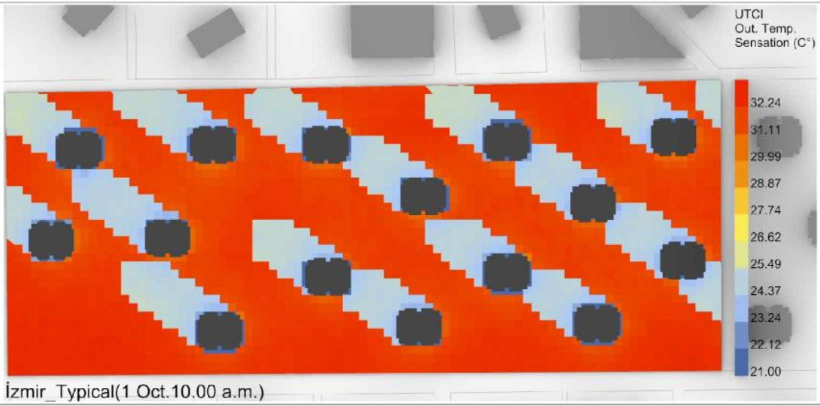
</td></tr>
<tr><td>Detached</td><td>U3</td><td>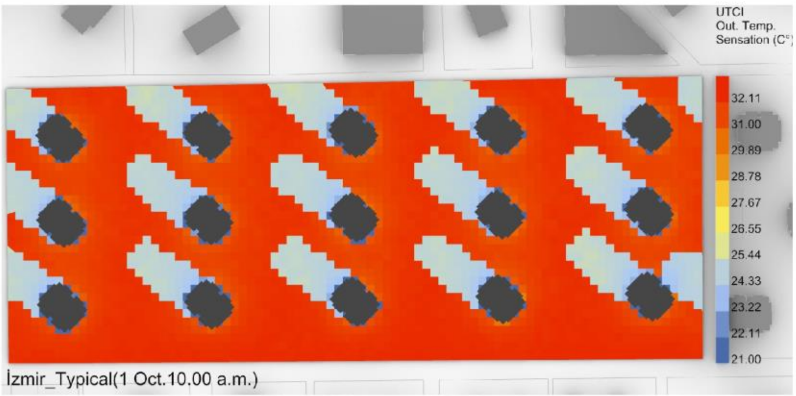
</td></tr>
<tr><td>Irregular Y-Axis</td><td>U11</td><td>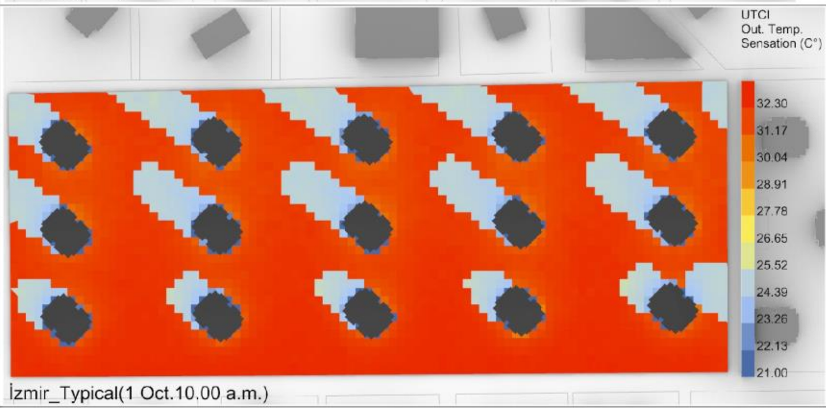
</td></tr>
<tr><td>Irregular Z-Axis</td><td>U24</td><td>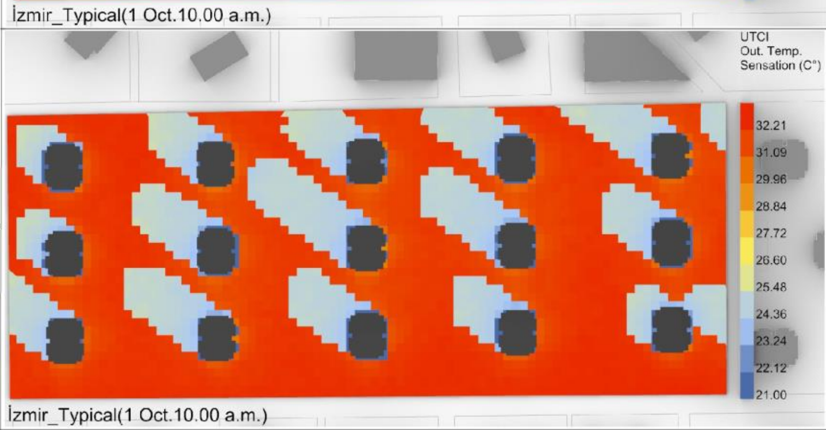
</td></tr>
</table>

Figure 43: Outdoor comfort for the typical period in İzmir

4.2.3 Indoor Comfort

The results of indoor comfort simulation consist of average operative temperature and PMV results. Table 27 indicates the average operative temperature for Ankara. For the existing situation, it is 16.7683 C° during the extremely cold hour, 26.3293 C° for the extremely hot period, and 19.9010 C° during the typical hour. It is advantageous to have the maximum operative temperature for the extreme cold and the typical period while it is minimum during the extremely hot hour. The U27 model has a 16.8095 C° operative temperature which is the maximum result for the extremely cold hour. Also, the same alternative has a minimum operative temperature of 26.3166 C° during the extremely hot period. The minimum consequence for the typical hour is 19.9056 C° with the U11 model.

Table 27: Indoor comfort results for Ankara

ANKARA *Average Operative Temperature (C°)*				
Urban Scenario		*Hourly Results*		
		Extreme Cold *(2 Jan. 11.00)*	*Extreme Hot* *(26 Aug. 10.00)*	*Typical* *(15 Oct. 10.00)*
Existing	**U0**	**16.7683**	**26.3293**	**19.9010**
Irregular X-Axis	U9	16.7569	26.3382	19.9004
	U11	16.7926	26.3389	19.9056
Irregular Z-Axis	U27	16.8095	26.3166	19.9000
	U28	16.6868	26.3251	19.8715

Figure 44, Figure 45, and Figure 46 show the indoor comfort simulation results for the hourly periods in Ankara. The Operative Temperature for the extremely cold period is between 6.99 C° and 19.55 C°. The corridors and toilets are cold, and others are slightly cool. For the extremely hot period, it is between 26.09 C° and 26.86 C°. The rooms on the north side of the building have lower operative temperatures than the rooms on the south. According to PMV results, the zones are neutral and slightly warm. For the typical period, the value is between 17.54 C° and 20.59 C°. The corridors and toilets are cool and cold, while the other spaces are slightly cool.

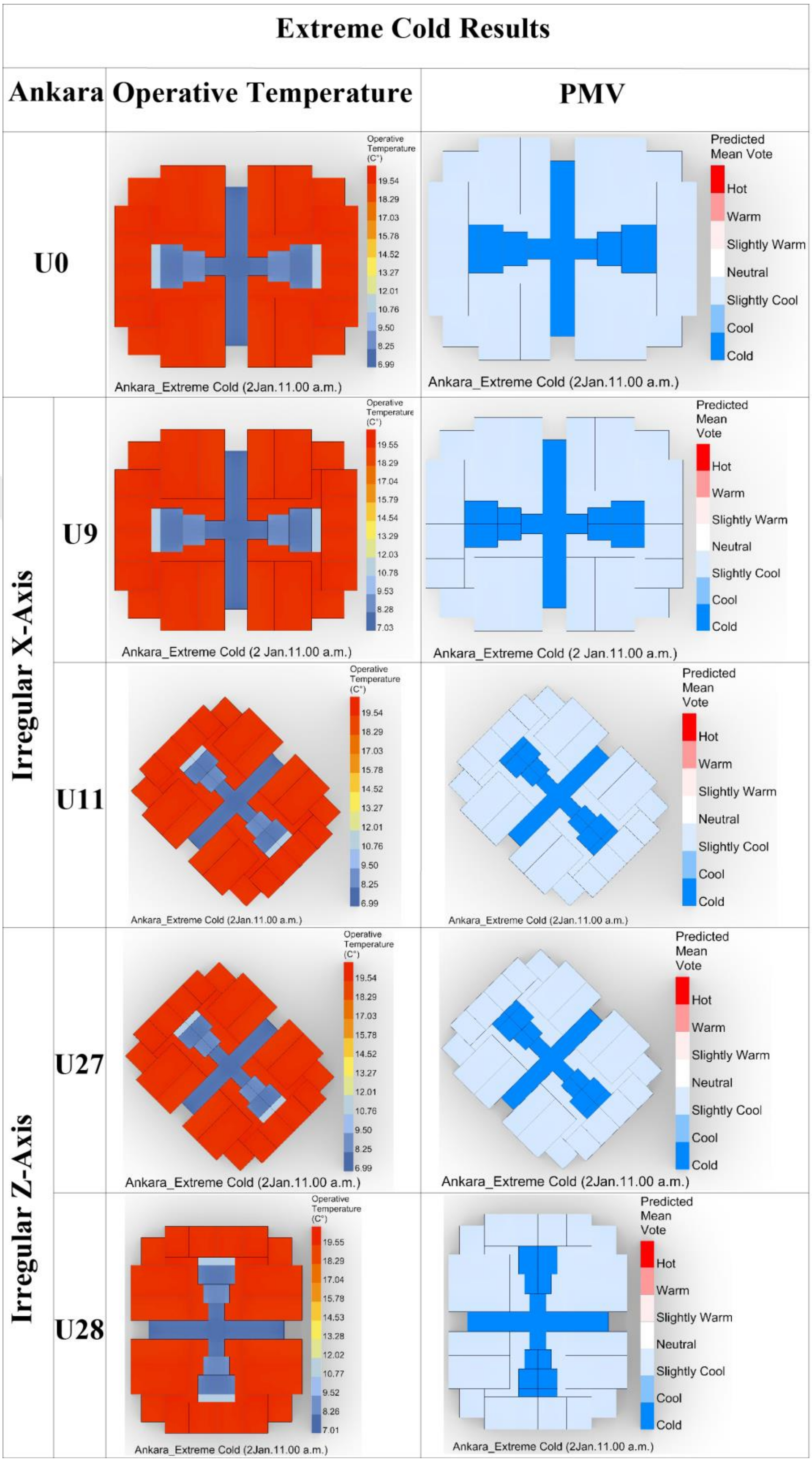

Figure 44: Indoor comfort for the extremely cold hour in Ankara

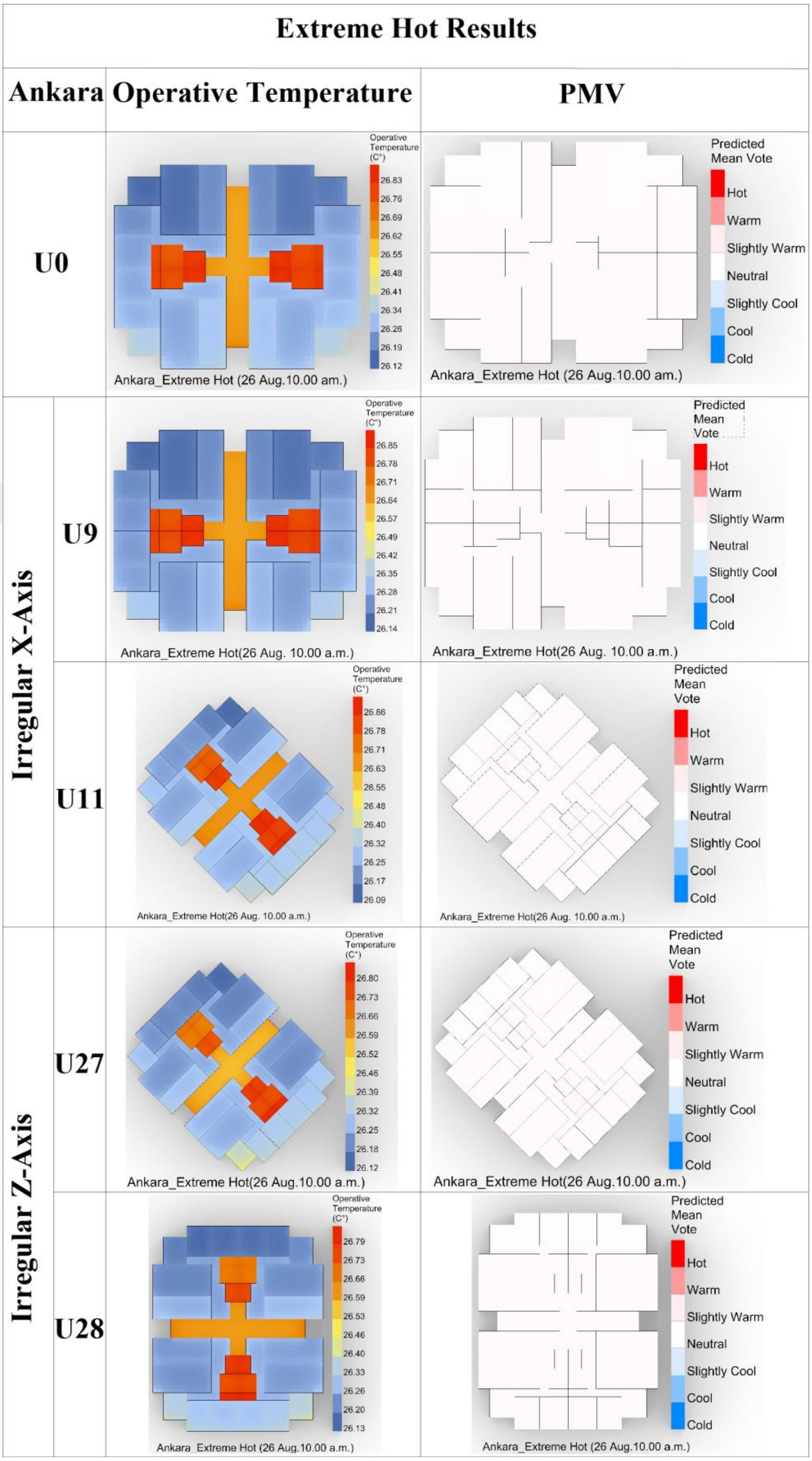

Figure 45: Extremely hot period’s indoor comfort results in Ankara

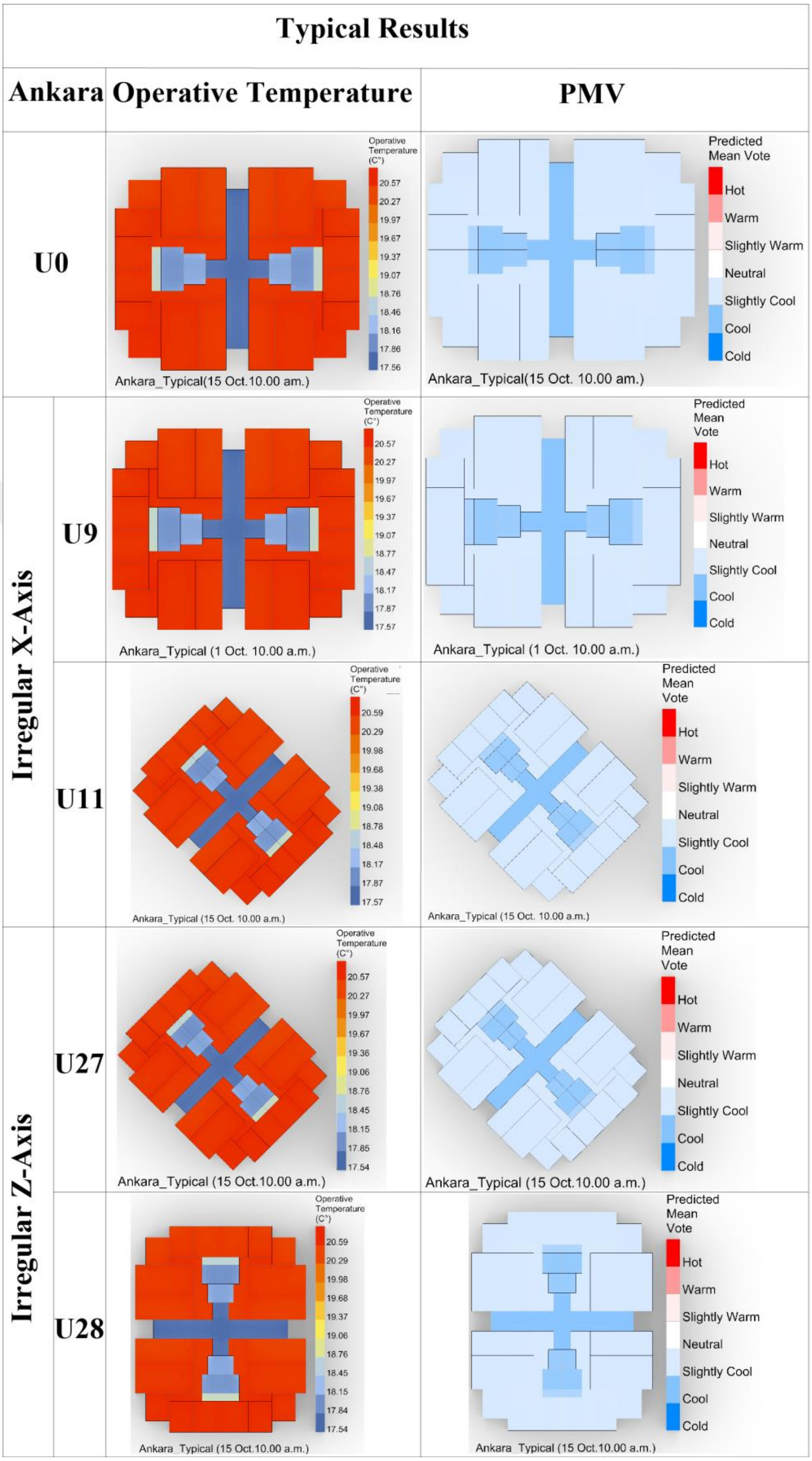

Figure 46: Indoor comfort during the typical period in Ankara

Table 28: Indoor comfort results for İzmir

Izmir *Average Operative Temperature (C°)*				
Urban Scenario		*Hourly Results*		
		Extreme Cold *(5 Dec. 09.00)*	*Extreme Hot* *(22 Jul. 16.00)*	*Typical* *(1 Oct. 10.00)*
Existing	**U0**	**18.4496**	**27.2321**	**21.8827**
Detached	U3	18.4540	27.2301	21.8728
Irregular Y-Axis	U11	18.4669	27.2309	21.8964
Irregular Z-Axis	U24	18.3821	27.2393	21.8370

The average operative temperature results for İzmir are indicated in Table 28. It is positive to have a maximum result for the extremely cold period, while the extremely hot and the typical hour has a minimum result. The existing situation has 18.4496 C°, 27.2321 C°, and 21.8827 C° regarding the extremely cold period, the extremely hot period, and the typical hour. The maximum operative temperature for the extreme cold hour is 18.4669 C° which belongs to U11model. The U3 alternative has the minimum result for the extreme hot period with 27.2301 C°. The minimum result for the typical hour is 21.8370 C° which belongs to the U24 model.

Figure 47, Figure 48, and Figure 49 show the indoor comfort simulation results for the hourly periods in İzmir. The Operative Temperature for the extremely cold period is approximately between 12.64 C° and 20.08 C°. The PMV results are generally between slightly cool and cold. During the extremely hot period, the value is between 26.52 C° and 29.70 C°. According to PMV results, the corridors are warm, the toilets are warm and slightly warm; the rooms are neutral. There is not any difference between North-oriented spaces and South-oriented ones. The typical period results are generally between 21.35 C° and 22.30 C°. The south-oriented zones have higher operative temperatures than the north-oriented ones. The PMV results are neutral and slightly cool.

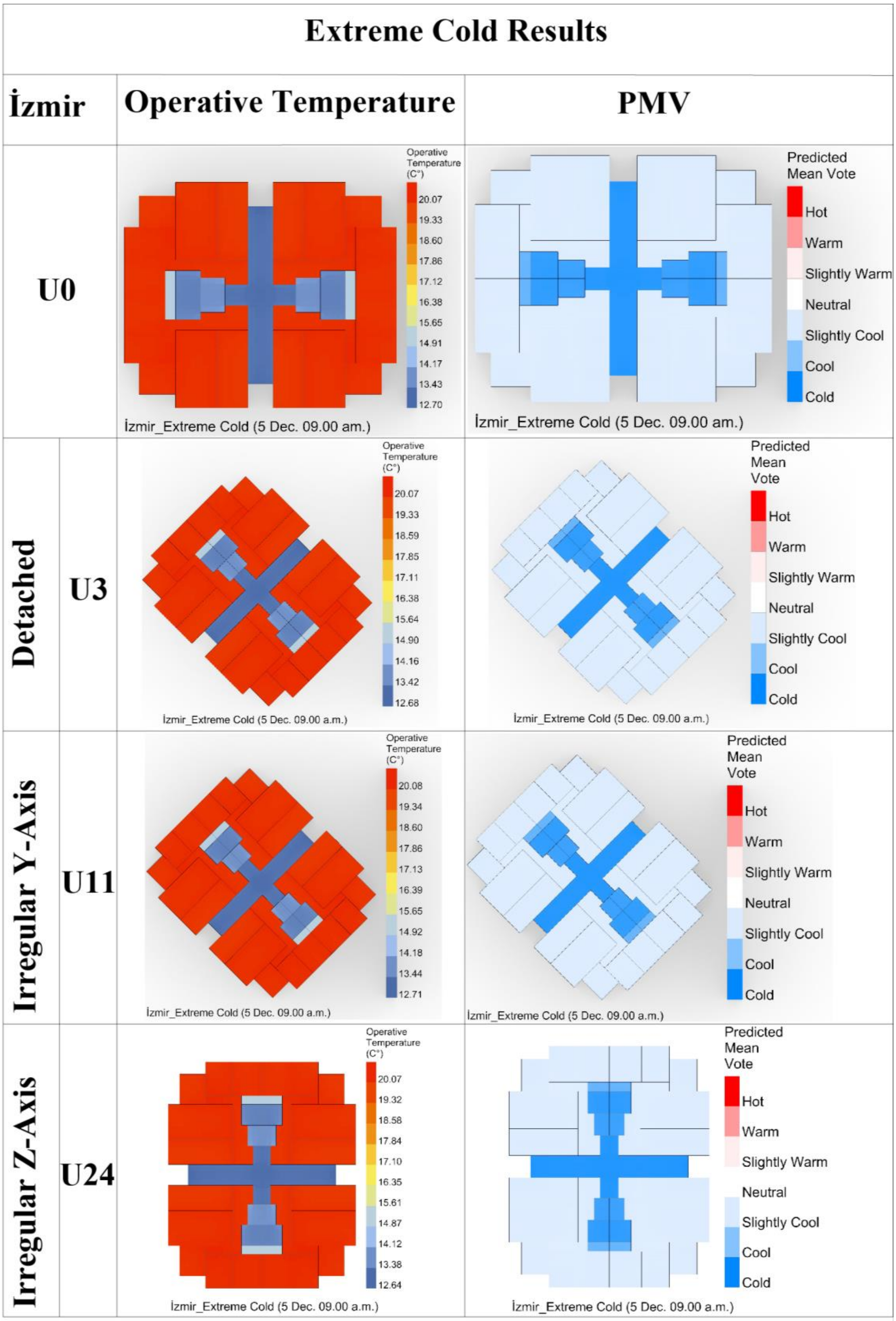

Figure 47: Indoor comfort for the extremely cold hour in İzmir

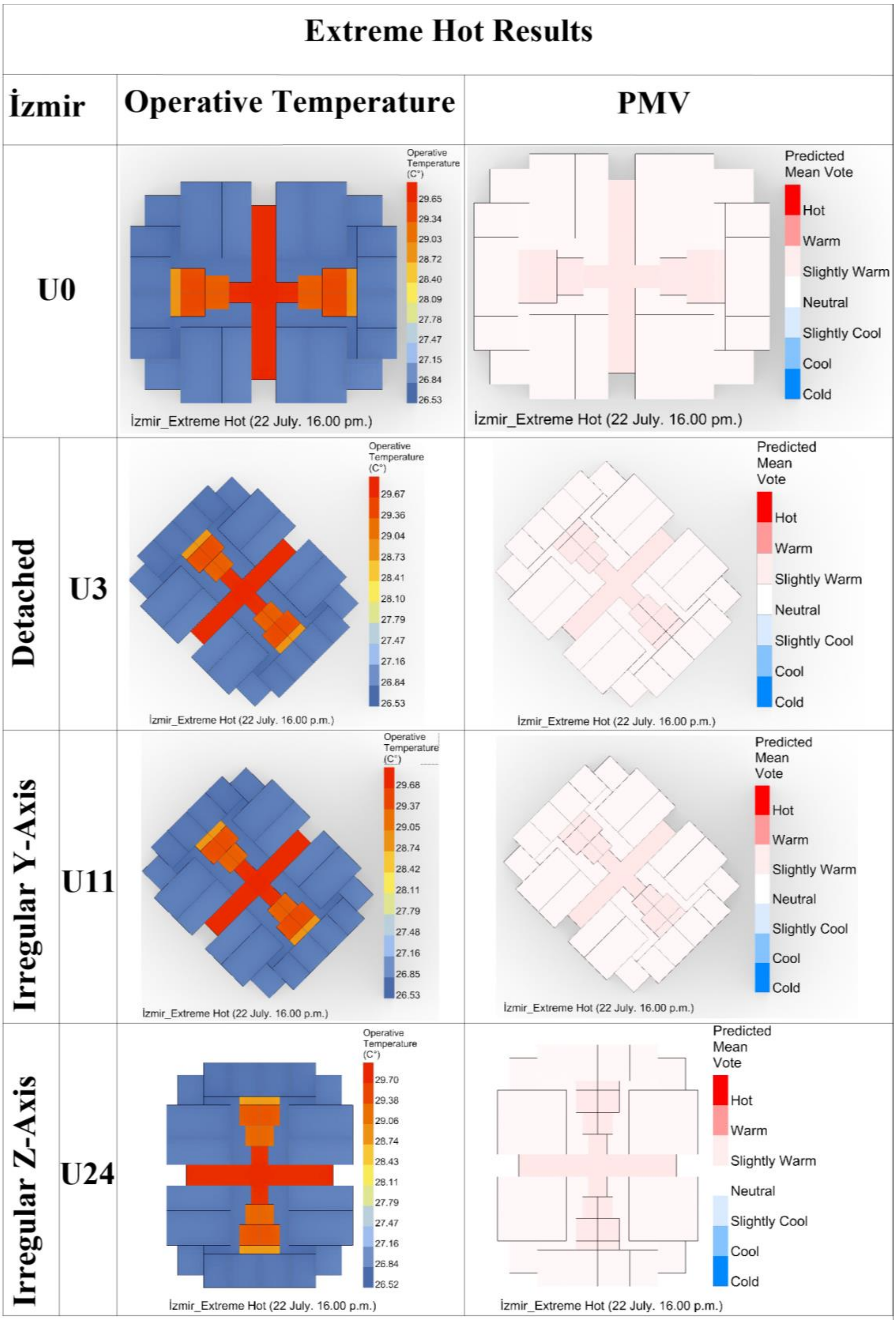

Figure 48: Extremely hot period's indoor comfort results in İzmir

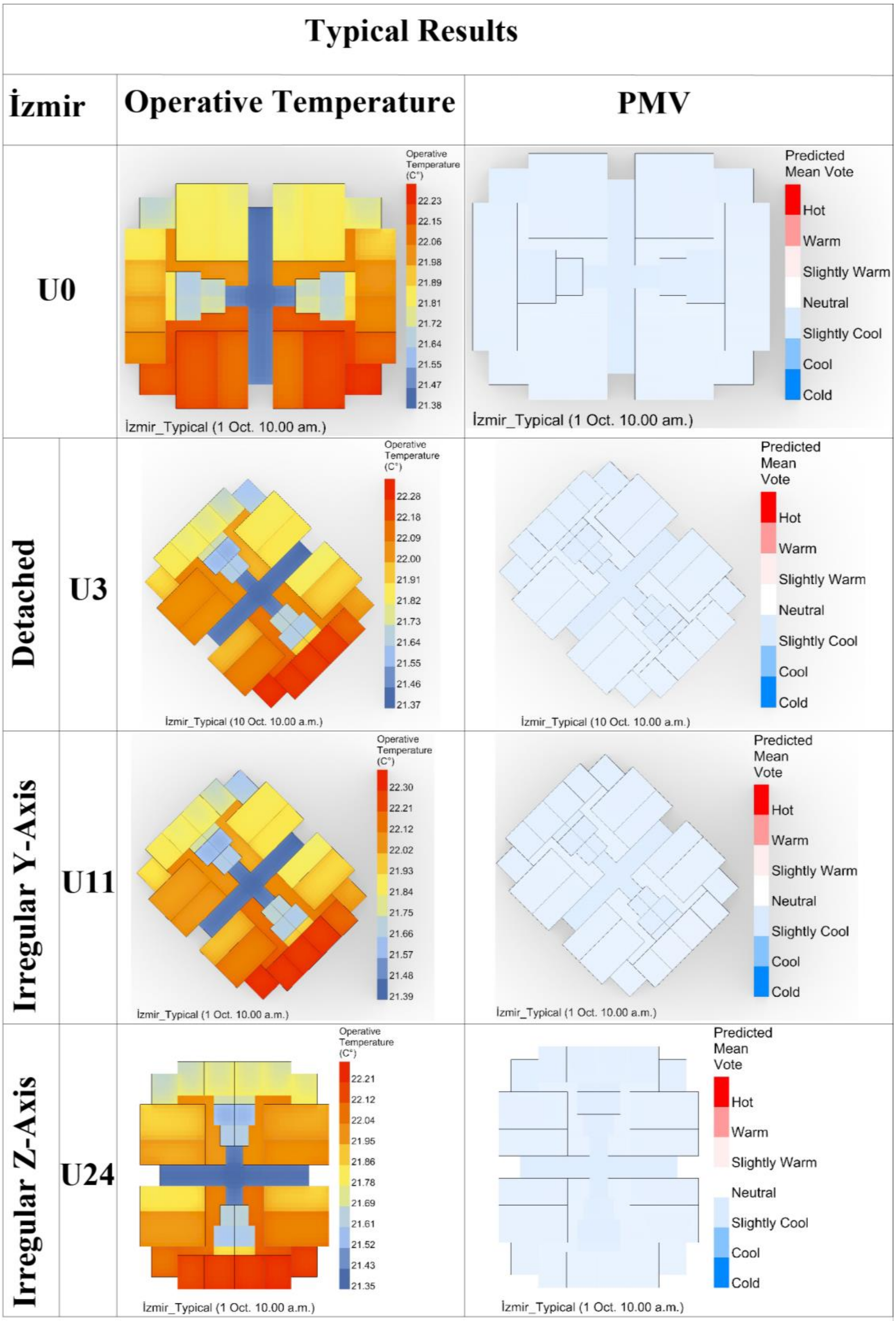

Figure 49: Indoor comfort results for the typical period in İzmir

4.2.4 Discussion of The Optimum Urban Block Models

Figure 50 shows the second positive point table for Ankara and İzmir.

ANKARA							
Scenarios			U0	U9	U11	U27	U28
CFD	Hourly	Ext.Cold			min		
		Ext.Hot			max		
		Typical				min	
Outdoor Comfort	Hourly	Ext.Cold			max		
		Ext.Hot	min				
		Typical			max		
Indoor Comfort	Hourly	Ext.Cold				max	
		Ext.Hot				min	
		Typical			max		
Positive Point.2			1	0	5	3	0
Positive Point.1			0	7	5	5	5
Total Positive Point			1	7	10	8	5

İzmir						
Scenarios			U0	U3	U11	U24
CFD	Hourly	Ext.Cold			min	
		Ext.Hot			max	
		Typical		max		
Outdoor Comfort	Hourly	Ext.Cold	max			
		Ext.Hot		min		
		Typical				min
Indoor Comfort	Hourly	Ext.Cold			max	
		Ext.Hot		min		
		Typical				min
Positive Point.2			1	3	3	2
Positive Point.1			0	4	4	3
Total Positive Point			1	7	7	5

Figure 50: Second positive point table for Ankara and İzmir

For Ankara, it is beneficial to have minimum wind velocity for the extremely cold and typical hours, to have maximum wind velocity for the extremely hot period. Therefore, the U11 model, and U27 model achieve positive points regarding the wind velocity results. According to outdoor temperature sensation, the maximum results for the extreme cold and the typical period provide an advantage in outdoor comfort. However, having a minimum result for the extremely hot period is beneficial. Therefore, the U11 alternative gains the positive remark for the extreme cold and the typical hours, while the existing situation achieves a positive point from the extremely hot period. The maximum results for the extreme cold and the typical period provide an advantage regarding operative temperature results within indoor comfort. In contrast, the minimum result offers an opportunity for the extremely hot hour. Hence, the U27 model gains a positive point for the extreme cold and the extremely hot periods. The U11 model achieves a positive response for the typical hour.

The main findings for Ankara are mentioned below.

- The existing situation gains only one positive point in total.
- Although the U9 model gains the best positive point regarding solar radiation analysis and energy performance simulations, the model does not achieve any positive remark regarding CFD analysis or outdoor and indoor simulations. Therefore, it gains seven positive points among the simulations. It shows that conducting only solar radiation analysis and/or energy performance analysis is not enough to determine the most optimum district morphology. There is a need to make comprehensive research.
- The U27 model achieves the three positive points from the second phase. In total, it has eight positive remarks which is the second placement for Ankara.
- The U11 achieves five positive points regarding CFD, outdoor, and indoor analysis. In total, the model gains ten positive points which is the best response in the analysis.

For İzmir, having minimum wind velocity during the extremely cold period and having maximum value for the extremely hot and the typical hour is advantageous since the climate is hot-humid. Therefore, the U11 model achieves positive points from the extremely cold and hot periods, while the U3 alternative acquires from the typical period. The minimum outdoor temperature sensation benefits the extremely hot, typical period. The maximum value is an advantage for the extremely cold period. Therefore, U0 has a positive response thanks to having a maximum result for the extremely cold period. The U3 model and U24 model achieve positive points by having minimum results for the extremely hot and the typical period. According to indoor comfort results, it is advantageous to have maximum operative temperature during the extremely cold period, and minimum values for extremely hot and typical hours. Among the results, the U11, the U3, and the U24 models gain positive points, respectively. The outputs are summarized below.

- The existing situation, the U0 has only one positive points.
- The U3 model and U11 model succeed in 3 positive responses from CFD analysis, outdoor comfort, and indoor simulations. The models have seven positive points, the best response among the results in İzmir.

As a result of the discussion, the models with the first and the second placement are determined. The U11 and U27 models became prominent for Ankara. The U3 and U11 models come to the forefront for İzmir. Their renewable energy potentials are discussed in Section 4.2.5.

4.2.5 Photovoltaic Panel Integration

Renewable energy potentials are discussed regarding the integration of photovoltaic (PV) panels. Most of the research examines solar energy production by integrating PV panels on facades and roofs. Mohajeri et al. [95] mentioned the benefit of solar potential on urban expansion by referring to the idea of “solar roads” or “solar streets,” which need to be explored in the near future. Therefore, it is valuable to examine the potential of the idea. Thus, the solar potential of PV panels is explored in this thesis by integrating them on roofs and “solar streets,” which are determined in the district.

There are some restrictions for the integration of PVs. When the PV panels are placed on roofs, the floor area of the roof is taken as the basis. Therefore, roofing elements and the location of technical and mechanical equipment have been ignored. For the solar streets, the condition of the landscape has been ignored. Both for the roof-integrated PVs and solar street-integrated PVs the angle of the panels has been ignored.

Figure 51 displays the PV panels' location on the roofs and "solar streets." The area of PV panels on the roofs is 8,676 m². The solar streets are determined between the buildings with a proper space to integrate PV panels. The size of the solar street for the existing situation is 12,881 m², while the alternative models have 32,560 m². The building organization is unequal and irregular in the current case. Therefore, the area of the solar street for the existing situation is lower than the other alternatives.

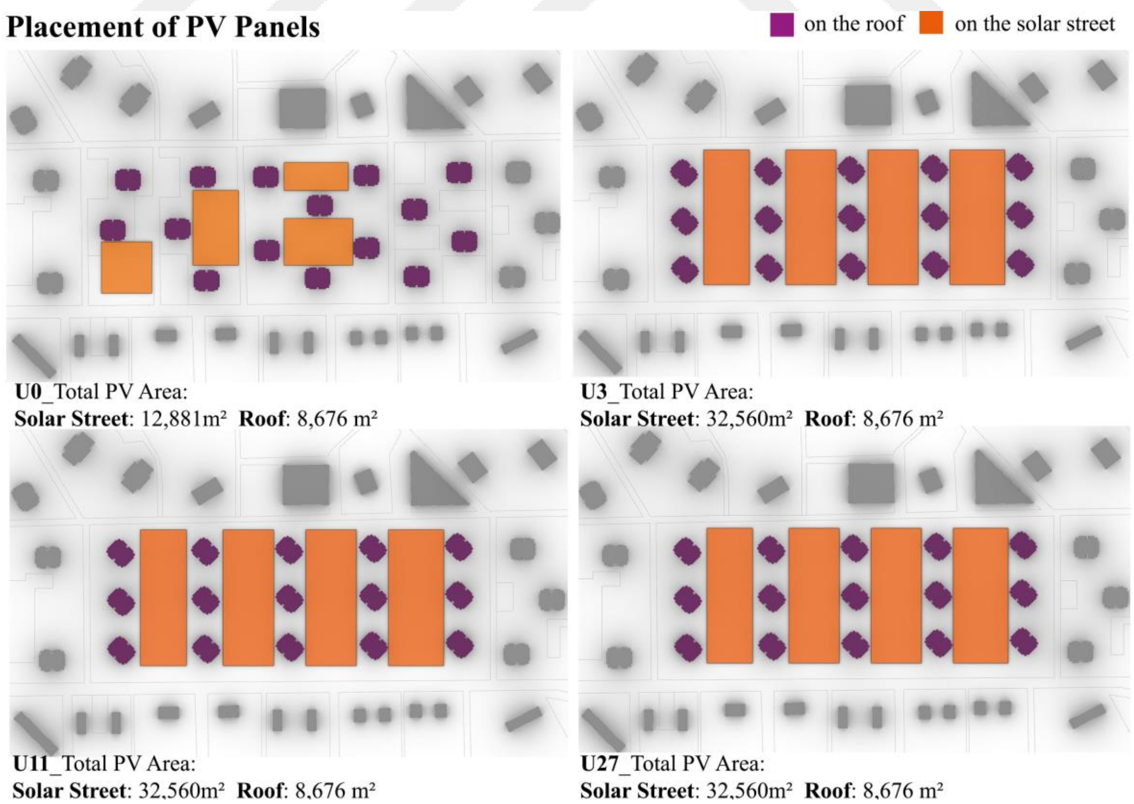

Figure 51: Placement of the PV panels

Table 29 includes the districts' T.P.E. for Ankara. The District T.P.E. for the existing situation is 18,023,398.70 kWh. While it is 18,009,922,44 kWh for the U11 model, the U27 model has 18,047,883.65 kWh.

Table 30 indicates the total produced electricity from PV panels on solar streets and roofs. For the existing situation, the solar streets have 2,194,104.48 kWh of electricity, while the PV panels on the roofs produce 1,756,826.87 kWh of electricity. The final district T.P.E decreases from 18,023,398.70 kWh to 15,829,294.22 kWh thanks to solar street-integrated PV panels, and 16,266,571.83 kWh thanks to roof-integrated PV panels. When the PV panels are integrated into solar streets, almost 1.5 times more electricity production is provided. Therefore, the final district T.P.E is lower for the solar streets.

Table 29: Calculation of the district's T.P.E. for Ankara

Urban Scenario		*T.P.E. (kWh/m²)*	*T.P.E. (kWh)*	*District T.P.E. (kWh)*
Existing	U0	207.727	120,155.99	18,023,398.70
Irregular X-Axis	U11	207.572	120,066.14	18,009,922.44
Irregular Y-Axis	U27	208.012	120,319.22	18,047,883.65

Table 30: Total produced electricity and final district T.P.E.for Ankara

ANKARA					
Urban Scenario		*Total Produced Electricity (kWh)*		*Final District T.P.E. (kWh)*	
		Solar Street	*Roof*	*Solar Street*	*Roof*
Existing	U0	2,194,104.48	1,756,826.87	15,829,294.22	16,266,571.83
Irregular X-Axis	U11	5,191,776.92	1,751,160.27	12,818,145.52	16,258,762.17
Irregular Y-Axis	U27	5,024,499.76	1,750,422.31	13,023,383.89	16,297,461.34

The PV panels on the solar streets produce 5,191,776.92 kWh of electricity for the U11 model, while it is 1,751,160.27 kWh for roofs. The PV panels on the solar streets have nearly three times more electricity production than the integration on roofs. Therefore, the final district T.P.E decreases from 18,009,922.44 kWh to 12,818,145.52 kWh thanks to the integration of PV panels on the solar streets. This is the minimum result for the final district T.P.E belongs to the U11 model. The final district T.P.E result is 16,258,762.17 kWh for the roof-integrated PV panels. This is also the lowest result among roof-integrated PV alternatives for Ankara.

The solar street electricity production for the U27 alternative is 5,024,499.76 kWh. This enables 13,023,383.89 kWh final district T.P.E. The roof-integrated PV panels produce 1,750,422.31 kWh of electricity, which provide 16,297,461.34 kWh of the final district T.P.E. Similarly, the solar street-integrated PV panels produce approximately three times more electricity than roof-integrated PV panels. Figure 52 shows the results in a graphical way.

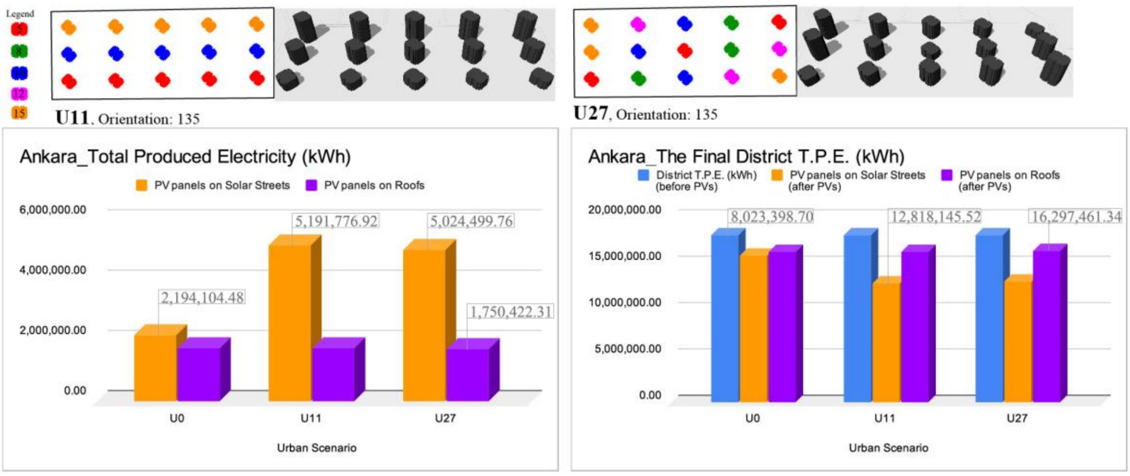

Figure 52: Total produced electricity and the final district’s T.P.E. in Ankara

- Among the results, the maximum electricity produced from roof-integrated PV panels belongs to the existing situation.
- Approximately, solar street-integrated PV panels produce three times more electricity than roof-integrated PV panels in Ankara.
- Among the results, the maximum electricity is produced thanks to solar street-integrated PV panels, which is 5,191,776.92 kWh with the U11 model. This model also has the lowest final district T.P.E. with 12,818,145.52 kWh. Therefore, the best optimum district model for Ankara is the U11 model, whose positive point is increased from 10 to 11 thanks to the final score.

Table 31 shows the districts' T.P.E. for İzmir. The District T.P.E. for the existing situation is 12,819,270.93 kWh. It is 11,463,337.54 kWh for the U3 model. The U11 model has 12,819,274.40 kWh. Among the models, the minimum District T.P.E. belongs to the U3 model in İzmir.

Table 31: District's T.P.E. for İzmir

Urban Scenario		*T.P.E. (kWh/m²)*	*T.P.E. (kWh)*	*District T.P.E. (kWh)*
Existing	U0	147.747	85,461.80	12,819,270.93
Detached	U3	132.120	76,422.25	11,463,337.54
Irregular X-Axis	U11	147.747	85,461.82	12,819,274.40

Table 32 indicates the total produces electricity and the final districts' T.P.E. for İzmir. For the existing situation, solar street-integrated PV panels have 2,243,565.90 kWh of electricity. It enables a decrease in the districts' T.P.E. with 10,575,705.03 kWh. When the PV panels are integrated into roofs, it produces 1,783,184.51 kWh of electricity, and the districts' T.P.E. becomes 11,036,086.42 kWh. Therefore, solar street-integrated PV panels are more beneficial.

For the U3 model, the solar street-integrated PV panels produce 4,887,786.00 kWh of electricity and provide a decrease for districts' T.P.E. from 11,463,337.54 kWh to 6,575,551.43 kWh. This is nearly half of the result. Also, this is the lowest result for İzmir. The roof-integrated PV panels produce 1,783,298.42 kWh of electricity, and the districts' T.P.E. is 9,680,039.12 kWh. Therefore, solar street-integrated PV panels produce about three times more electricity than roof-integrated PV panels.

For the U11 model, the roof-integrated PV panels produce 1,659, 290.56 kWh of electricity, while the solar street-integrated PV panels have 5,268,597.35 kWh of electricity. When the PV panels are utilized on solar streets, it produces approximately 3.5 times more electricity than roof-integrated PV panels.

Table 32: Total produced electricity and final district T.P.E.for İzmir

İzmir					
Urban Scenario		*Total Produced Electricity (kWh)*		*Final District T.P.E. (kWh)*	
		Solar Street	*Roof*	*Solar Street*	*Roof*
Existing	U0	2,243,565.90	1,783,184.51	10,575,705.03	11,036,086.42
Detached	U3	4,887,786.00	1,783,298.42	6,575,551.43	9,680,039.12
Irregular X-Axis	U11	5,268,597.35	1,659,290.56	7,550,677.05	11,159,983.84

Figure 53 shows the results in a graphical way for İzmir.

- The PV panels in İzmir produce more electricity than in Ankara. It can be related to the impact of climate since İzmir has a hot-humid climate zone.
- For the existing situation in İzmir, the solar street-integrated PV panels produce 1.5 times more electricity than the roof-integrated ones.
- For the U11 model, the solar street-integrated PV panels produce 3.5 times more

electricity than the roof-integrated PVs. This is the highest production among the alternatives. However, the final districts' T.P.E for the U11 model is not lower than the result for the U3 model.

- The solar street-integrated PV panels produce three times more electricity than the roof-integrated PVs with the U3 model. It provides to have the lowest final districts' T.P.E among the results. Therefore, the positive point of the U3 model increased from 7 to 8 finally. The U3 model acquires the best optimum district model for İzmir.

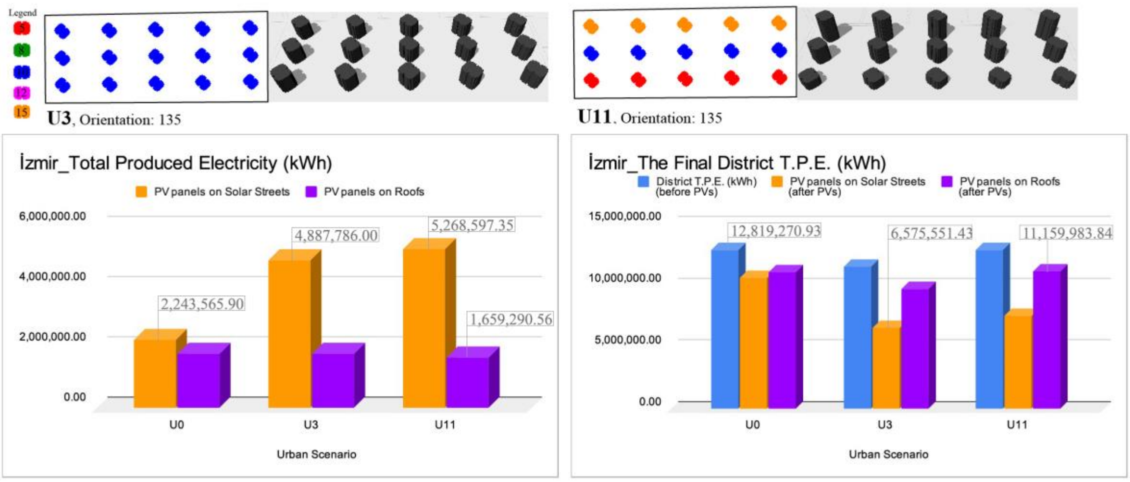

Figure 53: Total produced electricity results and the final district's T.P.E. in İzmir

As a result of the research, the solar radiation potential and energy performance of district models are discussed for Ankara and İzmir. The results for Ankara highlight the U9 model as the best positive response alternative. The U11, U27, and U28 models are at the second placement for Ankara. For İzmir, the best responses belong to the U3 model and U11 model, while the U24 gains the second placement.

In the second phase, these alternatives are tested regarding CFD simulation and outdoor and indoor analysis. This stage shows the necessity of comprehensive research to determine the most optimum district model. Although the U9 model gains the best positive points, the model does not achieve any points from the second stage. It shows the strong impact of conducting wind simulation and outdoor and indoor analysis. For Ankara, the U11 model successes the highest point, while the U27 model is in the second placement. For İzmir, the highest points belong to the U3, and U11 models.

In the third stage, the optimum district models about the potential of electricity production from PV panels located on roofs and solar streets are examined. The common output for İzmir and Ankara is that solar street-integrated PV panels produce nearly three times more electricity than roof-integrated PV panels. The best optimum urban scenario for Ankara is the U11 model, which produces the highest electricity thanks to solar streets and ensures the lowest final district T.P.E. The best optimum urban model for İzmir is the U3 model by having the lowest final district T.P.E. However, it should be highlighted that the highest amount of electricity from solar streets is produced with the U11 model.

CHAPTER V

CONCLUSION

This thesis aims to examine the impact of district morphology on environmental control, energy performance, outdoor comfort, and indoor comfort by considering different climatical regions of Turkey. Three features make the work original. The first and major one is conducting comprehensive research by including solar potential and wind behavior with environmental control parameters, energy performance levels, and thermal comfort analysis for outdoor and indoor environments. Secondly, arranging alternative district models by considering both homogeneous and heterogeneous morphology. Thirdly, PV panels are integrated into roofs and "solar streets," which is mentioned in the literature as one of the future explorations to benefit from solar energy by using urban expansion as a potential.

The case study district is in Ankara, Etimesgut. It has a temperate-dry climate. The comparing city is İzmir which has a hot-humid climate. Regarding variables and constant parameters, 28 district alternative models are developed. The existing situation and the 28 alternative models are examined using different plug-ins in Grasshopper/Rhinoceros software.

The performance analysis includes solar radiation simulation and energy performance analysis annually and hourly. The main outcomes are summarized below.

- Ankara has a temperate-dry climate. Therefore, it is advantageous to have maximum solar radiation for annual and hourly results while having minimum primary energy results. The U9 model achieves the first placement, while U11, U27, and U28 are in the second placement.

- İzmir has a hot-humid climate. Regarding solar radiation, it is advantageous to have minimum results for the annual and extremely hot periods while having maximum results for the extremely cold and typical periods. Regarding energy performance, having minimum primary energy is beneficial. Hence, the most positive alternative for İzmir is the U3 alternative; the others are U11 and U24 alternatives.

The optimization process includes wind simulation, outdoor analysis, and indoor analysis with alternatives that gain the first and the second placements. The outputs of wind simulation, outdoor analysis, and indoor analysis are summarized below.

Having minimum wind velocity for the extremely cold and the typical periods; having maximum result for the extremely hot period is an advantage for the temperate-dry climate. Therefore, the U11, and U27 are beneficial for the extremely cold, hot, and typical periods respectively, in Ankara. For hot-humid climates, it is positive to have maximum wind velocity for the extremely hot, and typical hours, to have minimum result for the extremely cold period. In İzmir, the U11 and U3 alternatives have the proper values.

Regarding outdoor comfort results, it is positive to have maximum outdoor temperature sensation values for extremely cold and typical periods. In contrast, the lowest result is beneficial for the extremely hot period in Ankara. The U0 model has the minimum consequence for the extremely hot period. The U11 model has the maximum result for the extremely cold and the typical results. For İzmir, the maximum result is advantageous for the extremely cold period; the minimum value benefits the extremely hot and the typical periods. Therefore, the U11, U3, and U24 alternatives are advantageous for İzmir.

Regarding indoor comfort simulation results, it is positive to have the maximum operative temperature for the extremely cold and the typical period and a minimum result for the extremely hot period in Ankara. U11 gains a positive response for the extremely cold, typical periods, while the U0 model has the lowest result for the extremely hot period. In İzmir, providing maximum values for the extremely cold period, minimum results for the extremely hot, and typical results are positive. Therefore, the U11, U3, and U24 models are advantageous in İzmir orderly.

- When the positive results are superimposing solar radiation analysis, energy performance simulations, CFD simulations, outdoor comfort analysis, and indoor comfort analysis, the optimum urban blocks are U11 and U27 for Ankara. Although the U9 model is the best for solar radiation and energy performance, the alternative does not gain any positive response from wind, outdoor comfort, and indoor comfort results. For İzmir, the optimum urban blocks are the U3 and U11 models. Also, all the optimum urban blocks have a 135° building orientation.

To ensure the best optimum urban block scenario, the renewable energy potentials of the alternatives are examined by integrating photovoltaic panels.

- Solar street-integrated PVs produce nearly three times more electricity than the roof-integrated ones for Ankara and İzmir.

- The best optimum district model for Ankara is the U11 model. It produces the highest amount of electricity through solar streets, which is 5,191,776.92 kWh. The model ensures the lowest final T.P.E., which is 12,818,145.54 kWh. This is almost 33% less than the current value.

- The best optimum district model for İzmir is the U3 alternative by ensuring the lowest final T.P.E., 6,575,551.43 kWh. This result is approximately 52% less than the existing one. The production of electricity, thanks to solar streets, is 4,887,786.00 kWh. Moreover, regarding the highest electricity production, the U11 model performs best with 5,268,597.35 kWh.

This study shows the importance of conducting comprehensive research to determine the best optimum district morphology in an urban environment for different climatical regions. Further studies can conduct research by expanding the boundary of the case study area, the competence of more urban alternatives can be tested by adding more variables, and the variables regarding landscape can be integrated into the research. Since the importance of the solar street is understood, this idea also can be further developed.

APPENDIX A

The Background of Algorithmic Analysis

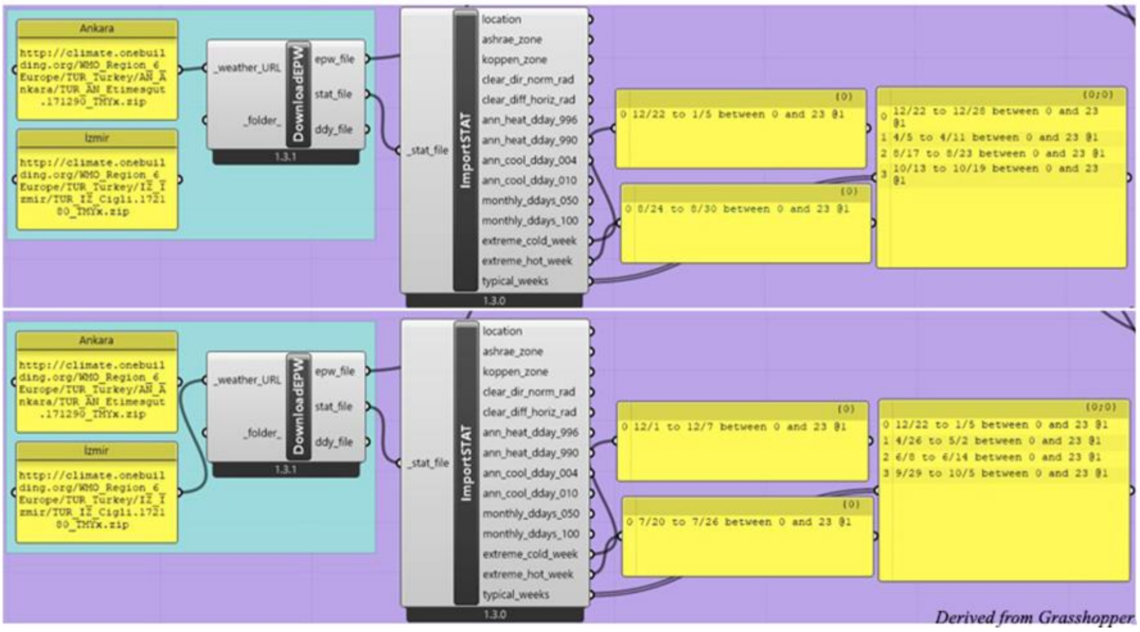

Appendix A1: Outputs of LB Import Stat

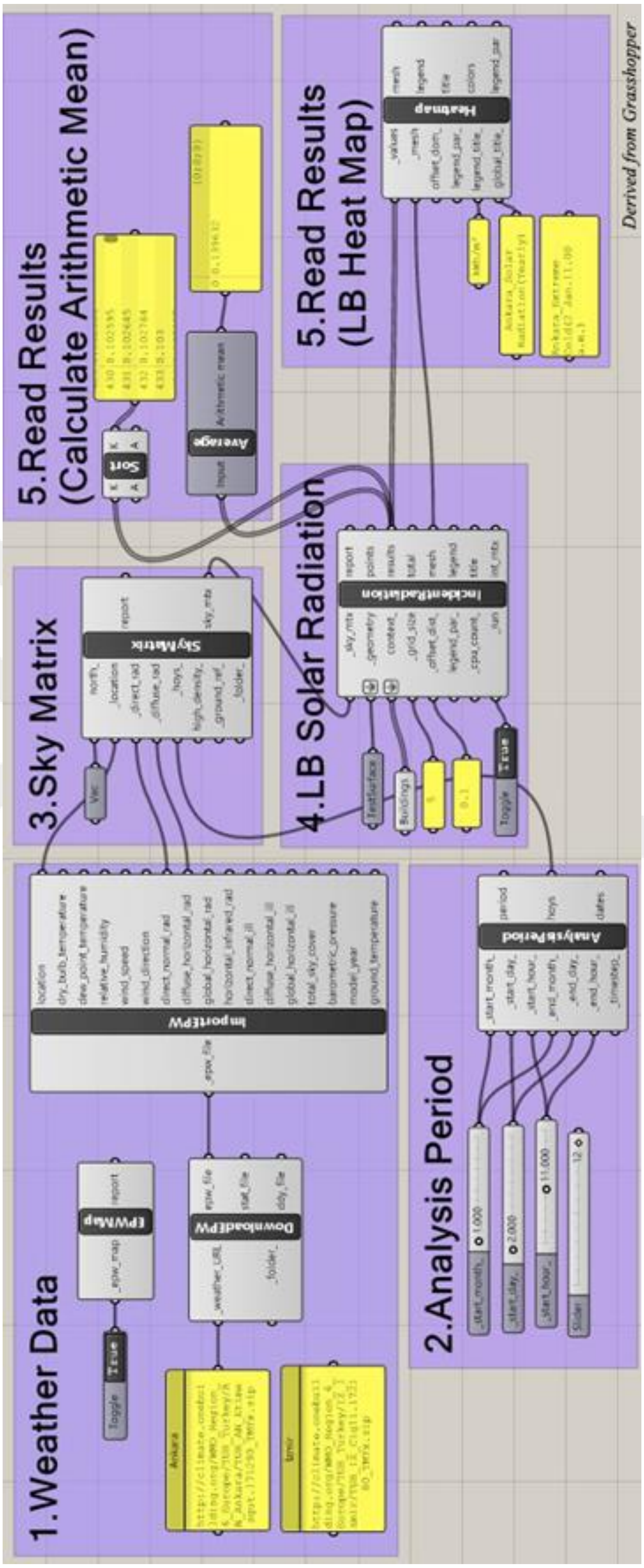

Appendix A2: Solar radiation script

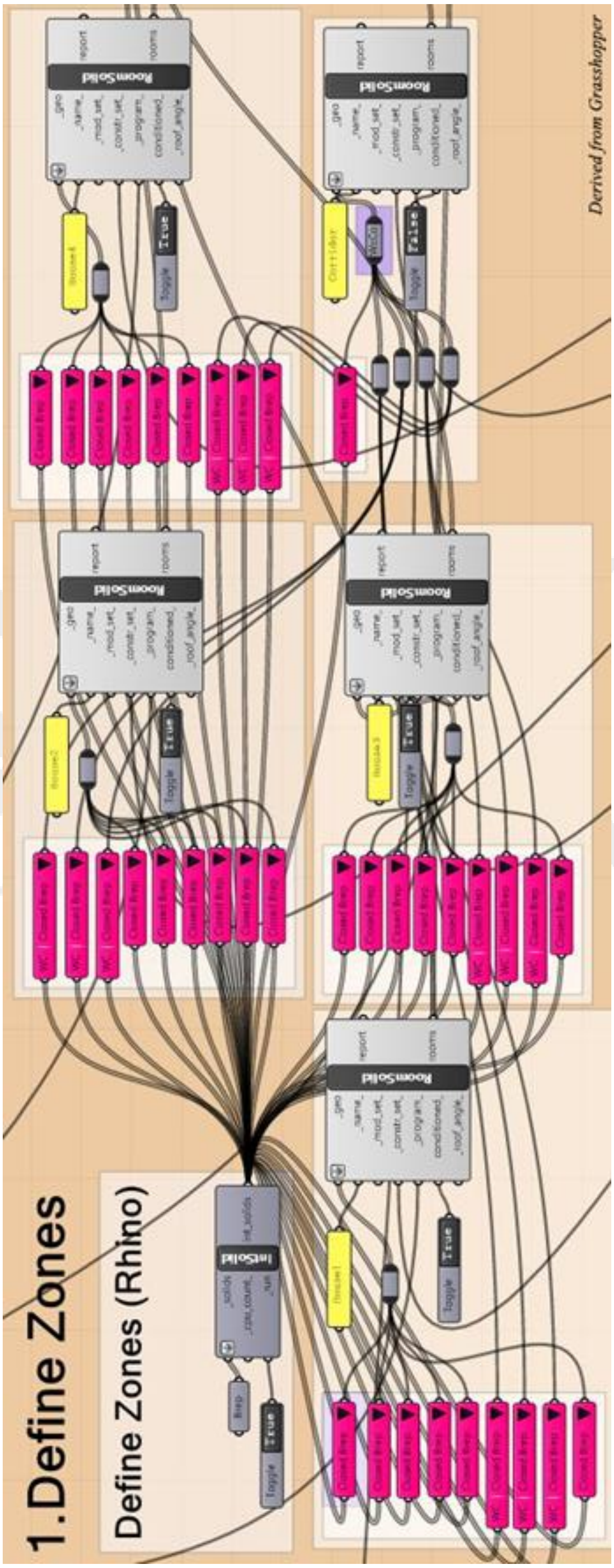

Appendix A3: First part of the algorithm: definition of zones

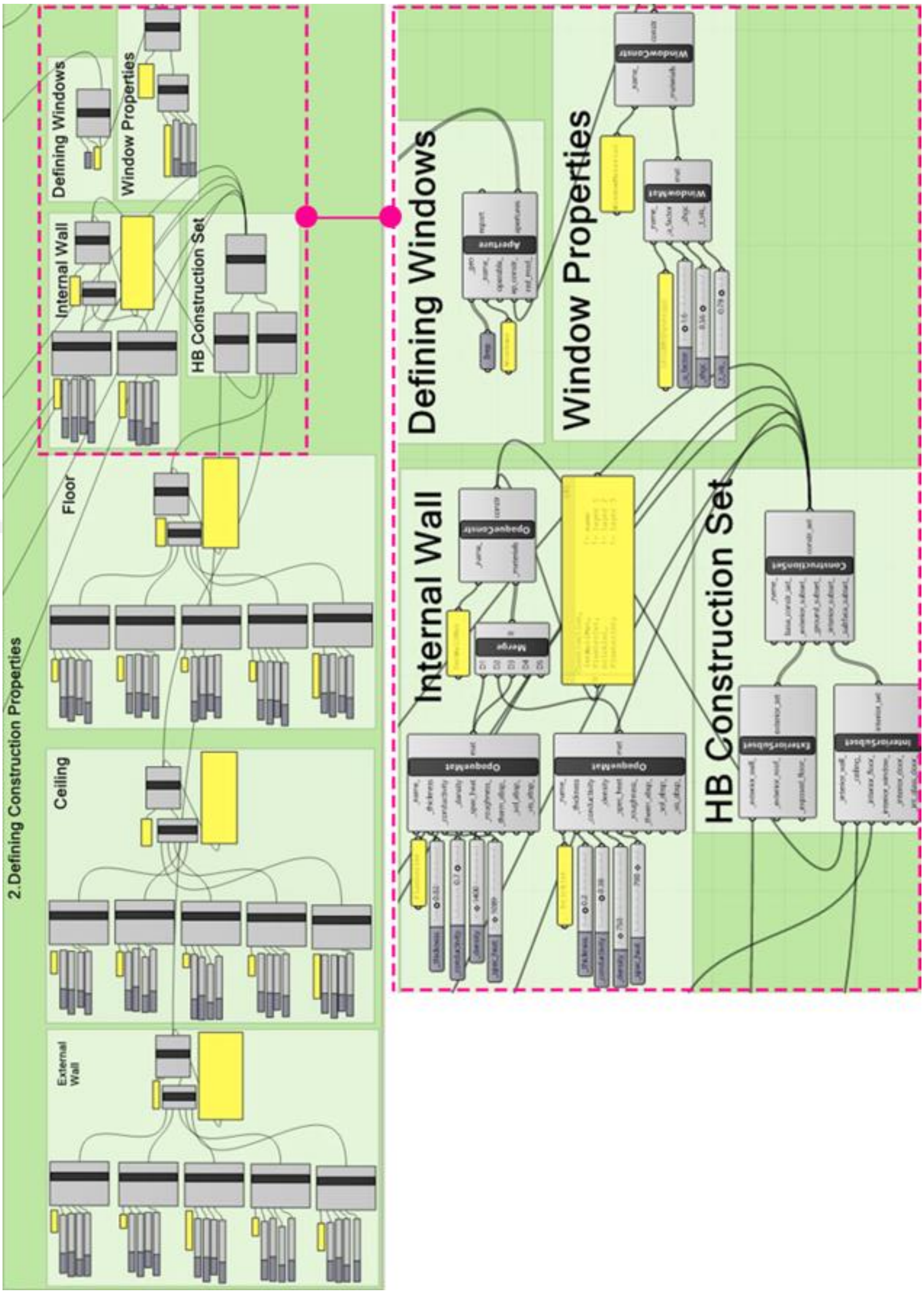

Appendix A4: Second part of the script: definition of construction properties

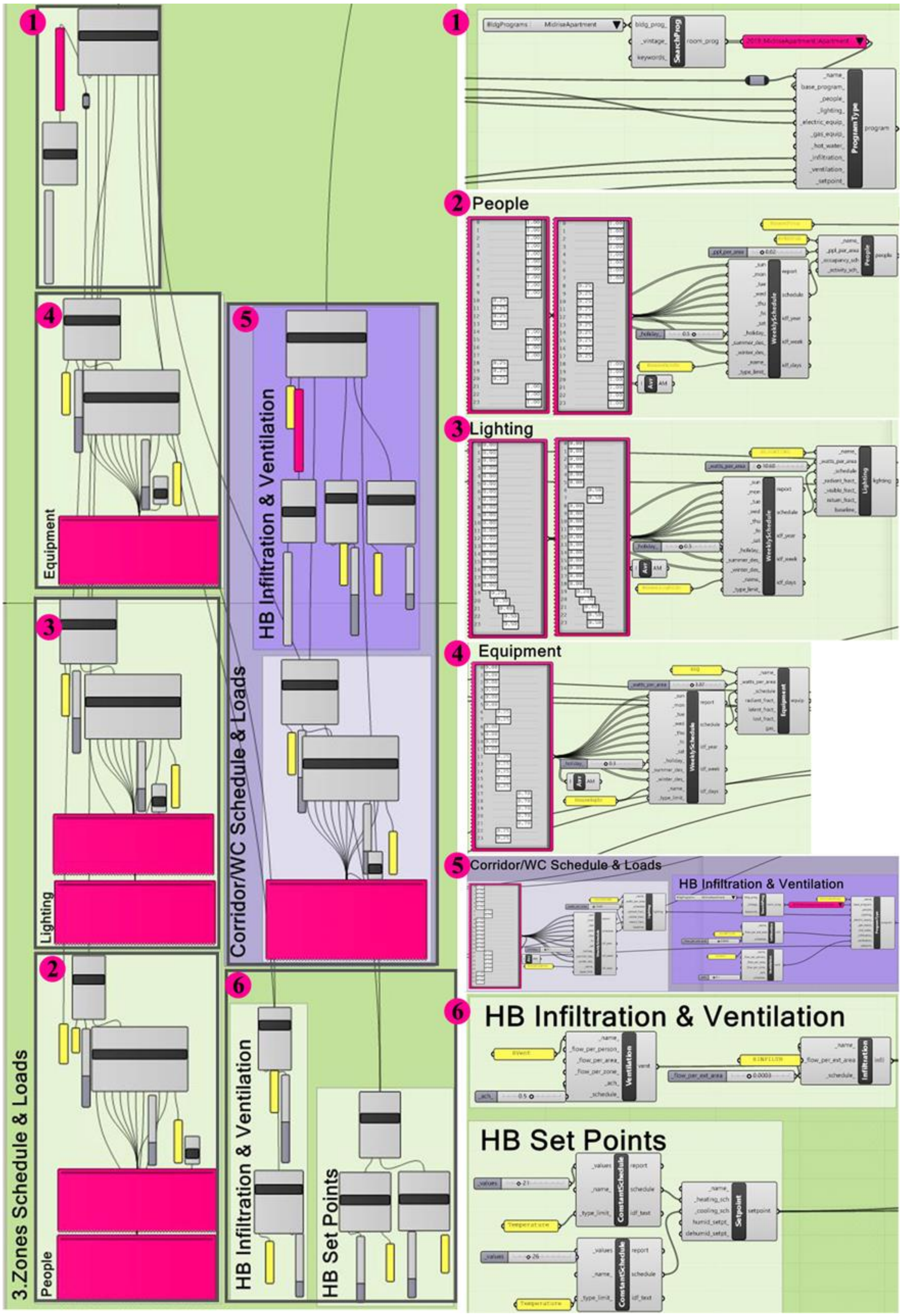

Appendix A5: Third part of the script: development of loads and schedules

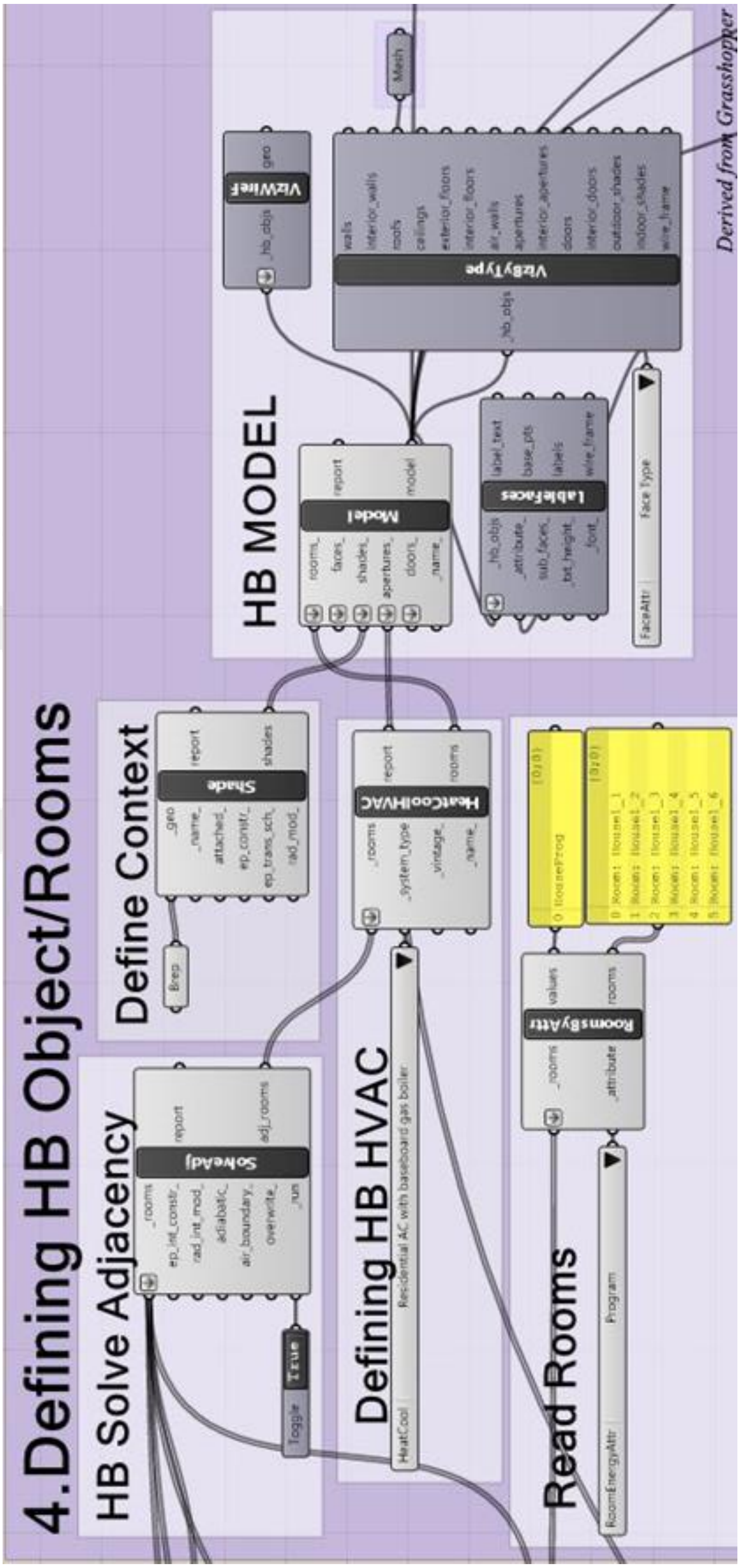

Appendix A6: Fourth part of the script: definition of HB Object

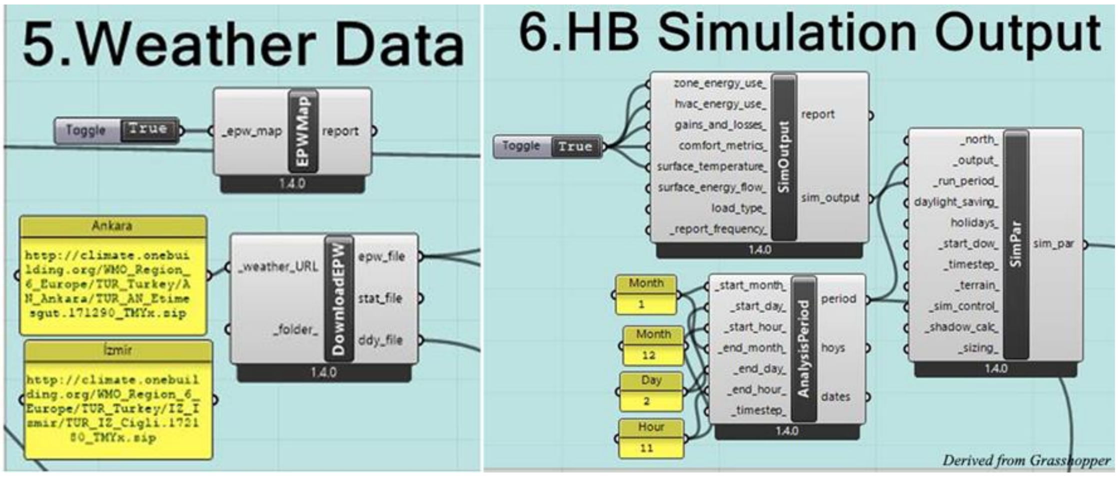

Appendix A7: Organization of weather data and simulation output

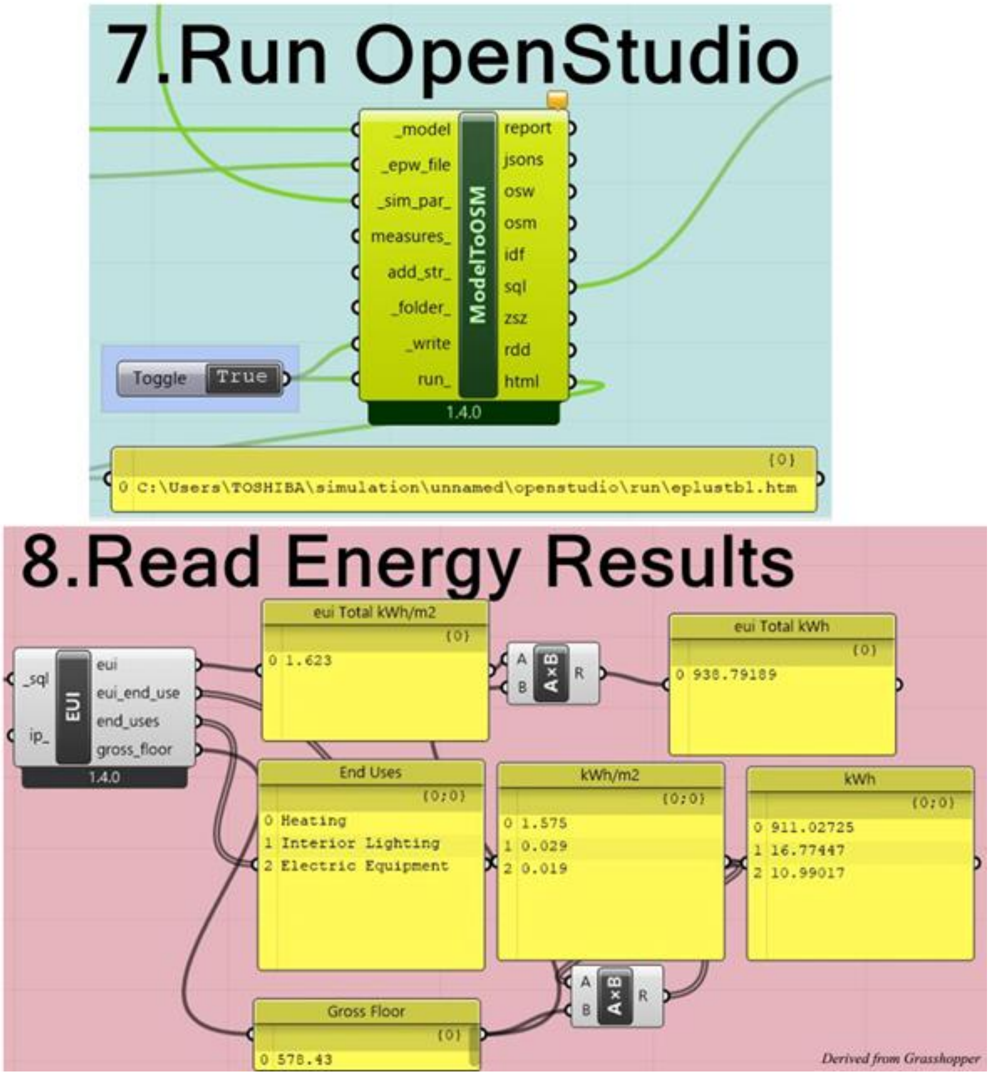

Appendix A8: Reading energy performance results

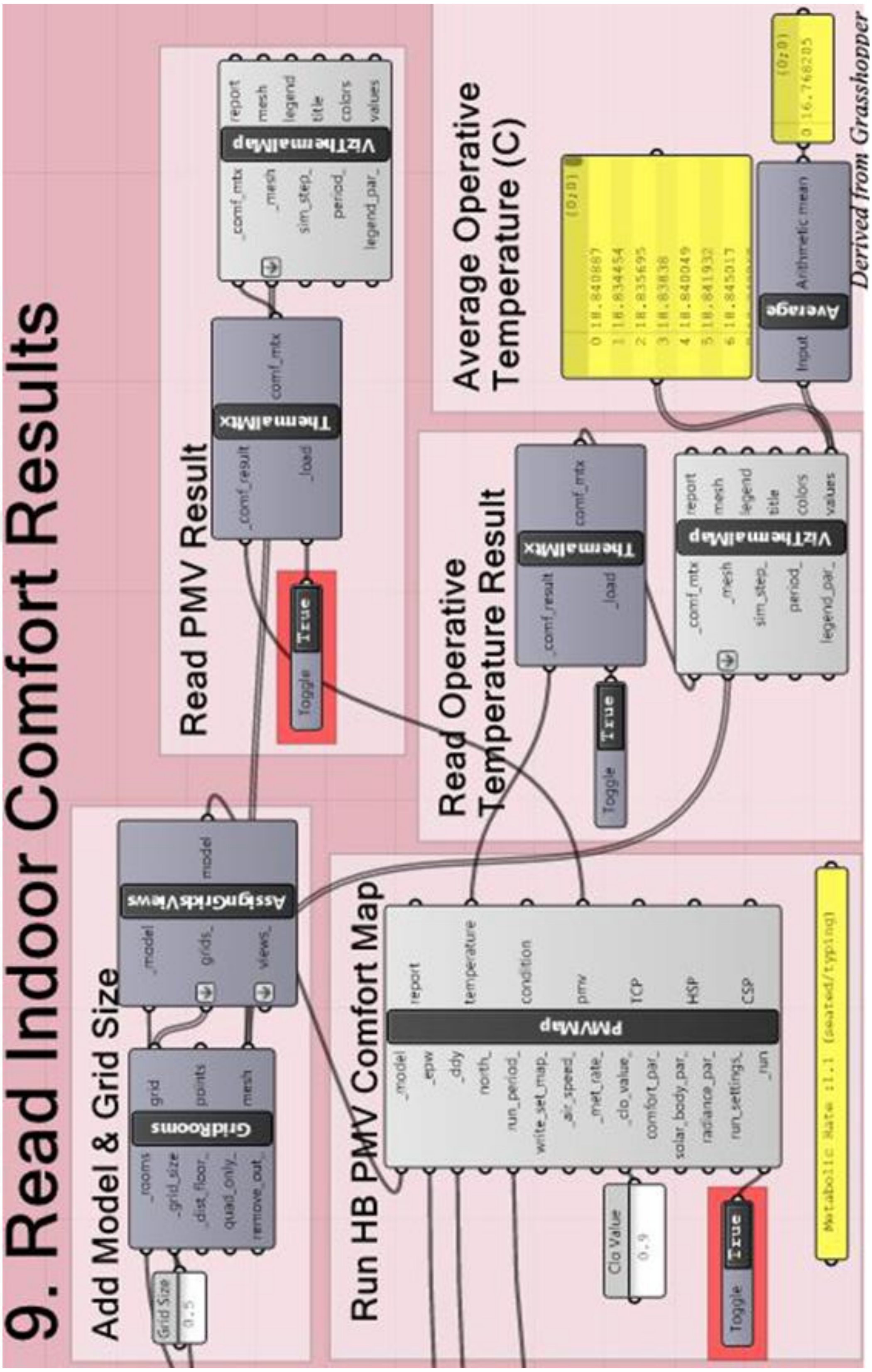

Appendix A9: Reading indoor comfort results

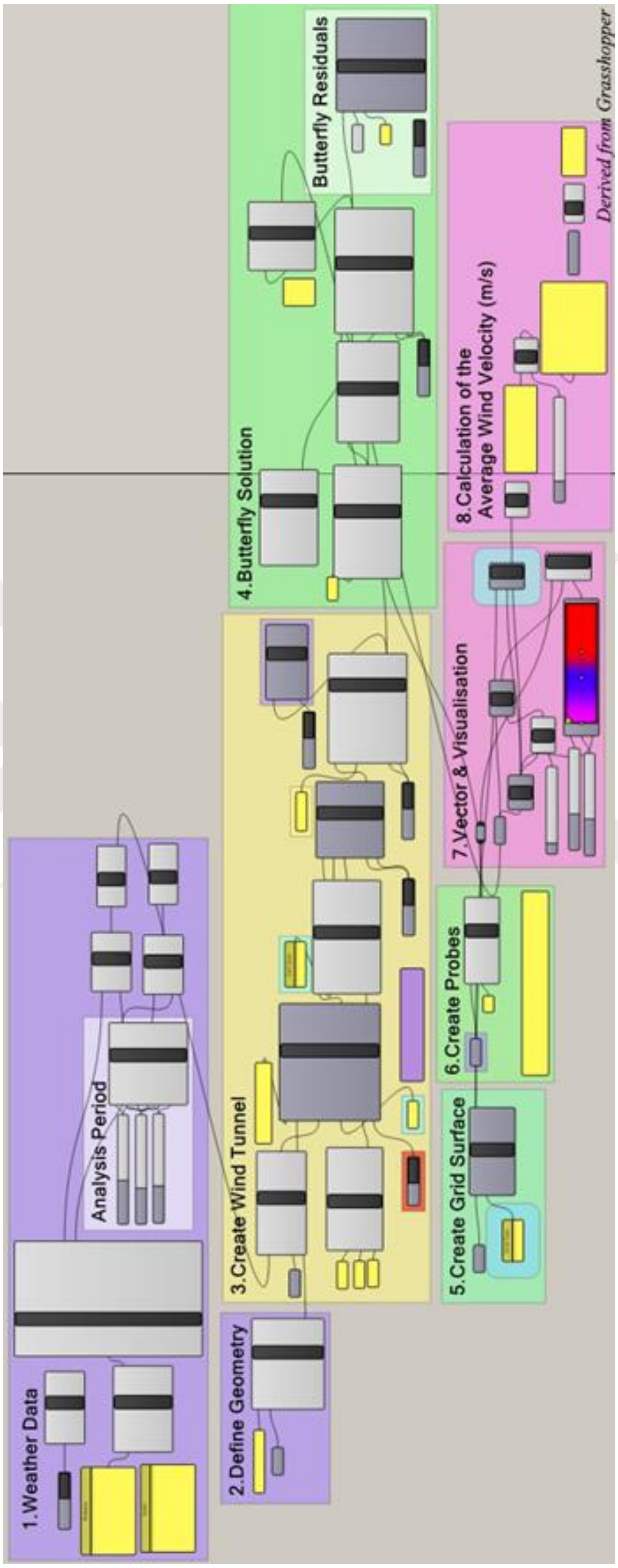

Appendix A10: CFD script

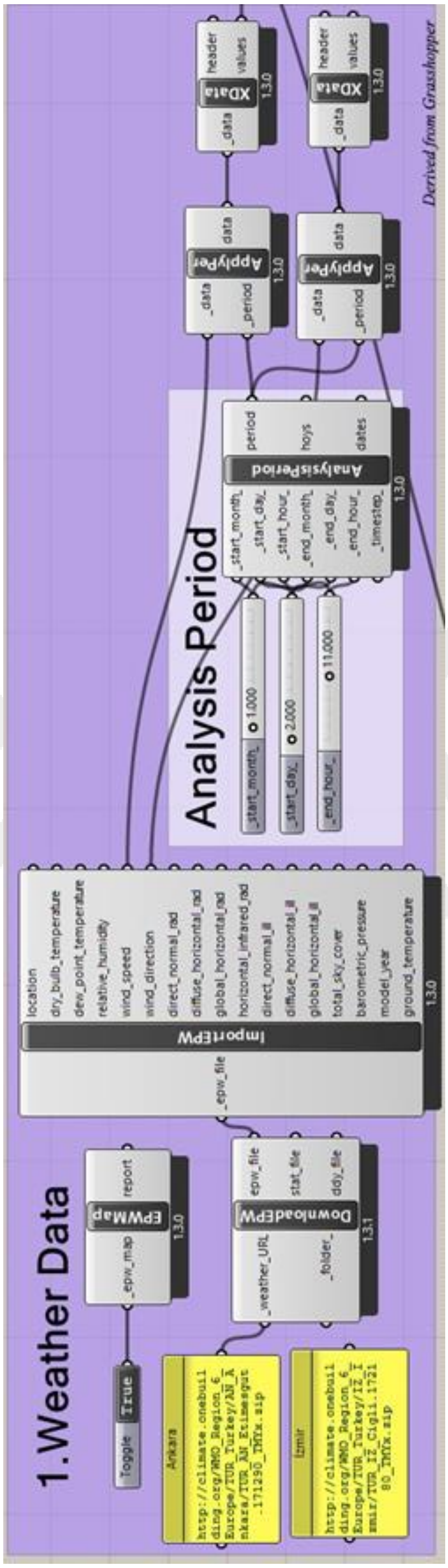

Appendix A11: Importing weather data and organization of run period

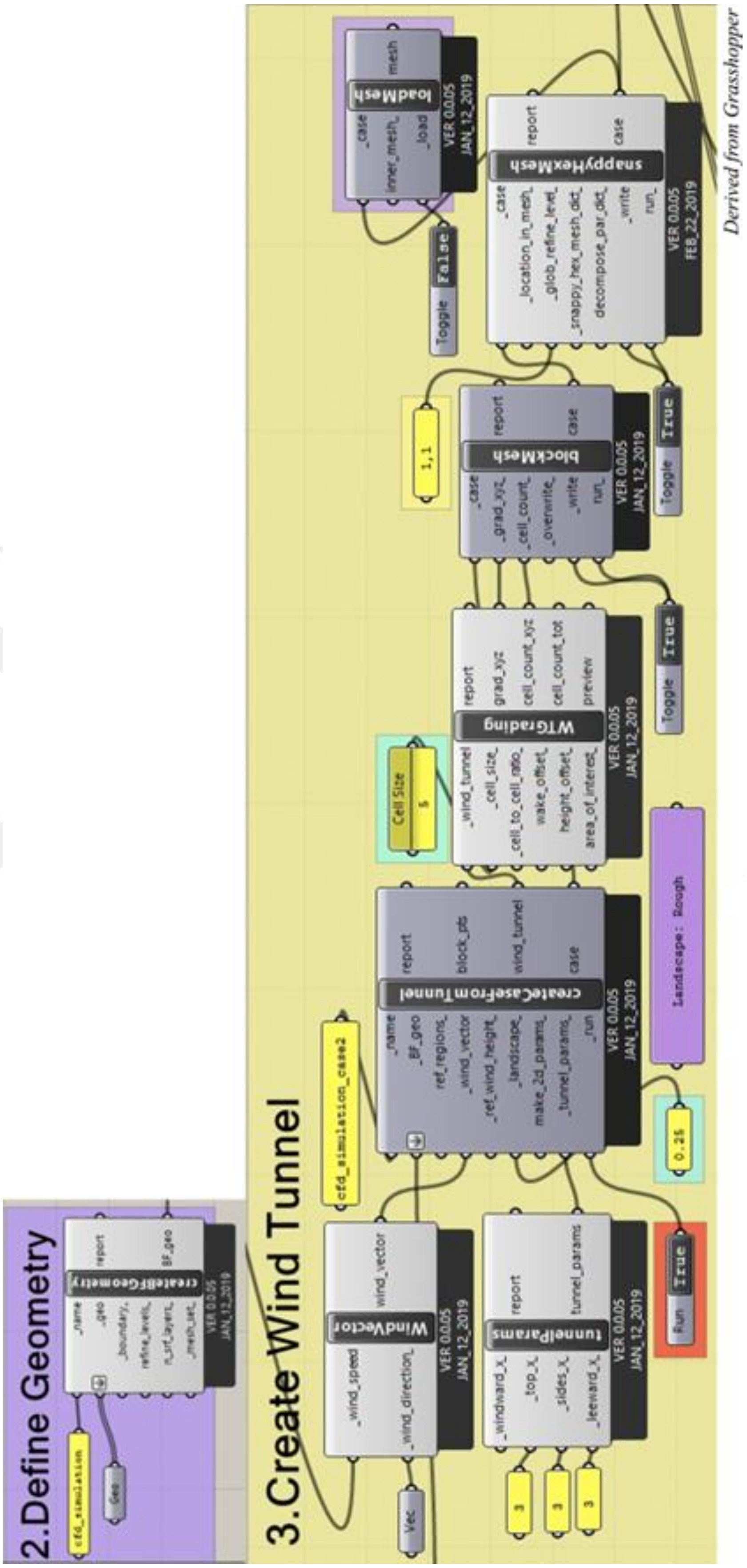

Appendix A12: Importing geometry and creating wind tunnel

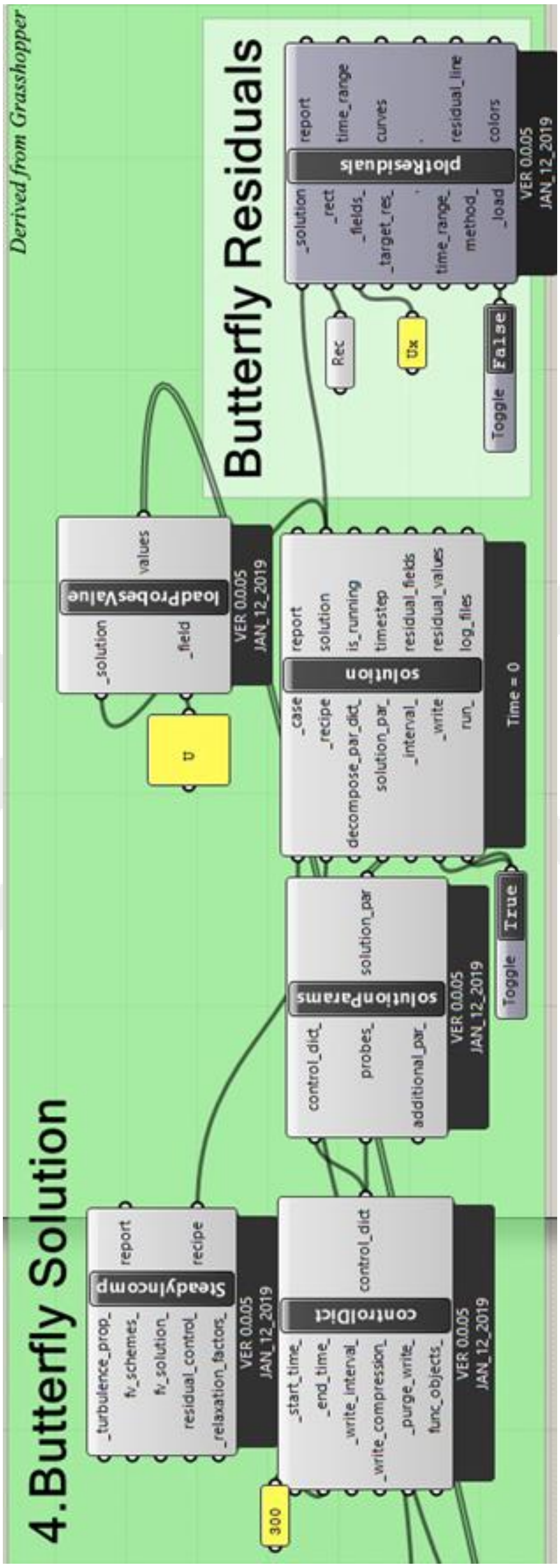

Appendix A13: Definition of Butterfly Solution

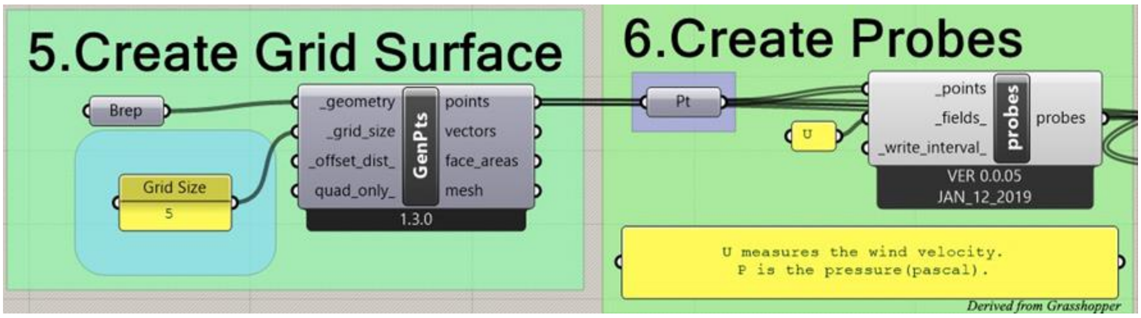

Appendix A14: Determination of test surface and probes

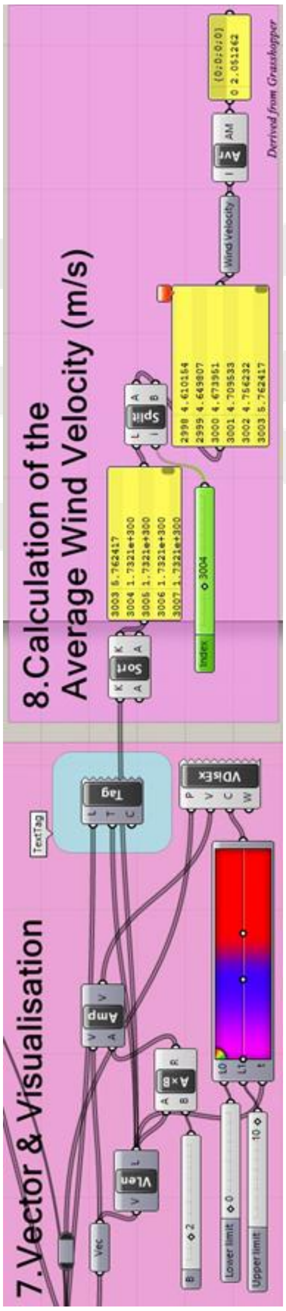

Appendix A15: Reading CFD Results

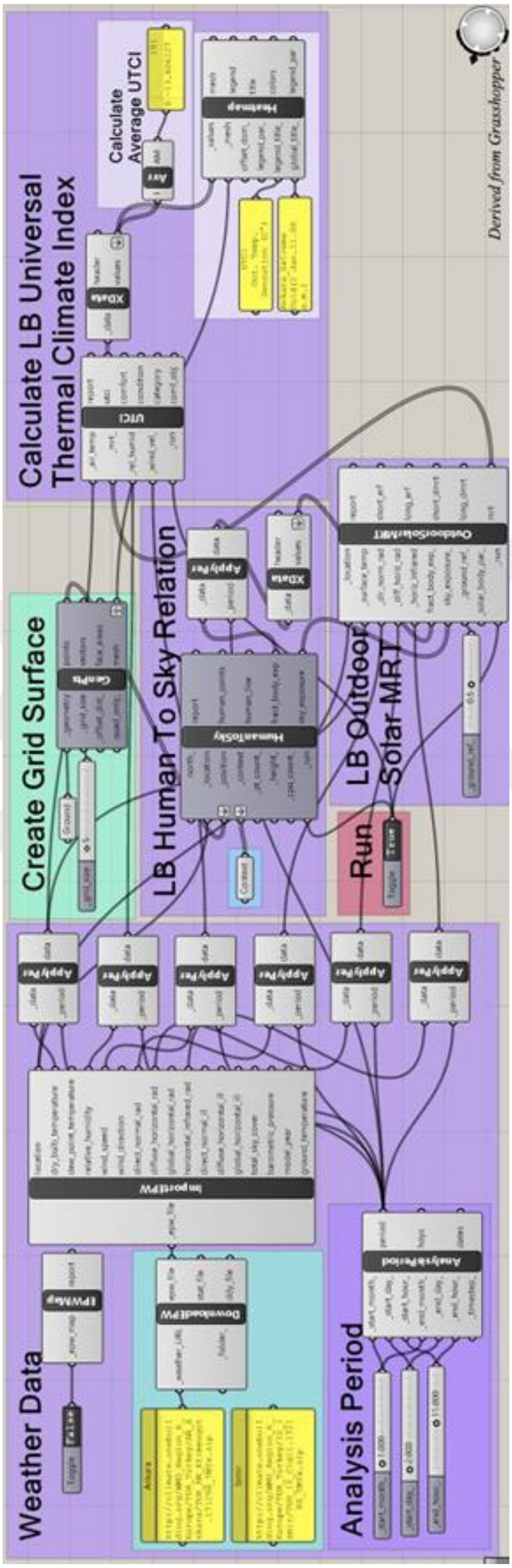

Appendix A16: Outdoor comfort script

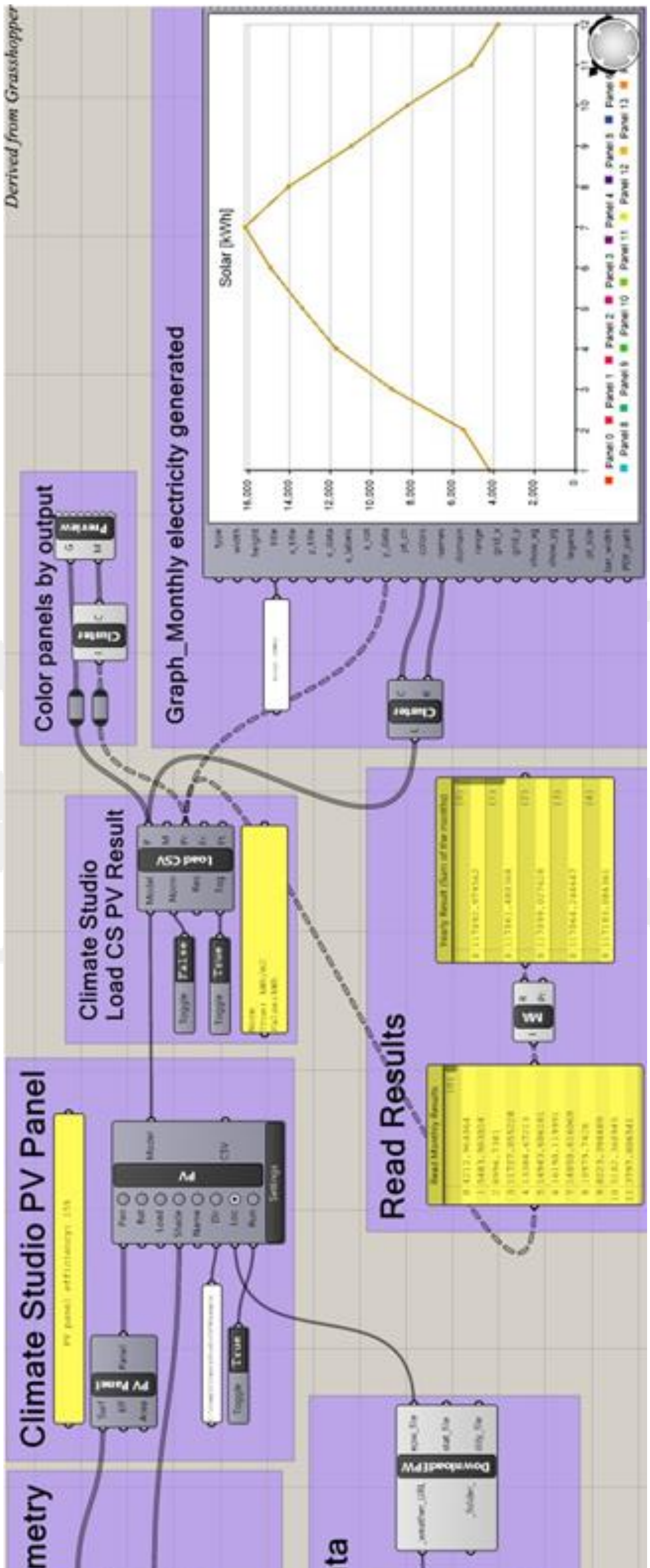

Appendix A17: S of the photovoltaic panels integration

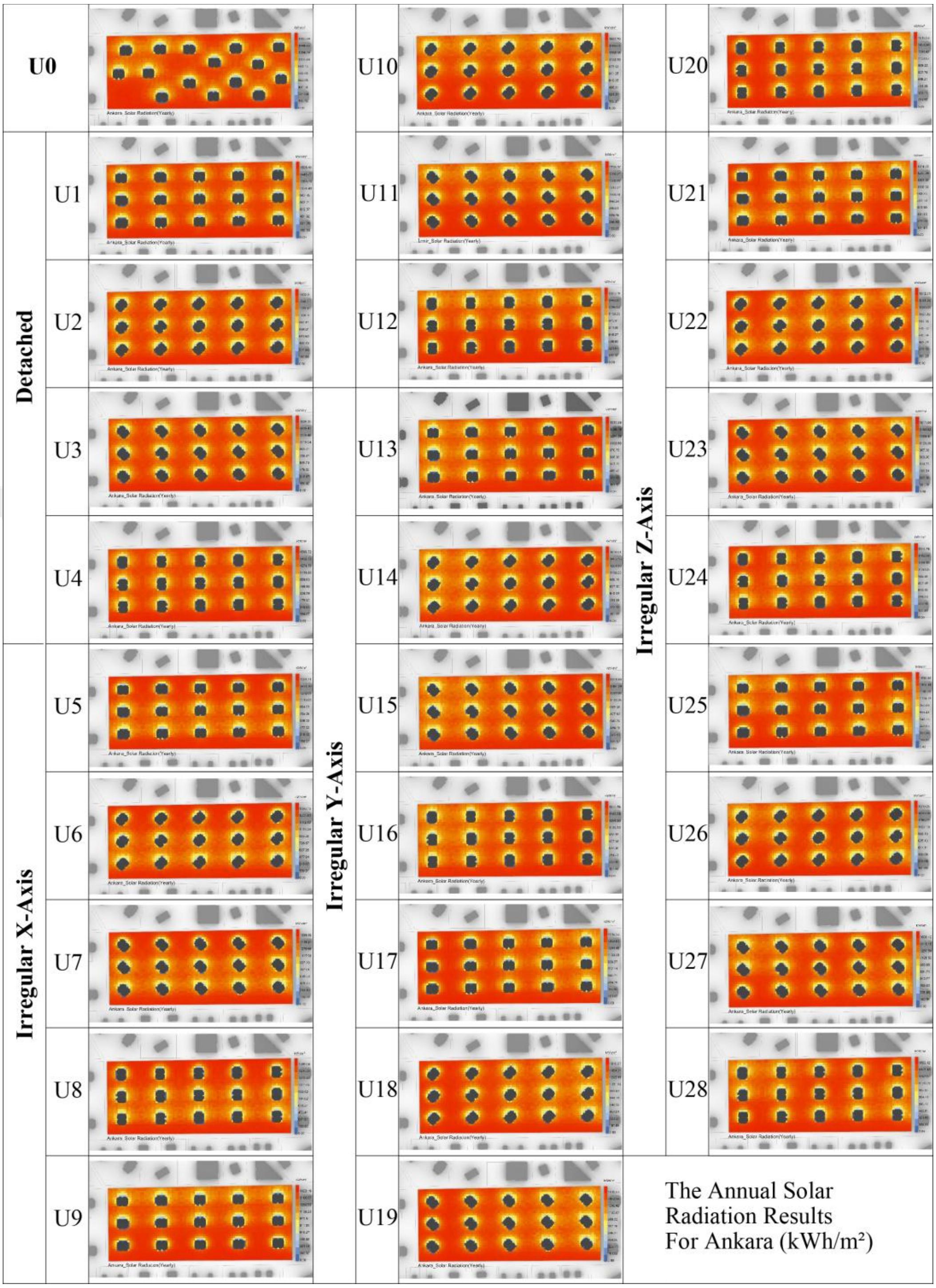

Appendix A18: Annual solar radiation results for Ankara

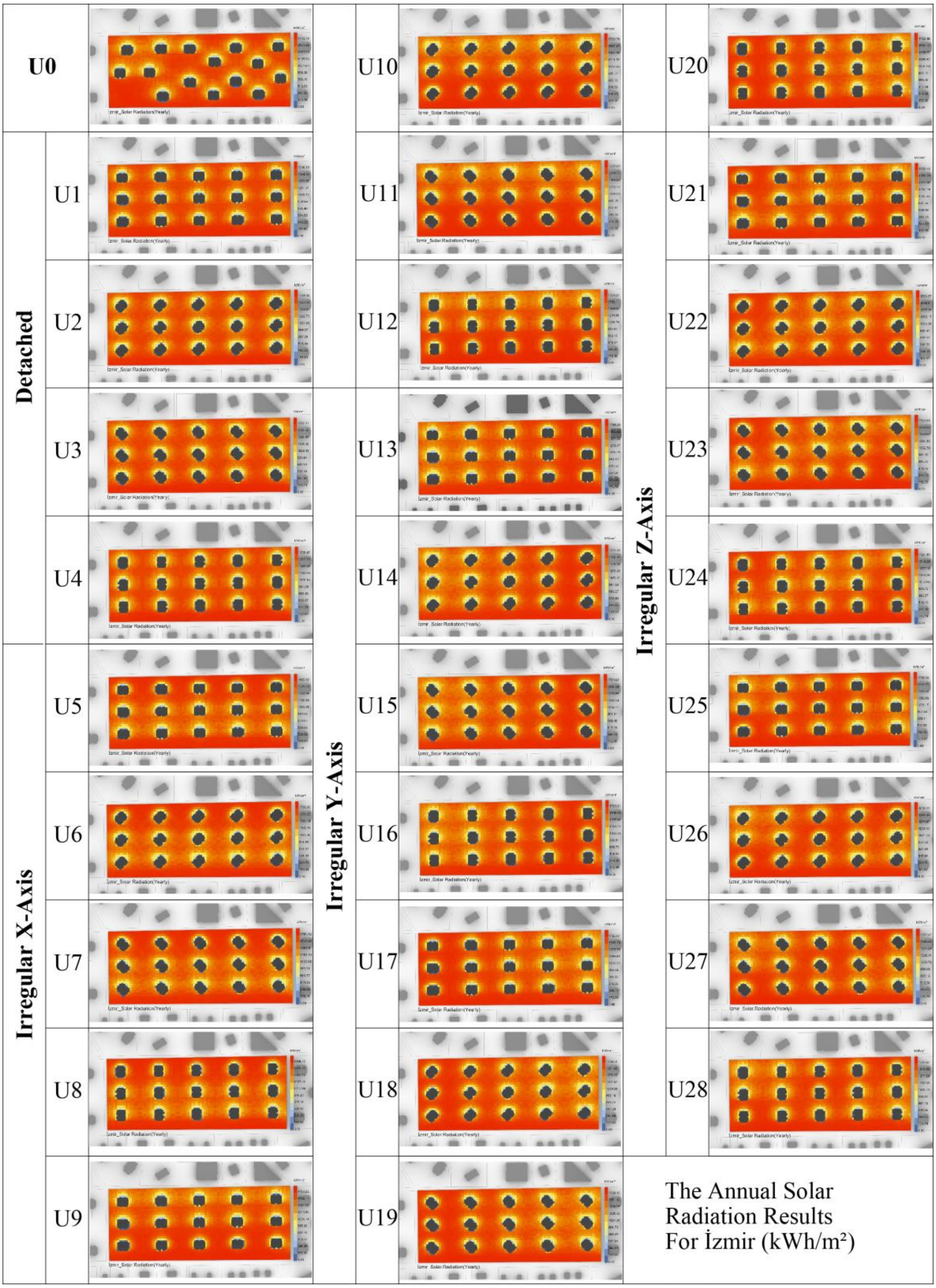

Appendix A19: Yearly solar radiation results for İzmir

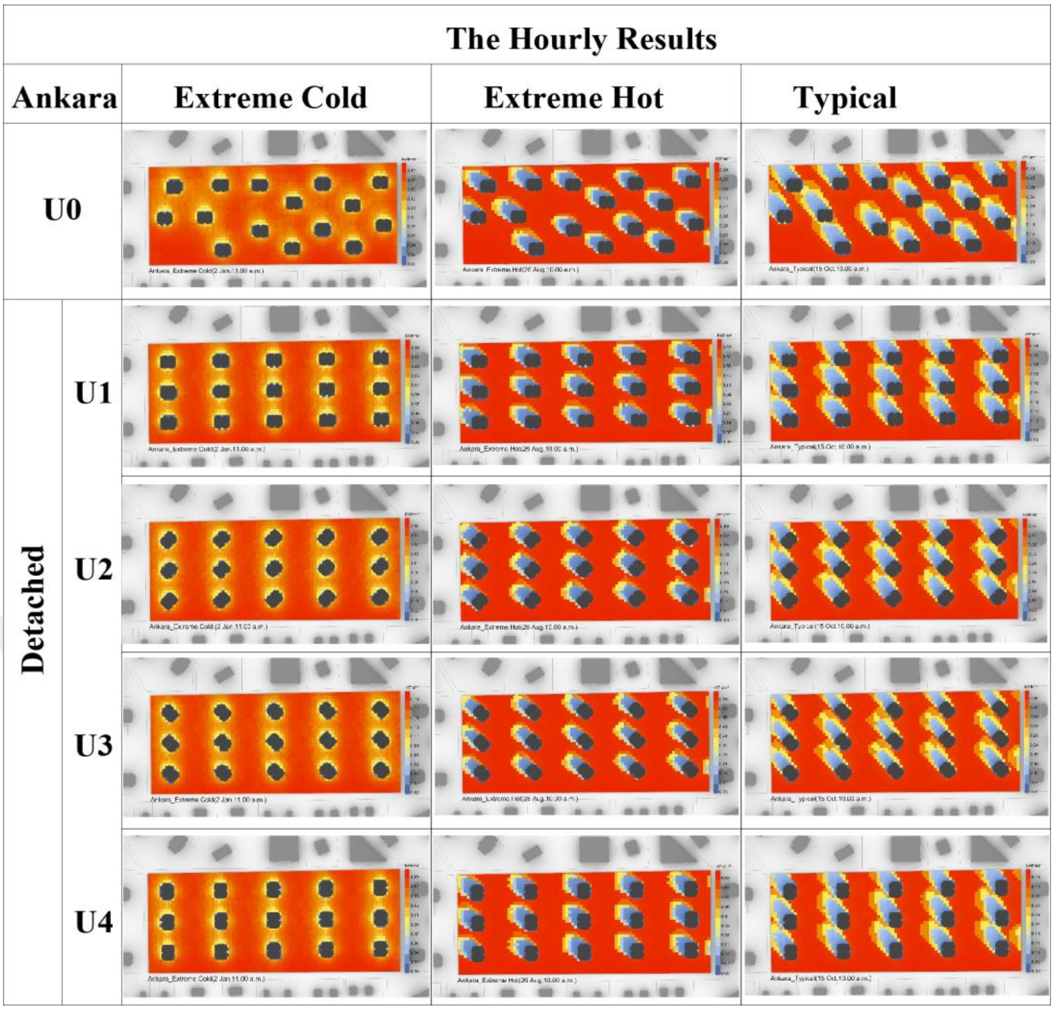

Appendix A20: Hourly solar radiation results for the U0, and the detached alternatives in Ankara

The Hourly Results				
Ankara		Extreme Cold	Extreme Hot	Typical
Irregular X-Axis	U5	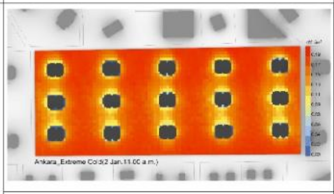	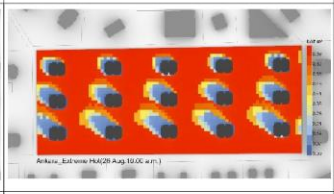	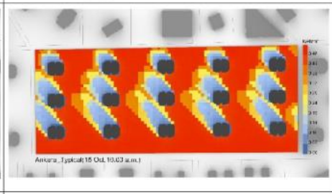
	U6	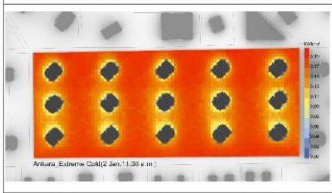	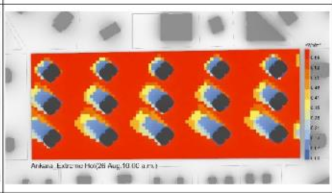	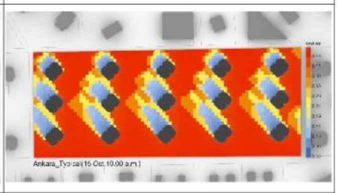
	U7	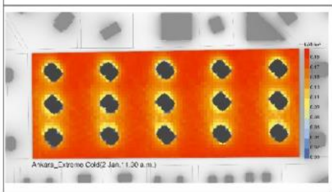	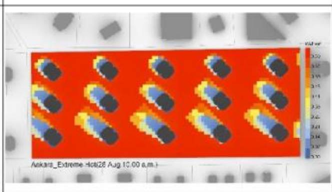	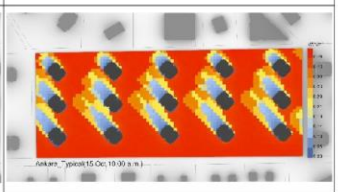
	U8	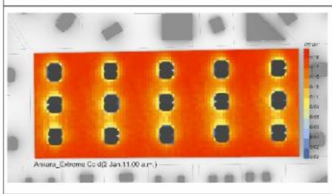	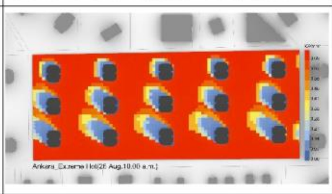	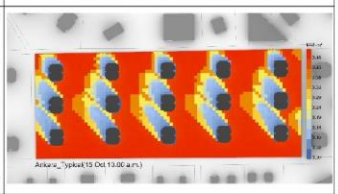
	U9	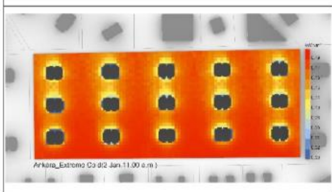	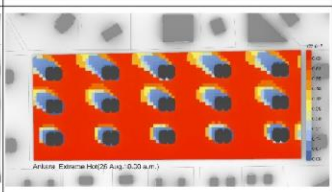	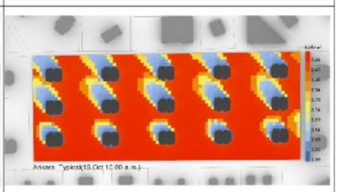
	U10	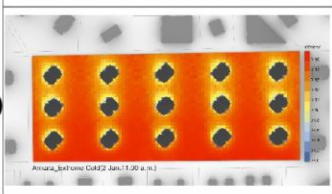	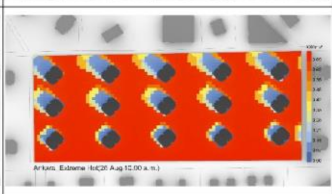	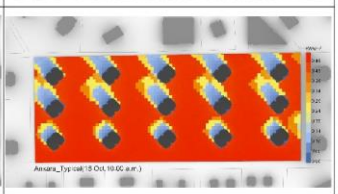
	U11	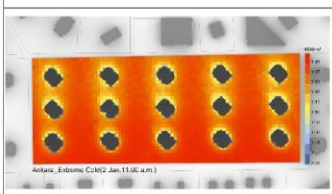	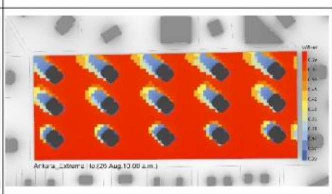	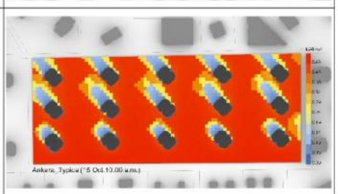
	U12	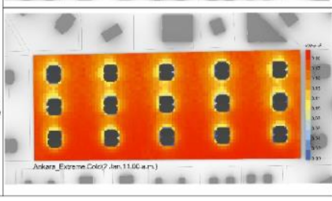	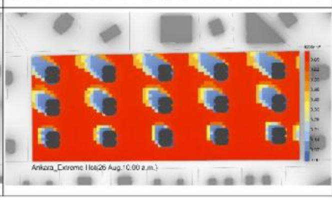	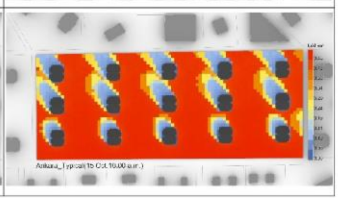

Appendix A21: Hourly solar radiation results for the Irregular X-Axis in Ankara

The Hourly Results				
Ankara		Extreme Cold	Extreme Hot	Typical
Irregular Y-Axis	U13	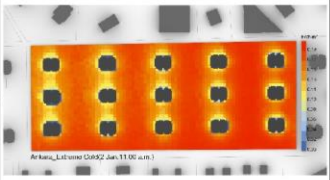	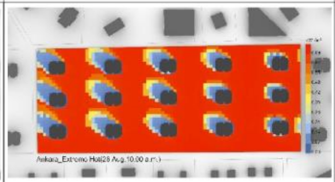	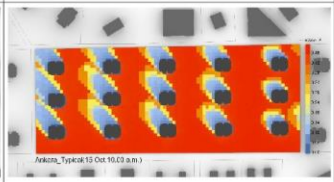
	U14	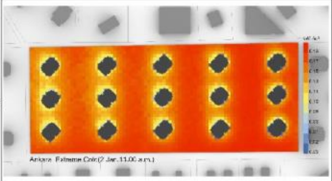	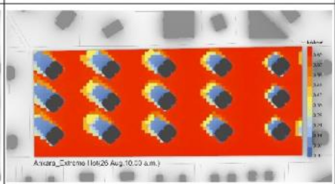	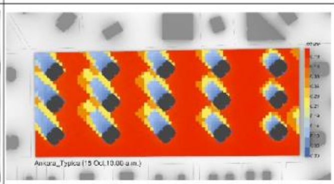
	U15	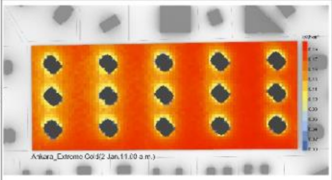	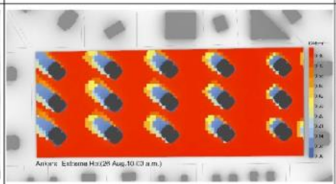	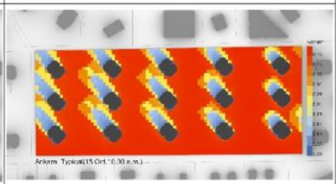
	U16	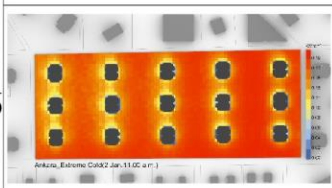	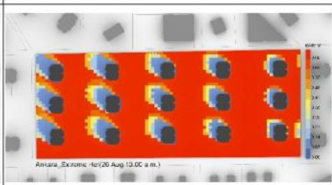	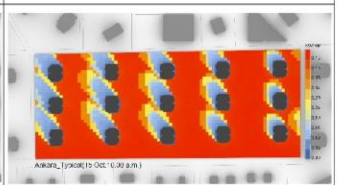
	U17	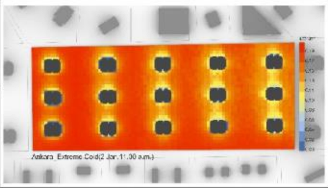	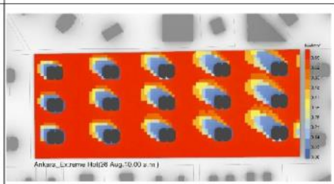	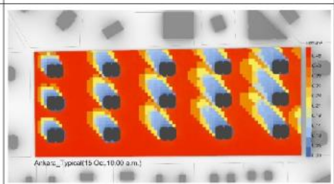
	U18	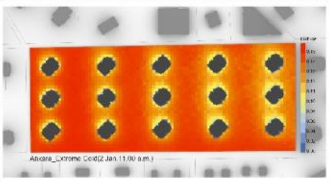	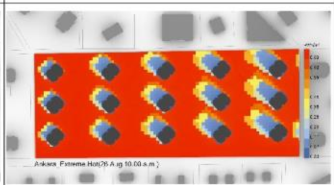	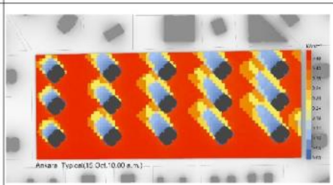
	U19	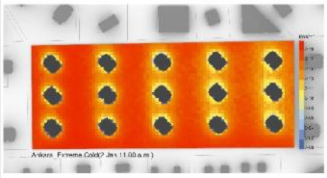	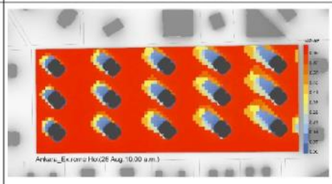	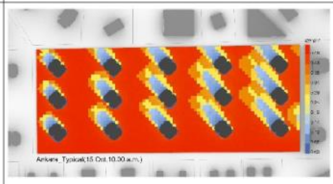
	U20	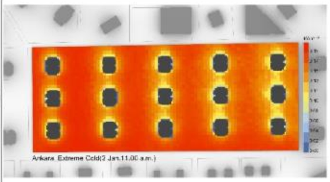	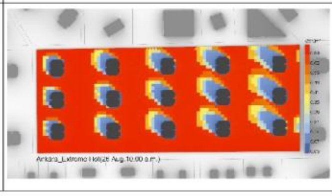	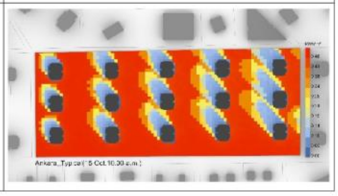

Appendix A22: Hourly solar radiation results for the Irregular Y-Axis in Ankara

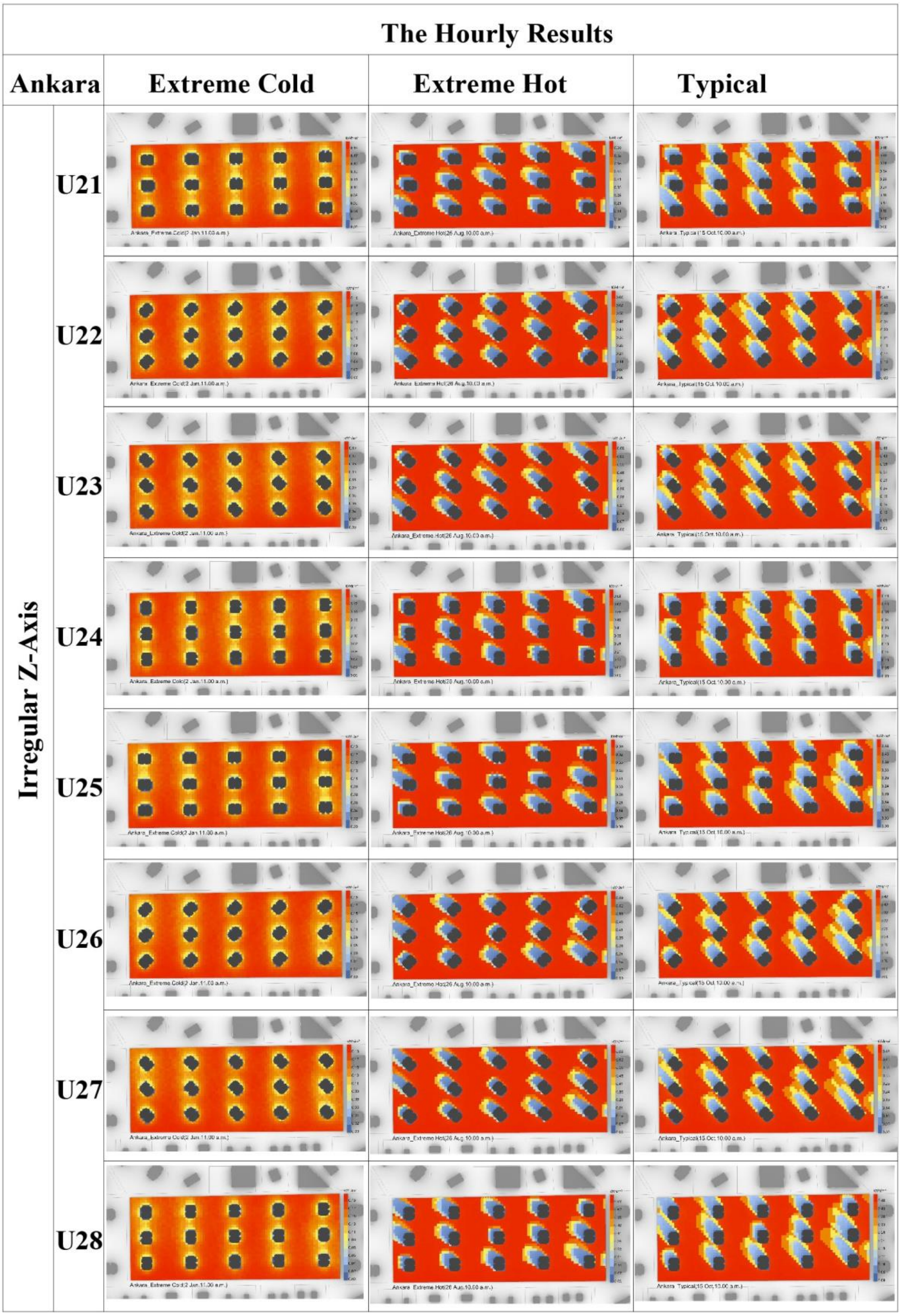

Appendix A23: Hourly solar radiation results for the Irregular Z-Axis in Ankara

		The Hourly Results		
İzmir		**Extreme Cold**	**Extreme Hot**	**Typical**
U0		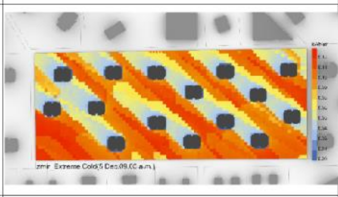	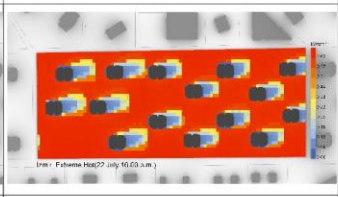	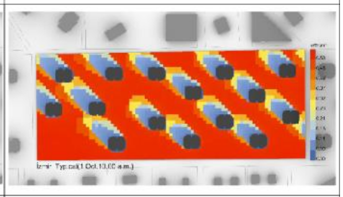
Detached	**U1**	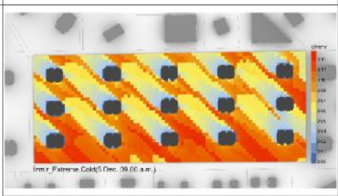	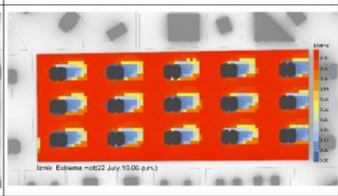	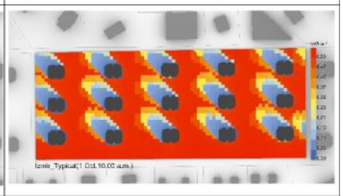
	U2	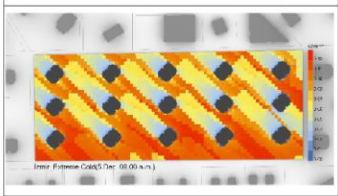	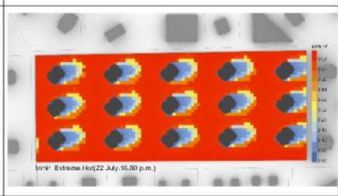	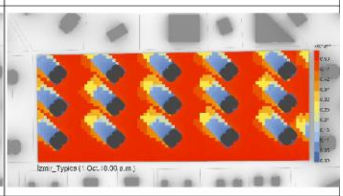
	U3	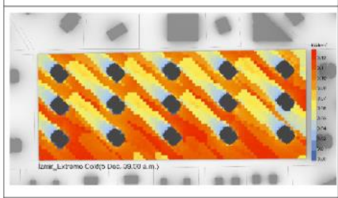	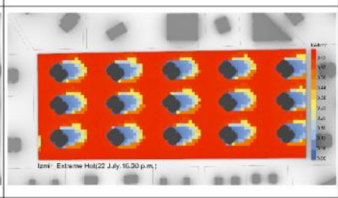	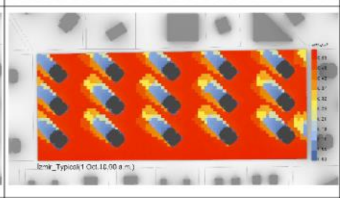
	U4	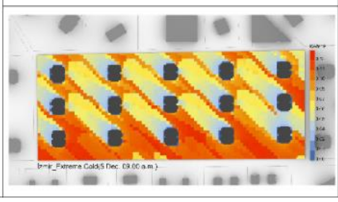	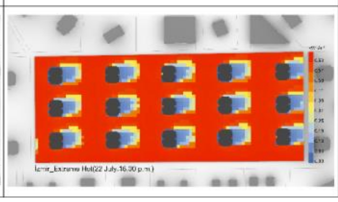	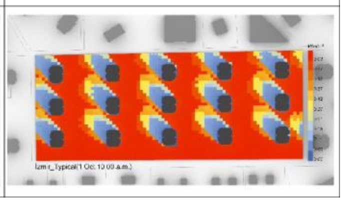

Appendix A24: Hourly solar radiation results for the U0 and detached alternatives in İzmir

The Hourly Results				
İzmir		Extreme Cold	Extreme Hot	Typical
Irregular X-Axis	U5	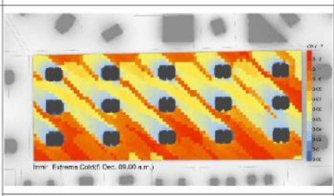	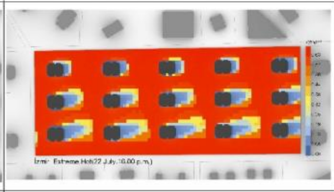	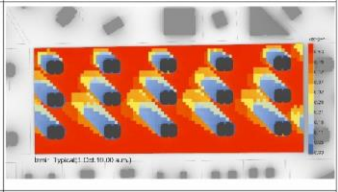
	U6	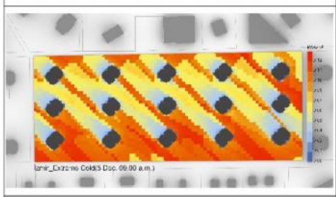	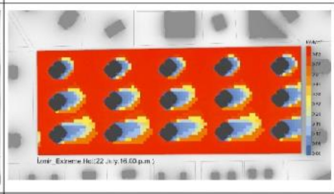	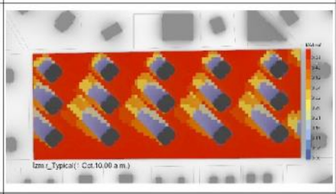
	U7	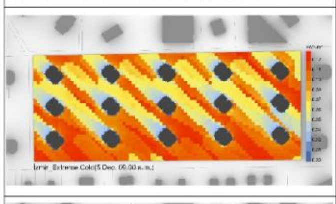	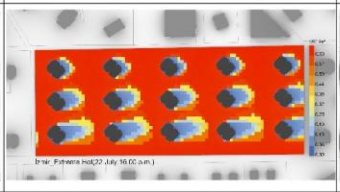	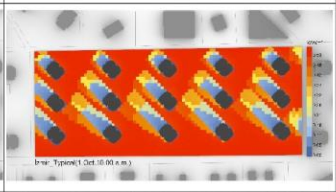
	U8	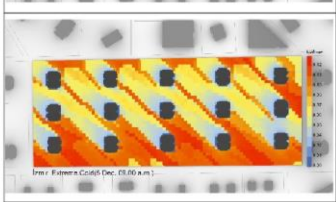	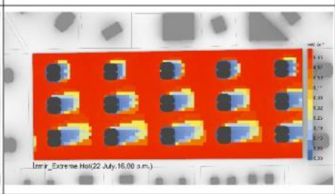	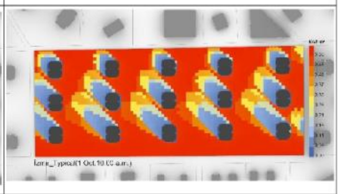
	U9	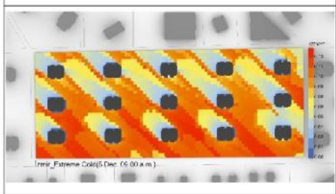	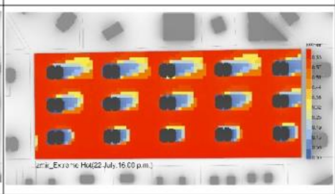	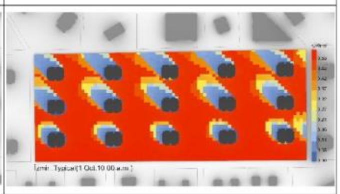
	U10	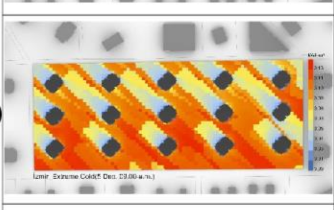	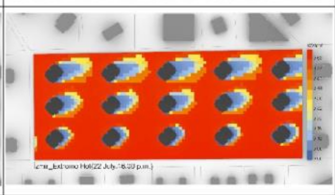	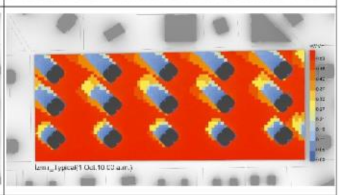
	U11	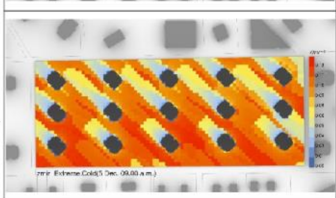	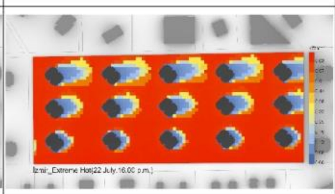	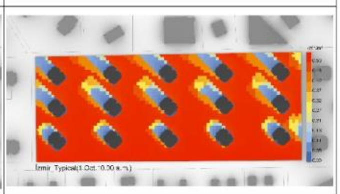
	U12	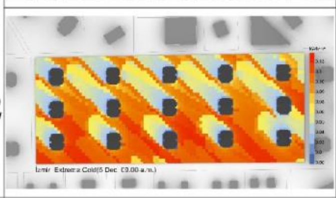	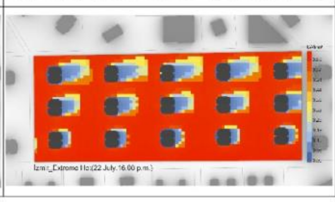	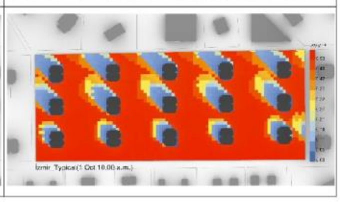

Appendix A25: Hourly solar radiation results for the Irregular X-Axis in İzmir

The Hourly Results				
İzmir		Extreme Cold	Extreme Hot	Typical
Irregular Y-Axis	U13	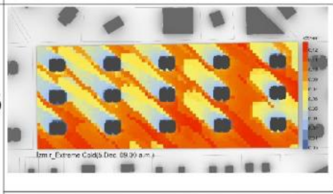	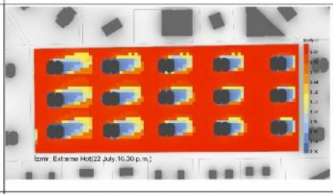	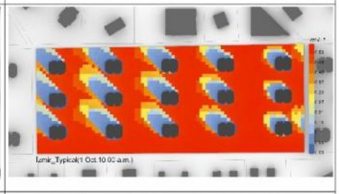
	U14	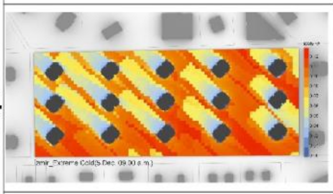	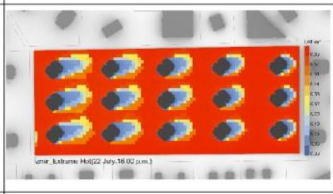	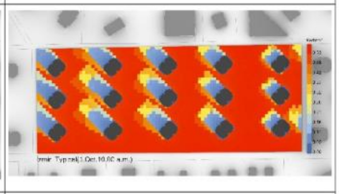
	U15	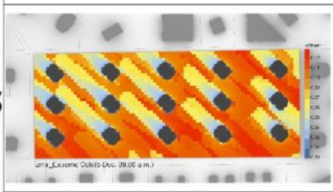	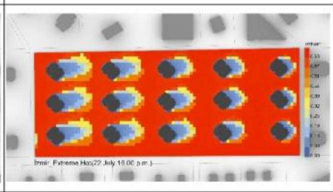	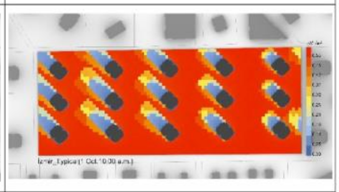
	U16	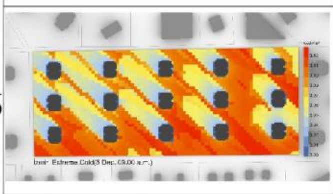	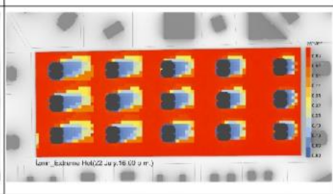	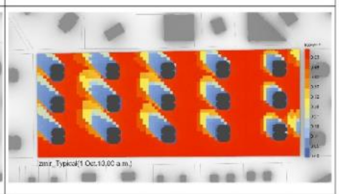
	U17	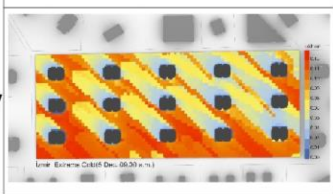	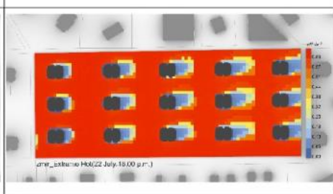	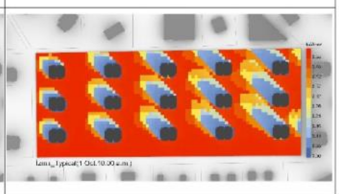
	U18	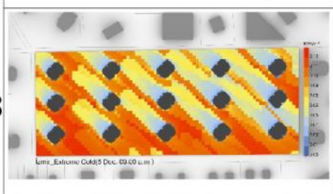	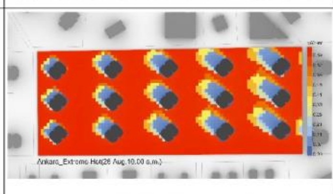	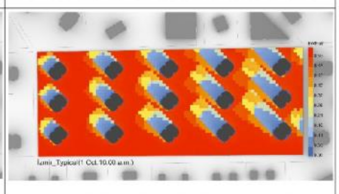
	U19	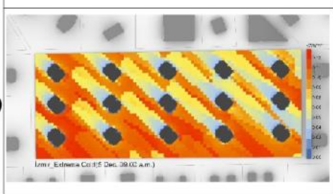	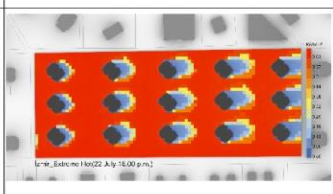	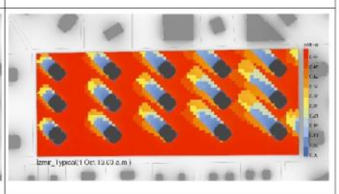
	U20	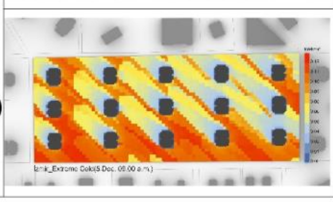	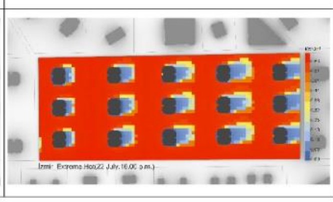	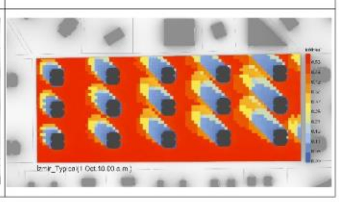

Appendix A26: Hourly solar radiation results for the Irregular Y-Axis in İzmir

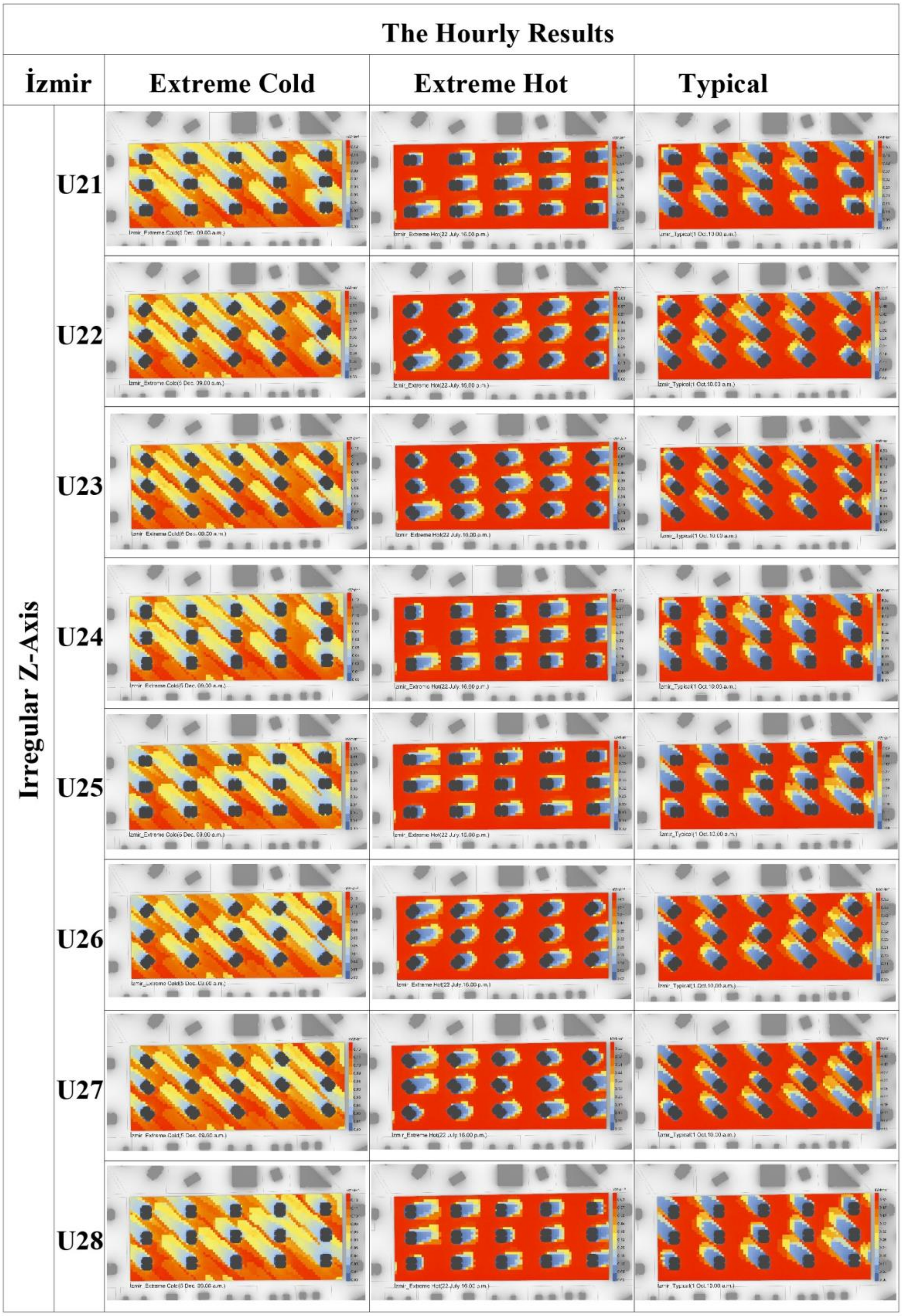

Appendix A27: Hourly solar radiation results for the Irregular Z-Axis in İzmir

REFERENCES

[1] International Energy Agency. (2020). *Tracking Buildings 2020* [Online]. Available: https://www.iea.org/reports/buildings

[2] The European Parliament and the Council of the European Union, "*Directive 2002/91/EC of the European Parliament and of the Council of 16 December 2002 on the energy performance of buildings," European Union: Official Journal of the European Communities*, vol. 1, pp. 65-71, 2002.

[3] The European Parliament and the Council of the European Union, "*Directive 2010/31/EU of the European Parliament and the council of 19 May 2010 on the energy performance of buildings (recast)," European Union: Official Journal of the European Communities*, vol. 153, pp.13-35, 2010.

[4] The European Parliament and the Council of the European Union, "*Directive (EU) 2018/844 of the European Parliament and of the council of 30 May 2018 amending directive 2010/31/EU on the energy performance of buildings and directive 2012/27/EU on energy efficiency (Text with EEA relevance)," European Union: Official Journal of the European Communities*, vol. 156, pp. 75-91, 2018.

[5] C. Becchio, M. C. Bottero, S. P. Corgnati, F. Dell'Anna, "Decision making for sustainable urban energy planning: an integrated evaluation framework of alternative solutions for a NZED (net zero-energy district) in Turin," *Land Use Policy*, vol.78, pp. 803-817, 2018.

[6] E. Kalaycıoğlu, Z.Yılmaz, "A new approach for the application of nearly zero energy concept at district level to reach EPBD recast requirements through a case study in Turkey," *Energy and Buildings*, vol. 152, pp. 680-700, 2017.

[7] S. Attia, S. "Towards regenerative and positive impact architecture: A comparison of two net zero energy buildings," *Sustainable Cities and Society*, vol. 26, pp.393-406, 2016.

[8] A. M. Hassan, A. A. ELMokadem, N. A. Megahed, A. Eleinen, "Urban morphology as a passive strategy in promoting outdoor air quality,". *Journal of Building Engineering*, vol. *29*, pp.1-14, 2020.

[9] S. D. Mangan, G. K. Oral, I. E. Kocagil, I. Sozen, "The impact of urban form on building energy and cost efficiency in temperate-humid zone," *Journal of Building Engineering*, vol. 33, pp. 1-15, 2021.

[10] S. Esfandi, L. Rahmdel, F. Nourain, A. Sharifi, "The role of urban spatial structure in energy resilience: An integrated assessment framework using a hybrid factor analysis and analytic network process model," *Sustainable Cities and Society*, vol.76, pp. 1-26, 2022.

[11] SHURA Energy Transition Center. (2019). *Enhancing Turkey's policy framework for energy efficiency of buildings, and recommendations for the way forward based on international experiences* [Online]. Available: https://www.shura.org.tr/wp-content/uploads/2019/06/Buildings-Energy-Efficiency-Policy-Working-Paper.pdf

[12] R. Loeffler, D. Österreicher, G. Stoeglehner, "The energy implications of urban morphology from an urban planning perspective-A case study for a new urban

development area in the city of Vienna," *Energy and Buildings*, vol. 252, pp. 1-12, 2021.

[13] B. C. Scheer, "Urban Morphology as a Research Method," in *Planning Knowledge and Research,* J. W. Sanchez, (Ed.), 2018, pp.167-181.

[14] C. Carneiro, V. Gori, G. Desthieux, C. Balocco, F. Golay, E. Morello, "Urban Morphology and energy consumption: Simplified tools for the estimation of energy needs and solar income at the urban and district level," in *Technologies for urban and spatial planning: Virtual cities and territories*, N. N Pinto, A. P. Antunes, R. Cladera, (Eds.), 2014, pp.173-195.

[15] S. D. Mangan, G. K. Oral, I. Sozen, I. E. Kocagil, "Evaluation of settlement textures in terms of building energy, economic performance, and outdoor thermal comfort," *Sustainable Cities and Society,* vol. 56, pp. 1-15, 2020.

[16] T.R. Oke, "Street design and urban canopy layer climate," *Energy and Buildings,* vol. 11,pp. 103-113, 1988.

[17] J. Strosmann-Andersen, P. A. Sattrup, "The urban canyon and building energy use: Urban density versus daylight and passive gains," *Energy and Buildings,* vol. 43, pp. 2011-2020, 2011.

[18] B. Meşe, "*Kentsel tasarımda pasif sistem kullanımı: Milas örneği*," M.Sc. dissertation, Dept. Architecture, İstanbul Technical University, İstanbul, Turkey, 2015.

[19] E. Trepci, P. Maghelal, E. Azar, "Urban built context as a passive cooling strategy for buildings in hot climate," *Energy and Buildings,* vol. 231, pp. 1-16, 2021.

[20] D. Jiang, W. Jiang, H. Liu, J. Sun, "Systematic influence of different building spacing, height, and layout on mean wind and turbulent characteristics within and over urban building arrays," *Wind and Structures*, vol.11, pp. 275-290, 2008.

[21] M. Ramalho Fontenelle, S. Lorente, L. E. Gonçalves Bastos, "The impact of urbanization on air flow pattern: the case of Rio de Janeiro," *International Journal of Green Energy*, vol. 12, pp. 908-916, 2015.

[22] J. Hang, M. Sandberg, Y. Li, "Effect of urban morphology on wind condition in idealized city models," *Atmospheric Environment*, vol. 43, pp. 869-878, 2009.

[23] J.J. Sarralde, J. D. Quinn, D. Wiesmann, & K. Steemers, "Solar energy and urban morphology: Scenarios for increasing the renewable energy potential of neighbourhoods in London," *Renewable energy,* vol. 73, pp. 10-17, 2015.

[24] Z. Shi, J. A.Fonseca, A. Schlueter, "A parametric method using vernacular urban block typologies for investigating interactions between solar energy use and urban design," *Renewable Energy,* vol. 165, pp. 823-841, 2021.

[25] M. M. E. Van Esch, R. H. J. Looman, G. J. de Bruin-Hordijk, "The effects of urban and building design parameters on solar access to the urban canyon and the potential for direct passive solar heating strategy," *Energy and Buildings,* vol. 47, pp. 189-200, 2012.

[26] D. Zhu, D. Song, J. Shi, J. Fang, & Y. Zhou, "The Effect of Morphology on Solar Potential of High-Density Residential Area: A Case Study of Shanghai," *Energies,* vol. 13, pp. 2215-2020, 2020.

[27] A. Khalid, "Passive Design, Urban-Rural Architectural Morphology for Subtropics," *European Journal of Sustainable Development*, vol. 9, pp. 376-399, 2020.

[28] N. El Dallal, F. Visser, “A climate responsive urban design tool: a platform to improve energy efficiency in a dry hot climate,” *International Journal of Sustainable Energy*, vol. 36, pp. 738-75, 2017.

[29] S. Uçlar, M.A. Buldurur, “Relation between urban form and heating energy consumption,” *A| Z ITU Mimarlık Fakültesi Dergisi*, vol. 17, pp. 89-102, 2020.

[30] X. Wang, Z. Li, “A systematic approach to evaluate the impact of urban form on urban energy efficiency: A case study in Shanghai,” *Energy Procedia*, vol. 105, pp. 3225-3231, 2017.

[31] T. A. De Lemos Martins, S. Faraut, L. Adolphe, “Influence of context-sensitive urban and architectural design factors on the energy demand of buildings in Toulouse, France,” *Energy and Buildings*, vol. 190, pp. 262-278, 2019.

[32] E. Garcia-Nevado, B. Beckers, “Radiative exchanges in the dense city,” in *Bioclimatic Approaches in Urban and Building Design,* G. Chiesa, Eds., 2021, pp. 321-349.

[33] K. R. D. C. C. Marins, “A method for energy efficiency assessment during urban energy planning,” *Smart and Sustainable Built Environment*, vol. 3, pp. 132-152, 2014.

[34] A. T. D. K. Perera, K. Javanroodi, V. M. Nik, “Climate resilient interconnected infrastructure: Co-optimization of energy systems and urban morphology,” *Applied Energy*, vol. 285, 2021.

[35] A. Salvati, M. Palme, G. Chiesa, M. Kolokotroni, “Built form, urban climate and building energy modelling: Case-studies in Rome and Antofagasta,” *Journal of Building Performance Simulation*, vol. 13, pp. 209-225, 2020.

[36] S. Shareef, “The impact of urban morphology and building’s height diversity on energy consumption at urban scale. The case study of Dubai,” *Building and Environment*, vol. 19, pp. 1-15, 2021.

[37] H. Leng, X. Chen, Y. Ma, N. H. Wong, T. Ming, “Urban morphology and building heating energy consumption: Evidence from Harbin, a severe cold region city,” *Energy and Buildings*, vol. 224, 2020.

[38] W. Wang, K. Liu, M. Zhang, Y. Shen, R. Jing, X. Xu, “From simulation to data-driven approach: A framework of integrating urban morphology to low-energy urban design,” *Renewable Energy*, vol. 179, pp. 2016-2035, 2021.

[39] B. Cody, W. Loeschnig, A. Eberl, “Operating energy demand of various residential building typologies in different European climates,” *Smart and Sustainable Built Environment,* vol.7, pp. 226-250, 2018.

[40] A. M. Salih, S. Dudek, “The impact of modified residential morphologies on the outdoor microclimate in hot-dry of Erbil, Kurdistan-Iraq,”in *Resilient and responsible smart cities,* N. Ujang, T. Fukuda, A. L. Pisello, B. Vukadinovic, D, Eds., 2021, pp. 155-168.

[41] A.Taki, J. Alabid, “Learning from bioclimatic desert architecture: a case study of Ghademes, Libya,” in *Research methodology in the built environment,* V. Ahmed, A.Opoku, Z. Aziz, Eds., 2016, pp.189-206.

[42] E. Ng, T. Chan, V. Cheng, N. H. Wong, M. Han, “Designing high density cities-parametric studies of urban morphologies and their implied environmental performance,” *Tropical Sustainable Architecture,* J. Bay, B. L.Ong, Ed., 2006, pp. 169-198.

[43] N. Jayaweera, U. Rajapakssha, I. Manthilake, “A parametric approach to optimize solar access for energy efficiency in high-rise residential buildings in dense urban tropics,” *Solar Energy,* vol. 220, pp. 187-203, 2021.

[44] E. Morello, V. Gori, C. Balocco, C. Ratti. *“Sustainable Urban Block Design through Passive Architecture: A tool that uses urban geometry optimization to compute energy savings,”*. In Conference of the 26. international conference on passive and low energy architecture: PLEA, 2009, pp. 146-151.

[45] P. E. Camporeale, P. Mercader-Moyano, “Towards nearly Zero Energy Buildings: Shape optimization of typical housing typologies in Ibero-American temperate climate cities from a holistic perspective,” *Solar Energy,* vol. 193, pp. 738-765, 2019.

[46] A. Jurelionis, D. G. Bouris, Impact of urban morphology on infiltration-induced building energy consumption,” *Energies,* vol. 9, 2016.

[47] N. Cardinale, M. Micucci, F. Ruggiero, “Analysis of energy saving using natural ventilation in a traditional Italian building,” *Energy and buildings*, vol. 35, pp. 153-159, 2003.

[48] K. Javanroodi, M. Mahdavinejad, Nik, V. M. “Impacts of urban morphology on reducing cooling load and increasing ventilation potential in hot-arid climate,” *Applied energy,* vol. 231, pp. 714-746, 2018.

[49] A. Gros, E. Bozonnet, C. Inard, M. Musy, “Simulation tools to assess microclimate and building energy–A case study on the design of a new district,” *Energy and Buildings*, vol. 114, pp. 112-122, 2016.

[50] N, Baker, K. Steemers, *Energy and environment in architecture: A tectnical design guide*, London, New York: E&FN Spon, 2000.

[51] N.Enteria, O. Cuertero-Enteria, M. Santamouris, U. Eicker, “Morphology of buildings and cities in hot and humid regions,” in *Urban Heat Island (UHI) Mitigation,* N.Enteria, M. Santamouris, U. Eicker, Eds., 2021, pp.1-13.

[52] V. Jankovic, “The city,” in *Research handbook on climate governance, K.* Backstrand, E. Lövbrand, Eds., 2015, pp.332-345.

[53] P. Smith, C. Lamarca, C. Henriquez, “A Comparative Study of Thermal Comfort in Public Spaces in the Cities of Concepción and Chillán, Chile,”in *Urban Climates in Latin America*, C. Henríquez, H. Romero, Eds., 2019, pp.111-134.

[54] K. K. Lau, Z. Tan, T. E. Morakinyo, C. Ren, “Dynamic response of pedestrian thermal comfort,” in *Outdoor Thermal Comfort in Urban Areas,* K. K. Lau, Z. Tan, T. E. Morakinyo, C. Ren, Eds., 2021, pp. 35-50.

[55] N. Mouada, N., Zemmouri, R. Meziani, “Urban morphology, outdoor thermal comfort and walkability in hot, dry cities: Case study in Sidi Okba, Algeria,” *International Review for Spatial Planning and Sustainable Development*, vol. 7, pp. 117-133. 2019.

[56] H. A. S. Othman, A. A. Alshboul, “The role of urban morphology on outdoor thermal comfort: The case of Al-Sharq City–Az Zarqa,” *Urban Climate,* vol. 34, pp. 1-12, 2020.

[57] O. M. Galal, D. J. Sailor, H. Mahmoud, “The impact of urban form on outdoor thermal comfort in hot arid environments during daylight hours, case study: New Aswan,” *Building and Environment*, vol. 184, pp. 1-15, 2020.

[58] İ. Sözen, G. K. Oral, “Outdoor thermal comfort in urban canyon and courtyard in hot arid climate: A parametric study based on the vernacular settlement of Mardin,” *Sustainable Cities and Society,* vol. 48, pp. 1-15. 2019.

[59] S. Sabrin, M. Karimi, R. Nazari, J. Pratt, J. Bryk, “Effects of different urban-vegetation morphology on the canopy-level thermal comfort and the cooling benefits of shade trees: Case-study in Philadelphia,” *Sustainable Cities and Society*, vol. 6, pp. 1-14, 2021.

[60] E. L. Krüger, F. O. Minella, F. Rasia, “Impact of urban geometry on outdoor thermal comfort and air quality from field measurements in Curitiba, Brazil,” *Building and Environment*, vol. 46(3), pp. 621-634, 2011.

[61] K. M. Wai, C. Yuan, A. Lai, & K. N. Peter, “Relationship between pedestrian-level outdoor thermal comfort and building morphology in a high-density city,” *Science of the total environment*, vol. 708, 1-7, 2020.

[62] W, Ghaffour, M. N. Ouissi, M. A. V. Dabat, “Analysis of urban thermal environments based on the perception and simulation of the microclimate in the historic city of Tlemcen,” *Smart and Sustainable Built Environment*, vol. 10, pp. 141-168, 2020.

[63] G. S. Song, & M. Jeong, “Morphology of pedestrian roads and thermal responses during summer, in the urban area of Bucheon city, Korea,” *International journal of biometeorology*, vol. 60, pp. 999-1014, 2016.

[64] L. Tsichritzis, M. Nikolopoulou, “The effect of building height and façade area ratio on pedestrian wind comfort of London,” *Journal of wind engineering and industrial aerodynamics*, vol. 191, pp. 63-75. 2019.

[65] A. Chatzidimitriou, S. Yannas, “Microclimate design for open spaces: Ranking urban design effects on pedestrian thermal comfort in summer,” *Sustainable Cities and Society*, vol. 26, pp. 27-47. 2016.

[66] B. Ekinci, “*Kentsel Alanlarda Oluşan Isı Adası Etkisinin Kentsel Tasarım Yöntemleri İle Azaltılması: Aksaray Meydanı Örneği,”* Ph.D dissertation, Dept. Architecture, İstanbul Technical University, Istanbul, Turkey, 2016.

[67] A. Ö. Alpaslan, A. Ö. “*Enerji etkin planlama kapsamında Antalya kenti için bir yöntem yaklaşımı,”* Ph.D dissertation, Dept. Architecture, University of Akdeniz, Antalya, Turkey, 2019.

[68] G.Kazancı, “*İklim Değişikliğine Uyum Kapsamında Akıllı Kentlerin Rolü: Muğla Metropoliten Alanı Üzerine Bir Değerlendirme,”* M.Sc. dissertation, Dept. Architecture, İstanbul Technical University, İstanbul, Turkey, 2019.

[69] M. F. U. Moazzam, Y. H. Doh, B. G. Lee, “Impact of urbanization on land surface temperature and surface urban heat Island using optical remote sensing data: A case study of Jeju Island, Republic of Korea,” *Building and Environment*, vol. 222, 2022.

[70] A. Gülten, “*Kentsel yüzeylerde ısı adası etkisinin simülasyon ile araştırılması,”* Ph.D dissertation, Dept. Architecture, İstanbul Technical University, Istanbul, Turkey, 2014.

[71] C. Apreda, A. Reder, P. Mercogliano,. “Urban morphology parameterization for assessing the effects of housing blocks layouts on air temperature in the Euro-Mediterranean context,” *Energy and Buildings*, vol. 223, pp. 1-20, 2020.

[72] O. Tabanoğlu, “*Antalya için iklim değişikliğine uyum stratejileri önerisi,”* M.Sc. dissertation, Dept. Architecture, İstanbul Technical University, İstanbul, Turkey, 2018.

[73] E. H. S. Rajan, L. R. Amirtham, “Urban heat island intensity and evaluation of outdoor thermal comfort in Chennai, India,” *Environment, Development and Sustainability*, vol. 23, pp. 16304-16324. 2021.

[74] C. Yuan, A. S. Adelia, S. Mei, W. He, X. X. Li, L. Norford, "Mitigating intensity of urban heat island by better understanding on urban morphology and anthropogenic heat dispersion" *Building and Environment*, vol. 176 ,pp. 1-12. 2020.

[75] K. K. L. Lau, Z. Tan, T. E. Marakinyo, C. Ren, "Urban Greening Strategies for Enhancing Outdoor Thermal Comfort," in *Outdoor Thermal Comfort in Urban Environments,* in SpringerBriefs in Architectural Design and Technology, 2022, pp.85-100.

[76] B. J. He, L. Ding, D. Prasad, "Relationships among local-scale urban morphology, urban ventilation, urban heat island and outdoor thermal comfort under sea breeze influence," *Sustainable Cities and Society*, vol. 60, pp. 1-20, 2020.

[77] Y. Liu, Q. Li, L. Yang, K. Mu, M. Zhang, J. Liu, "Urban heat island effects of various urban morphologies under regional climate conditions," *Science of the Total Environment*, vol. 743, pp. 1-14, 2020.

[78] L. G. Santos, I. Nevat, G. Pignatta, L. K. Norford, (2021). "Climate-informed decision-making for urban design: Assessing the impact of urban morphology on urban heat island," *Urban Climate*, vol. 36, pp. 1-14, 2021.

[79] S. Mirzabeigi, M. Razkenari, "Design optimization of urban typologies: A framework for evaluating building energy performance and outdoor thermal comfort," *Sustainable Cities and Society*, vol. 76, pp. 1-15. 2022.

[80] F. De Luca, E. Naboni, G. Lobaccaro, "Tall buildings cluster form rationalization in a Nordic climate by factoring in indoor-outdoor comfort and energy," *Energy and Buildings*, vol. 238, pp. 1-16. 2021.

[81] G. Evola, V. Costanzo, C. Magrì, G. Margani, L. Marletta, E. Naboni, "A novel comprehensive workflow for modelling outdoor thermal comfort and energy demand in urban canyons: Results and critical issues," *Energy and Buildings*, vol. 216, pp. 1-19, 2020.

[82] T. Sharmin, K. Steemers, A. Matzarakis, "Analysis of microclimatic diversity and outdoor thermal comfort perceptions in the tropical megacity Dhaka, Bangladesh," *Building and Environment*, vol. 94, pp.734-750, 2015.

[83] T. Sharmin, K. Steemers, A. Matzarakis, "Microclimatic modelling in assessing the impact of urban geometry on urban thermal environment," *Sustainable cities and society*, vol. 34, pp. 293-308, 2017.

[84] S. Tsoka, T. Leduc, A. Rodler, "Assessing the effects of urban street trees on building cooling energy needs: The role of foliage density and planting pattern," *Sustainable Cities and Society*, vol. 65, pp. 1-16, 2021.

[85] Google Earth. (n.d.). *Google Earth* [Online]. Available: https://earth.google.com/web/

[86] CADMAPPER. (n.d.). *Worldwide map files for any design program* [Online]. Available: https://cadmapper.com/

[87] Autodesk. (n.d.). *Autodesk AutoCAD* [Online]. Available: https://www.autodesk.com/products/autocad/overview?term=1-YEAR&tab=subscription

[88] OpenStreetMap. (n.d.). *OpenStreetMap* [Online]. Available: https://www.openstreetmap.org/about/

[89] Robert McNell & Associates. (n.d.). *Rhinoceros 3D* [Online]. Available: https://www.rhino3d.com/

[90] Bilgi Ofisi. (n.d.). *46277 Ada Burçak Apt. A2 (66) Blok* [Online]. Available: https://eryaman.bilgiemlak.com.tr/yer/burcak-apt-a2-66-blok-3007#yertab=katplanlari

[91] Isıcam Sistemleri. (n.d.). *Isıcam Cam Yalıtımı Sistemleri* [Online]. Available: https://www.isicam.com.tr/tr

[92] Isıcam Sistemleri. (n.d.). *S Serisi Cam Sistemleri ile Etkin Isı ve Gürültü Yalıtımı* [Online]. Available: https://www.isicam.com.tr/tr/urunler/isicam-sistemleri-s-serisi#undefine

[93] *Thermal insulation requirements for buildings*, TS-825, 1-154, 2013.

[94] Ladybug Tools. (n.d.). *Epwmap* [Online]. Available: https://www.ladybug.tools/epwmap/

[95] N. Mohajeri, A. Gudmundsson, G. Upadhyay, D. Assouline, "Neighbourhood morphology ans solar irradiance in relation to urban climate," in *9th International Conference on Urban Climate Jointly With 12th Symposium on the Urban Environment*, Switzerland, EPFL, 2015, pp.1-6.

VITA

In 2019, Ayşe Özlem DAL obtained her bachelor's degree from Özyeğin University, from the department of Architecture and Design (English) as a high honor student. She has been conducting her master's degree in Özyeğin University from MSc in Architecture. Dal worked as a graduate scholar in the research project whose name is *"Developing National Approach of Long-term Renovation Strategies for Existing Educational Campuses in Turkey Towards Nearly Zero Energy Target"*. The project is organized by TÜBİTAK 3501 Career Development Program, and numbered 219M552. She worked as a teaching assistant for architectural studios, construction technology classes, and environmental control courses between 2019 and 2022.

Since 2022, she is working as a research assistant at OzU with the department of Construction Technologies. She is also the member of Building Envelope Design and Technology Lab, and Building Material and Physics Lab. During this period, Dal concluded national, and international conference papers, and have continuing journal papers. Her research area includes energy efficiency in urban design, building material and its physics, parametric analysis, computer-aided design, disaster risk reduction and resilience in cities.